SEA No. 93-554-06-A:1

Parametric Study of the Potential for BWR ECCS Strainer Blockage Due to LOCA Generated Debris

Preliminary Draft Report

Prepared by:

Science and Engineering Associates, Inc.

Prepared for:

U.S. Nuclear Regulatory Commission

Science & Engineering Associates, Inc.

SEA No. 93-554-06-A:1

Parametric Study of the Potential for BWR ECCS Strainer Blockage Due to LOCA Generated Debris

Preliminary Draft Report

Date: January 20, 1994

Prepared by: G. Zigler, J. Brideau, D.V. Rao, N. Ruiz, C. Shaffer, W. Thomas, R. Walsh

Science and Engineering Associates, Inc.

SEA Plaza
6100 Uptown Blvd. NE
Albuquerque, NM 87110

Prepared for:

U.S. Nuclear Regulatory Commission

Office of Nuclear Regulatory Research
Washington, DC 20555

NRC Contract No. NRC-04-91-071

Table of Contents

Section				Page
List of Acronyms				iv
Executive Summary				v
1.0	BACKGROUND			1-1
	1.1	Unresolved Safety Issue A-43		1-1
	1.2	Summary of the Perry and Barsebäck Events		1-3
	1.3	Objectives and Scope		1-5
2.0	METHODOLOGY FOR ANALYSIS OF INSULATION DEBRIS EFFECTS			2-1
	2.1	Overall Methodology		2-1
	2.2	Reference BWR Selection Considerations		2-1
	2.3	Pipe Break Frequency Considerations		2-5
	2.4	Debris Generation Considerations		2-5
	2.5	Debris Transport Considerations		2-6
	2.6	Strainer Blockage Considerations		2-7
	2.7	Pump Performance Considerations		2-8
	2.8	BLOCKAGE 2.0 Overview		2-8
3.0	REFERENCE BWR PLANT DATA			3-1
	3.1.	Introduction		3-1
	3.2	Piping Layout in the Drywell		3-1
	3.3	Primary Piping Weld Locations		3-4
		3.3.1	Recirculation Loops A and B	3-4
		3.3.2	Feedwater Loops A, B and C, D	3-7
		3.3.3	Main Steam Lines A, B, C and D	3-7
	3.4	Drywell Piping Insulation		3-7
	3.5	Drywell and Suppression Pool Layout		3-18
	3.6	RHR and CS Systems Description		3-18
4.0	PRIMARY PIPE BREAK FREQUENCIES			4-1
	4.1	Approach Used to Estimate Weld Break Frequencies		4-1
	4.3	BLOCKAGE 2.0 Pipe Break Frequency Estimates		4-7
5.0	SCREEN BLOCKAGE MODELS			5-1
	5.1	Introduction		5-1
	5.2	Debris Generation Model		5-1
		5.2.1	Review of USI A-43 Debris Generation Model	5-1
		5.2.2	BWR Debris Generation Model	5-4
		5.2.3	Application to DAEC Unit 1	5-6
	5.3	Debris Transport to the Suppression Pool		5-15
		5.3.1	Review of USI A-43 Debris Transport Model	5-15
		5.3.2	BWR Debris Transport Model	5-16
	5.4	Debris Transport Within the Sump		5-17
	5.5	Strainer Head Loss Model		5-18
		5.5.1	Review of USI A-43 Head Loss Model	5-19
		5.5.2	NUKON™ Head Loss Model	5-21
		5.5.3	Application to DAEC-Unit 1 Plant	5-24
	5.6	Loss of ECCS NPSH Model		5-24

6.0 COMPUTER PROGRAM BLOCKAGE 2.0 6-1
- 6.1 Background 6-1
- 6.2 BLOCKAGE Overview 6-1
- 6.3 Functional Description of BLOCKAGE 2.0 6-2
  - 6.3.1 Input Description 6-2
  - 6.3.2 Calculational Algorithm 6-2
  - 6.3.3 Output Description 6-6
- 6.4 Application to DAEC-Unit 1 Plant 6-7

7.0 DUANE ARNOLD BLOCKAGE ESTIMATES 7-1
- 7.1 Base Case Results 7-1
  - 7.1.1 ECCS Strainer Blockage Frequency Estimates for the Base Case 7-2
  - 7.1.2 ECCS Strainer Blockage Frequency Estimates by System 7-2
  - 7.1.3 ECCS Strainer Blockage Frequency Estimates by Pipe Size 7-2
  - 7.1.4 ECCS Strainer Blockage Frequency Estimates by Pipe Location 7-3
- 7.2 Major Analysis Assumptions and Limitations 7-4
  - 7.2.1 Major Analysis Assumptions 7-4
    - 7.2.1.1 Pipe Break Initiator Assumptions 7-4
    - 7.2.1.2 Debris Generation Assumptions 7-7
    - 7.2.1.3 Debris Transport Assumptions 7-7
  - 7.2.2 Major Analysis Limitations 7-7
    - 7.2.2.1 General Limitations 7-8
    - 7.2.2.2 Pipe Break Initiator Limitations 7-8
    - 7.2.2.3 Debris Generation Limitations 7-9
    - 7.2.2.4 Debris Transport Limitations 7-9
    - 7.2.2.5 Head Loss Limitations 7-10
    - 7.2.2.6 Pump Performance Limitations 7-11
- 7.3 Sensitivity Analyses 7-11
  - 7.3.1 Variation of Head-Loss Correlation Coefficients 7-11
  - 7.3.2 Variation of NPSH Margin 7-12
  - 7.3.3 Variations of Debris Generation Insulation Destruction Fractions 7-13
  - 7.3.4 Variations of Debris Transport Fractions 7-13
- 7.4 Summary and Conclusions 7-17

Appendix A: BWR Coolant Pipe Weld Break Frequencies for Estimating the Potential for LOCA Generated ECCS Strainer Blockage (Revision 2)

Appendix B: Overview of BLOCKAGE 2.0

List of Acronyms

ARL	Alden Research Laboratory
ASME	American Society of Mechanical Engineers
BPVC	Boiler and Pressure Vessel Code
BWR	Boiling Water Reactor
CEESI	Colorado Engineering Experiment Station, Inc.
CS	Core Spray
D	Diameter of broken pipe
DAEC	Duane Arnold Energy Center
DEGB	Double-Ended Guillotine Break
ECCS	Emergency Core Cooling System
GPM	Gallons per Minute
HDR	Heissdampfreaktor
HPCI	High Pressure Coolant Injection
IGSCC	Intergranular Stress Corrosion Cracking
IPE	Individual Plant Examination
KKL	Kernkraftwerk Leibstadt Ag
L	Distance from break to target
LLNL	Lawrence Livermore National Laboratory
LOCA	Loss of Coolant Accident
LPCI	Low Pressure Coolant Injection
LPCS	Low Pressure Core Spray
MSL	Main Steam Line
NPSH	Net Positive Suction Head
NRC	Nuclear Regulatory Commission
P&ID	Piping and Instrumentation Diagram
PCI	Performance Contracting, Inc.
PWR	Pressurized Water Reactor
RCIC	Reactor Core Isolation Cooling
RG	Regulatory Guide
RHR	Residual Heat Removal
RWCU	Reactor Water Clean-up
SNL	Sandia National Laboratories
SRV	Safety Relief Valve
TAP	Task Action Plan
USI	Unresolved Safety Issue
WPI	Worcester Polytechnic Institute

Executive Summary

Unresolved Safety Issue (USI) A-43, "Containment Emergency Sump Performance," dealt with concerns about the availability of long term recirculation cooling provided by the Emergency Core Cooling Systems (ECCS) in a Pressurized Water Reactor (PWR) following a LOCA. USI A-43 addressed concerns related to destruction and dislodgement of fibrous insulation from the pipes in the areas surrounding the break by the steam/water jet originating from the break, and subsequent transport of the debris to the sump ECCS pump intake screen. USI A-43 evaluated the potential for such debris to block flow through the debris screen to an extent where the net positive suction head available at the ECCS pump suction is below that required to prevent ECCS pump cavitation. Major findings of this study were documented in NUREG-0897, Rev. 1,[1] and NUREG-0869, Rev. 1[2].

Although USI A-43 was derived principally from concerns about emergency sump performance in PWRs, the concerns about debris blockage applies to Boiling Water Reactors (BWRs) as well. This concern at BWRs was heightened by recent suppression pool strainer blockage incidents at the Perry nuclear plant in the U. S. and at the Barsebäck-2 plant in Sweden. In response, the NRC staff undertook a study to estimate the potential for loss of low pressure coolant injection (LPCI) and low pressure core spray (CS) capabilities due to LOCA-generated debris for a representative BWR using the methodology previously applied to PWRs as part of the USI A-43 study. The major elements of this current study were:

1. the selection of a reference BWR for analysis,
2. the estimation of primary pipe break frequencies,
3. a parametric study of debris generation and debris transport to the suppression pool,
4. calculation of head loss due to accumulation of fibrous insulation debris on RHR/CS pump suction intake strainers, and
5. analysis of RHR/CS pump performance during post-LOCA conditions.

These elements were combined to yield ECCS strainer blockage frequency estimates for a reference BWR. The reference plant selected for this analysis was Duane Arnold Energy Center (DAEC)-Unit 1. DAEC Unit 1 is a BWR/4 with a Mark I containment, and it retains the original 304-stainless steel (304SS) recirculation loops. The 304SS material is more susceptible to intergranular stress corrosion cracking (IGSCC) than more resistant materials used at other plants, for example 316 nuclear grade stainless steel (316NG).

---

[1] A. W. Serkiz, "Containment Emergency Sump Performance," US Nuclear Regulatory Commission, NUREG-0897, Rev. 1, October 1985.

[2] A. W. Serkiz, "USI A-43 Regulatory Analysis," US Nuclear Regulatory Commission, NUREG-0869, Rev. 1, October 1985.

Other studies have identified that pipe breaks in reactor cooling systems are most likely to occur at the weld locations, and that weld break frequency is strongly dependent on the type of weld and operating environment. As a result, considerable effort was devoted in this study to identify the number, type, location and orientation of welds in the entire primary system piping subjected to high pressures during normal operation. For each weld type, a weld break frequency was obtained based on data extracted from a Lawrence Livermore National Laboratory BWR pipe break study described in NUREG/CR-4792[3]. Based on a detailed analysis, it was concluded that debris generation in the DAEC Unit 1 is dominated by breaks postulated in the recirculation, feedwater, and main steam system piping. Pipe break frequencies for these three systems were then estimated as a sum of weld break frequencies over the entire length of the system piping. The estimated overall pipe break frequency (per Rx-year) obtained from this study, based on the DAEC Unit 1 configuration, is 1.5E-4. The pipe break frequencies sorted by systems were 1.2E-4, 1.4E-5 and 1.9E-5 (per Rx-year), respectively, for the recirculation, feedwater and main steam lines. It is important to note that only Double-Ended Guillotine Breaks (DEGBs) were considered in the analysis.

The LOCA debris generation model used in the present study was very similar to the three-region, two-phase jet expansion model proposed in NUREG-0897 for PWRs. Physical boundaries of these regions were modified to account for (a) lower stagnation pressures typical of postulated breaks in BWRs compared to PWRs and (b) 304SS jacketed NUKON™ insulation used in DAEC Unit 1. The zone of influence was assumed to extend up to an axial length (L) of 7 times the inside diameter (D) of the pipe where the break occurs, and this zone is in the shape of a right-angle cone. Also, the present model conservatively assumed that about 75% of the available insulation in Region I ($L/D < 3$), 60% in Region II ($3 < L/D < 5$), and 40% in Region III ($5 < L/D < 7$) is actually destructed into transportable form and dislodged from the target pipes by the expanding jet. These fractions were parametrically varied to examine their impact on ECCS strainer blockage frequency. For the sake of simplification, results presented here assumed that only insulation on the broken pipe would have the potential to cause strainer blockage. Other possible targets were not considered. Also, no credit was given to operator actions for mitigating strainer blockage conditions to overcome this potential cause of ECCS failure.

The debris transport model used in the present study was parametric in nature and was keyed to the DAEC Unit 1 drywell configuration. This model did not make any distinction between transport during short-term (or blowdown) and long-term (or recirculation) phases of ECCS operation following a LOCA. Instead, the present study divided the drywell into three regions: High, Mid-level, and Low, depending on break location with respect to gratings located at elevations 757' and 776'. The base case assumed that 75% of the debris generated below an elevation of 757', 50% of the debris generated between

---

[3] C. S. Holman and C. K. Chou, "Probability of Failure in BWR Reactor Coolant Piping," published as Lawrence Livermore National Laboratory Report UCID-20914, NUREG/CR-4792, March 1989.

757′ and 776′, and 25% of the debris generated above an elevation of 776′ would be transported to the suppression pool. This base case was based on engineering judgement and very limited experimental data. Sensitivity analyses performed as part of this study then varied these fractions to examine their impact on ECCS strainer blockage frequency.

Debris transport within the suppression pool was simplified by conservatively assuming that all debris reaching the suppression pool will ultimately be deposited uniformly on the RHR/CS pump strainers. The head loss across these strainers was then calculated using a correlation developed as a part of this study which was based on experimental data for uniformly packed NUKON™ shreds, fines and 'as-fabricated' blankets. Finally, the RHR/CS pumps were assumed to fail when the estimated head loss was greater than or equal to the NPSH-margin for the RHR pumps. In estimating the NPSH-margin, no credit was given for possible effects of suppression pool pressurization due to blowdown, or decrease in NPSH margin due to an increase in the pool temperature. The present analysis, however, examined the impact of NPSH margin on the ECCS strainer blockage by varying this parameter between 1 and 20 ft of water.

The point estimate of overall DEGB pipe break frequency (per Rx-year) obtained from this study is 1.5E-4, with a corresponding overall ECCS strainer blockage frequency (per Rx-year) of 4.6E-5. The overall conditional strainer blockage probability was calculated to be 0.31 by dividing the above strainer blockage frequency (4.6E-05 per Rx-yr) by the pipe break initiator frequency (1.5E-04 per Rx-yr). This conditional blockage probability represents the probability of strainer blockage given the class of DEGB pipe break initiators considered in the analysis, and given the set of assumptions and bases used in carrying out the analysis.

Figures A and B illustrate point estimates of ECCS strainer blockage frequency as a function of system, pipe diameter and location (drywell elevation) where the breaks can occur. As shown in Figure A, the recirculation system contributes the largest fraction to the ECCS strainer blockage frequency (3.1E-5 per Rx-year). This result is a direct reflection of the large pipe break frequency associated with the recirculation piping (1.2E-4 per Rx-year). However, the conditional probability for ECCS strainer blockage given a LOCA in the recirculation piping is only 0.26. This low conditional probability is primarily due to the large number of small diameter instrumentation welds in the recirculation loops which contribute to the high break frequency, but whose potential for debris generation is limited. Note that this conclusion may not be valid if the insulation of interest is not metallic-jacketed.

The conditional probability for ECCS strainer blockage given a LOCA in piping less than 6 inches in diameter is close to zero. This result is due to the fact that the volume of debris generated is a direct function of the break diameter since only insulation on the broken pipe was not accounted for. However, this conclusion may not be valid for 4" - 6" diameter breaks if all the target pipes and other components

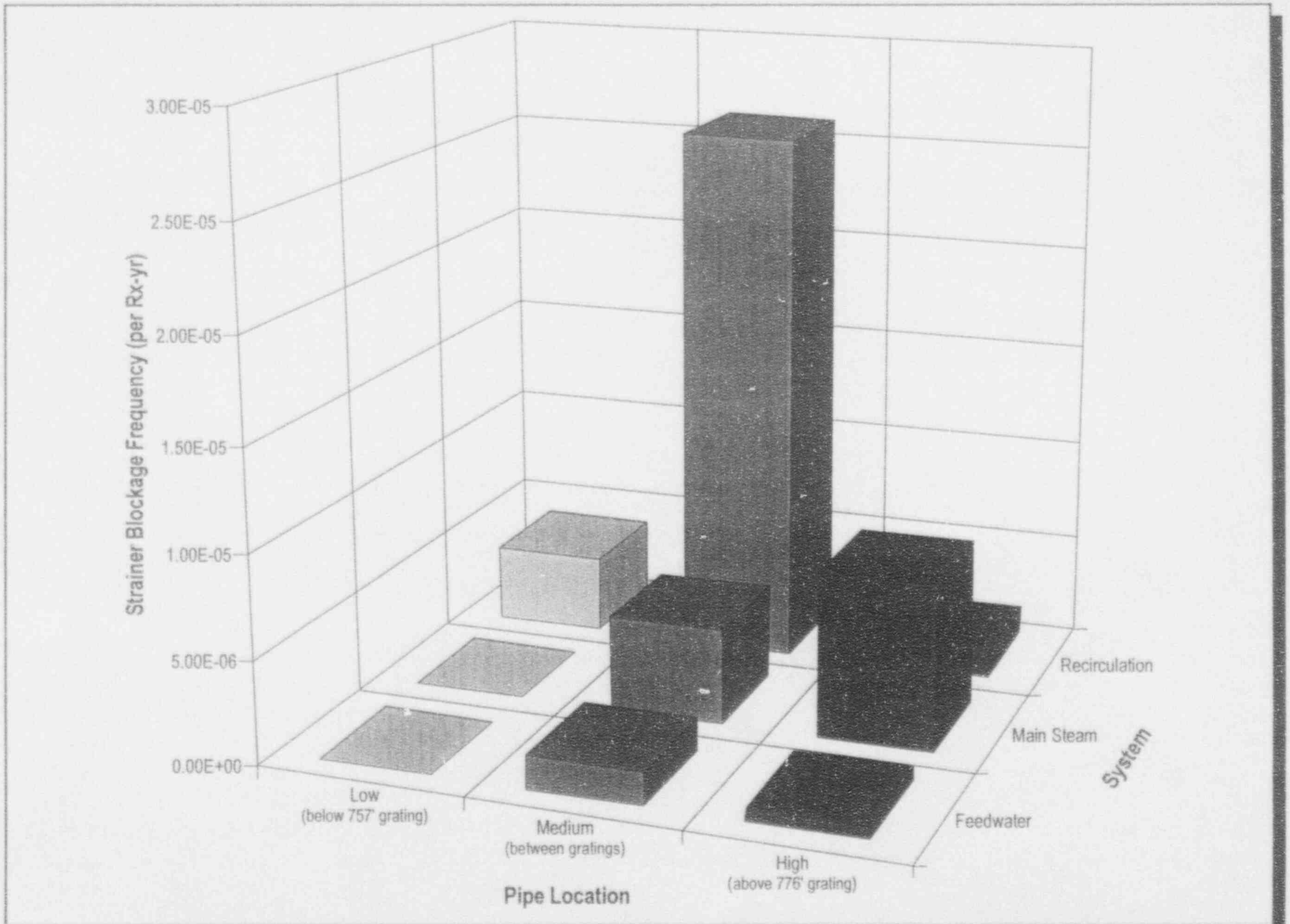

Figure A. Blockage Frequency by System and Location

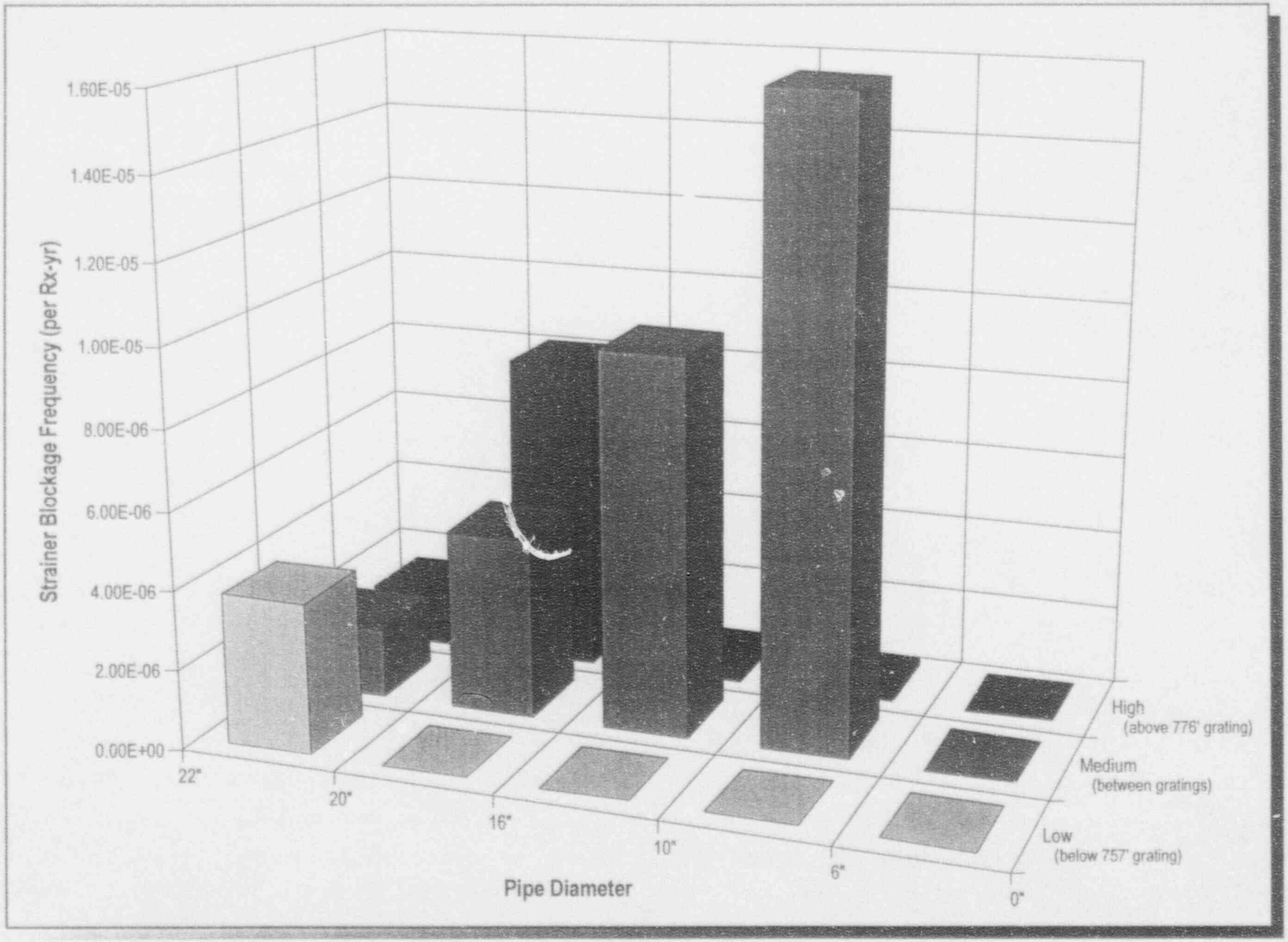

Figure B. Blockage Frequency by Diameter and Location

in the zone of influence had been included in the analysis. Conditional blockage probabilities for the main steam and feedwater breaks were 0.68 and 0.16, respectively. The relatively large main steam conditional blockage probability is due to the fact that a main steam break generates a much larger volume of debris compared to feedwater or recirculation breaks.

The present study included parametric analyses that examined the effect of variations in destruction factors, transport factors, and head-loss equations on the overall conditional probability of blockage. The analysis indicated that increasing destruction factors for Regions I, II and III from the base case values of 75%, 60% and 40% by 25% will not change the overall conditional probability for ECCS strainer blockage substantially. On the other hand, decreasing the destruction factors by 25% will reduce the conditional probability to 0.20, from the present value of 0.31. This result clearly demonstrates that the assumed base case represents a very conservative scenario. However, the results were found to be very sensitive to (a) the transport factors used to estimate the fraction of debris transported to the suppression pool as a function of break elevation, (b) the head-loss equation (used to estimate pressure - drop across the strainer due to debris accumulation), and (c) NPSH margin.

Based on the present study it is concluded that the overall ECCS strainer blockage frequency for DAEC Unit 1 due to LOCA generated insulation debris is about 4.6E-5 per Rx-year. However, the present study does not address several important issues, including time-dependent effects, the dependence of debris generation models on the type of insulation used (mineral wool vs fiber glass, and metallic-jacketed vs unjacketed), the effects of containment type and layout, the strong dependence of pressure drop across the strainer on debris material and size, and pressurization or heat-up of the suppression pool. Also, an uncertainty analysis was beyond the scope of this study. As a result, large uncertainties may be associated with the conclusions of this study and, therefore, caution should be observed in generalizing the insights gained by this study. However, the study identified important parameters and models that have the greatest influence on the study results. Also, the study provided key insights into what further refinements would most improve the our ability to predict ECCS failure due to strainer blockage from LOCA-generated debris.

1.0 BACKGROUND

Unresolved Safety Issue (USI) A-43, "Containment Emergency Sump Performance," dealt with concerns about the availability of adequate recirculation of cooling water following a loss-of-coolant accident (LOCA). One concern was the effects of LOCA-generated insulation debris that is transported to the sump debris screen, blocking the screen and reducing net positive suction head (NPSH) margin below that required for the recirculation pumps to maintain long-term cooling.

Although USI A-43 was derived principally from concerns about containment emergency sump performance in Pressurized Water Reactors (PWRs), the concern about debris blockage also applies to Boiling Water Reactors (BWRs). The BWR Residual Heat Removal (RHR) system performs the Low Pressure Coolant Injection (LPCI) function of the Emergency Core Cooling System (ECCS). In addition BWR designs incorporate a low pressure Core Spray (CS) System as part of the ECCS. The suction strainers in the suppression pool of a BWR RHR system are analogous to the PWR sump debris screen, and both BWRs and PWRs must have adequate recirculation cooling capacity to prevent core melt.

This report provides estimates of the potential for BWR ECCS strainer blockage due to LOCA-generated debris for a representative BWR using methods based on those used to analyze a PWR in NUREG-0869, Rev. 1 (Ref. 1.1). The following sections provide further background to USI A-43 and reported incidents at the Barsebäck nuclear power plant in Sweden and at the Perry nuclear power plant in the U.S. The final section describes the objectives and scope of the current efforts discussed in the remainder of the report.

1.1 Unresolved Safety Issue A-43

Emergency core cooling systems require a clean, reliable water source to maintain long-term recirculation following a LOCA. In PWRs, the containment emergency sump provides such a water supply to residual heat removal pumps and containment spray systems. BWRs rely on pump suction intakes in the suppression pool or wet well to provide water to residual heat removal and core spray systems. Successful long-term recirculation depends on the sump design for PWRs, or the suction intake design for BWRs, to provide adequate water free of debris to the RHR pumps for extended periods of time.

The primary areas of safety concern addressed in NUREG-0869, Rev. 1 (Ref. 1.1) were as follows:

- post-LOCA hydraulic effects (i.e., air ingestion potential)
- generation of insulation debris as a result of a LOCA, with subsequent transport of the debris to PWR sump screens (or BWR suppression pool strainers) and blockage thereof
- the combined effects of the above two items on the required recirculation pumping capacity (i.e., impact of NPSH on the recirculation pumps).

NPSH requirements, operational verification, and sump design requirements have been evolving and were addressed in the following NRC Regulatory Guides (RGs):

R.G. 1.1	Net Positive Suction Head for Emergency Core Cooling and Containment Heat Removal Systems Pumps, 1970 (Ref. 1.2)
R.G. 1.79, Rev. 1	Preoperational Testing of Emergency Core Cooling Systems for PWRs, 1975, (Ref. 1.3)
R.G. 1.82, Rev. 1	Sumps for Emergency Cooling and Containment Sprays Systems, 1985 (Ref. 1.4)

Concerns of the NRC Staff regarding emergency sump performance evolved over time. In-plant tests were initially called for in RG 1.79, Rev. 1 (Ref. 1.3), followed by a transition to containment and PWR sump model tests in the mid-1970s. Considerable emphasis was placed on adequate sump hydraulic performance, with vortex formation as the key determinant. Formation of an air-core vortex may result in unacceptable levels of air ingestion and lead to severely degraded pump performance. Another concern involved sump damage or blockage of the flow as a result of insulation debris generated by LOCAs, missiles, and break jet loads. These concerns led to the formulation of some of the guidelines set forth in RG 1.82, Rev. 1 (Ref. 1.4), including those relating to cover plates, debris screens, and a 50% blockage criterion.

In 1979, the NRC designated the issue of safe operation of ECCS sumps as Unresolved Safety Issue (USI) A-43, Containment Emergency Sump Performance. To assist in the resolution of this issue, the Department of Energy funded construction of a full-scale sump hydraulic test facility at the Alden Research Laboratory (ARL) of Worcester Polytechnic Institute (WPI). In addition, an NRC Task Action Plan (TAP) A-43 was developed to address all aspects of this issue. Potential debris effects were investigated through plant insulation surveys, sample plant calculations, and supplemental experiments conducted at ARL to determine the transport characteristics of various types of insulation debris and attendant screen blockage head losses.

Several of the technical findings reported in NUREG-0869, Rev. 1 (Ref 1.1) relate to LOCA-generated debris. Surveys of plant insulation materials showed a wide variability in the types and quantities of insulation employed in nuclear power plants. Also, changes made in operating plants have changed the types and quantities of insulation. Therefore, debris blockage assessments become very plant specific and time dependent.

Estimating the effects of debris blockage requires an estimation of 1) the quantity of debris that might be generated by a LOCA, 2) the transport of such insulation debris to the PWR sump screen or BWR suppression pool strainer, and 3) the potential blockage as a result of flow entrainment of debris to the screen or strainer surface. According to plant-specific studies, debris effects are strongly dependent on PWR sump and BWR suction intake design features and on plant layout, which affects migration of debris.

Blowdown experiments performed using HDR Test-Facility have demonstrated the destructive power of a LOCA jet, particularly regarding the destruction of fibrous insulation materials. Because finely shredded insulation can be transported at low recirculation flow velocities and distributed uniformly over debris screens or suction strainers, NUREG-0869, Rev. 1 (Ref 1.1) recommends strong consideration of such insulation in estimating the effects of post-LOCA blockage on pump NPSH margin. Experiments also showed that reflective metallic insulation can suffer severe damage from LOCA jets, and that fragments or pieces of thin foils can be transported at velocities as low as 0.2 to 0.4 ft/sec.

Sample plant analyses and experiments demonstrated that the uniform 50% blockage criterion in the first version of RG 1.82 (Rev. 0) was not adequate. Sump screen or suppression pool strainer blockage should be evaluated on a plant-specific basis, based on the insulation materials employed, and a plant-specific assessment of potential debris transport and debris screen blockage should be performed. RG 1.82 was revised accordingly and issued as RG 1.82, Rev. 1 (Ref. 1.4) in 1985.

Finally, methods for estimation of debris generation and transport developed in NUREG/CR-2791 (Ref. 1.5) are superseded by those outlined in NUREG-0869, Rev. 1 (Ref. 1.1). Certain assumptions in NUREG/CR-2791 (Ref. 1.5) were not supported by more recent evaluations.

For the resolution of USI A-43 (Ref. 1.1), the NRC Staff evaluated the loss of post-LOCA recirculation capability due to debris generation, focusing primarily on PWRs. The NRC Staff also performed a value-impact analysis and concluded that backfit action could not be justified. The blockage probabilities for PWRs were calculated on the basis of a detailed analysis contained in NUREG/CR-3394 (Ref. 1.6). As is briefly described in NUREG-0869, Rev. 1 (Ref. 1.1), the NRC also made estimates of BWR blockage probabilities. Although the estimates for BWR blockage probabilities were somewhat lower than the calculated values for PWRs, the plant types with the largest potential for net averted exposure per reactor were BWRs with Mark I and Mark II containments. It is important to recognize, however, that these BWR blockage probability estimates were made without the benefit of a detailed analysis.

1.2 Summary of the Perry and Barsebäck Events

As described in a Licensee Event Report (Ref. 1.7) and NRC Information Notice 93-34 (Ref. 1.8), the Perry nuclear power plant recently experienced problems with fouling of RHR pump strainers. During a refueling outage in May 1992, a video camera inspection of the suppression pool revealed various foreign objects on the pool floor. In addition, accumulations of dirt and debris were seen on the suction strainers for RHR pumps A and B. While inspection personnel noted the RHR strainer fouling, the system operability was not questioned because all required surveillance activities had been successfully completed.

During a subsequent maintenance outage in January 1993, the licensee cleaned and inspected the strainers. The RHR A and B strainers were found to be deformed. Specifically, the region of the strainer surface located between the internal stiffeners was partially collapsed inward along the direction of flow. The licensee determined that strainer fouling during pump operation had caused the strainer deformation.

In March of 1993, an unexpected shutdown occurred at Perry that involved use of the RHR A and B pumps in the suppression pool cooling mode. The A pump was operated for a total of 2 hours with suppression pool suction, while the B pump was operated for 7 hours with suppression pool suction. During a subsequent inspection in April of 1993, the RHR pump B strainer was found to be fouled and deformed in the same manner as was observed during the January maintenance outage. However, the remaining ECCS strainers displayed no signs of fouling. An operability test was run on the RHR B pump with the strainer in its undisturbed condition. This test was terminated after 10 hours when the pump suction pressure dropped from the initial reading at pump start of 6.4 psig to 0.0 psig. A second test was conducted on the same RHR loop with improved instrumentation. During this additional test, the pump suction pressure dropped to 0.0 psig after 18 hours. The pump was allowed to run for an additional 8 hours during which no further decrease in pump suction pressure was observed. In both of the tests, there was no observed change in the system flow rates or pump motor amperage. An engineering evaluation by the licensee determined that excessive strainer differential pressures could have adversely affected cooling during and following 100 days of post-LOCA operation.

In conjunction with an analysis of the Perry plant suppression pool debris, video tapes of the RHR strainers taken in during 1992 and 1993 were reviewed. These tapes showed the presence of debris and corrosion products that were attached or entangled in fibrous materials. From samples of the debris, it was determined that glass fiber used in the Drywell Air Cooler System was the predominant fibrous material. From other evidence, it was concluded that the fibrous material entered the suppression pool in the form of intact pieces as opposed to individual fibers.

In July 1992, a strainer plugging incident also occurred at the Barsebäck-2 BWR in Sweden. As described in a news release (Ref. 1.9), this incident occurred as the unit was being re-started following an annual refueling outage. During the re-start activities, steam was released into the containment from a relief valve that had been inadvertently been left open. The release of steam dislodged mineral wool insulation used on adjacent piping. Pieces of this dislodged insulation material were subsequently transported by steam and water into the wetwell located at the bottom of containment. Within one hour, the mineral wool material had clogged the ECCS inlet strainers. This type of strainer clogging had previously been considered as a possibility, but it was believed that ten hours would have to elapse before clogging would take place. A ten hour delay in clogging would allow operating personnel time to remove the strainer clogging by manually reversing flow through the strainers. Such a flow reversal activity would interrupt ECCS flow for 5-10 minutes, but this interruption would be acceptable after ten hours following reactor shutdown because of the large decrease in decay heat levels. As stated in Ref. 1.9, subsequent calculations based on the Barsebäck incident indicated that clogging of the strainers could occur in less than 30 minutes. At 30 minutes after reactor shutdown from operation, the decay heat levels would not allow interruption of ECCS flow to correct strainer clogging.

1.3 Objectives and Scope

The Perry and Barsebäck incidents highlight the importance of evaluating BWR suppression pool performance following a loss of coolant accident. In response, the NRC Staff initiated a study to estimate the potential for loss of low pressure coolant injection capability in BWRs due to LOCA-generated debris blockage. This report provides preliminary estimates of the frequency of loss of LPCI/RHR/CS in a reference BWR using analysis method similar to those reported in NUREG-0869, Rev. 1 (Ref. 1.1). The scope of the methodology is limited, i.e., ECCS strainer blockage frequencies were obtained for a single reference BWR plant with steel jacketed NUKON™ insulation. Additionally, only limited parametric analyses were carried out. Therefore, the results documented in this report are point-estimates in nature and may not be applicable to other BWRs. Future efforts are anticipated to address some of these limitations.

References for Section 1

1.1 A. W. Serkiz, "USI A-43 Regulatory Analysis," US Nuclear Regulatory Commission, NUREG-0869, Rev. 1, October 1985.

1.2 USNRC, "Net Positive Suction Head for Emergency Cooling and Containment Heat Removal System Pumps (Safety Guide 1)," Regulatory Guide 1.1, November 1970.

1.3 USNRC, "Preoperational Testing of Emergency Core Cooling Systems for Pressurized Water Reactors," Regulatory Guide 1.79, Revision 1, September 1975.

1.4 USNRC, "Water Sources for Long-Term Recirculation Cooling Following a Loss-of-Coolant Accident," Regulatory Guide 1.82, Revision 1, November 1985.

1.5 J. Wysocki and R. Kolbe, "Methodology for Evaluation of Insulation Debris Effects: Containment Emergency Sump Performance, Unresolved Safety Issue A-43," Burns and Roe, Inc., published as Sandia National Laboratories Report No. SAND82-7067, NUREG/CR-2791, Sept. 1982.

1.6 J. J. Wysocki, "Probabilistic Assessment of Recirculation Sump Blockage Due to Loss of Coolant Accidents, Containment Emergency Sump Performance USI A-43," Vols. 1 and 2, Burns & Roe, Inc., published as Sandia National Laboratories Report No. SAND83-7116, NUREG/CR-3394, July 1983.

1.7 Perry Nuclear Power Plant, "Excessive Strainer Differential Pressure Across the RHR Suction Strainer Could Have Compromised Long-Term Cooling During Post-LOCA Operation," Licensee Event Report 93-011, Docket 50-440, May 19, 1993.

1.8 USNRC, "Potential for Loss of Emergency Cooling Function Due to a Combination of Operational and Post-LOCA Debris in Containment," NRC Information Notice 93-34, April 26, 1993.

1.9 European Nuclear Society Nuclear News Network, "Swedish N-Utilities Explain BWR Emergency Core Cooling Problem," News No. 358/92, September 18, 1992.

2.0 METHODOLOGY FOR ANALYSIS OF INSULATION DEBRIS EFFECTS

2.1 Overall Methodology

The methodology used for estimating the potential for BWR ECCS strainer blockage due to insulation debris is very similar to that used previously in USI A-43 study for PWRs; the minor differences pertain mainly to its adaptation to BWR systems and improved understanding of the problem. Figure 2-1 illustrates the present methodology. Important elements of the present methodology can be summarized as follows:

- Selection of a reference BWR for analysis;
- Analysis of initiating events, i.e. location and probability of primary breaks;
- Parametric analysis of debris generation and transport to the suppression pool;
- Calculation of pressure drop across the strainer due to debris accumulation;
- Estimation of probability for loss of ECCS due to inadequate NPSH.

Figure 2-1 also lists section numbers of this report where each element of this methodology is discussed in detail and results of the pertinent analyses are presented. In documenting these analyses and results, a minimal degree of prior knowledge concerning pipe break analysis, jet impingement effects, general nature of boiling water reactor (BWR) operation, and critical safety system operation is assumed. In addition, minimal familiarity with previous USI A-43 analyses and their results was assumed. Readers unfamiliar with these aspects are referred to previous pertinent reports, for example NUREG-0869, Rev. 1 (Ref 2.1), NUREG-0897, Rev. 1 (Ref. 2.2), and NUREG/CR-5460 (Ref. 2 3).

2.2 Reference BWR Selection Considerations

Duane Arnold Energy Center (DAEC) - Unit 1 was selected as the reference BWR for use in this study to estimate pipe break frequencies and attendant debris generation and transport in a manner similar to the PWR analysis reported in Appendix D of NUREG-0869, Rev. 1 (Ref. 2.1). DAEC-Unit 1 is a General Electric BWR/4 with a Mark I containment. Per design, this unit has a relatively small suppression pool and large strainer flow velocities, especially in comparison to BWRs with MARK II and MARK III containments. Also, more than 99% of the primary piping in this unit is insulated by fibrous insulation, which maximizes the volume of fibrous debris generated following a LOCA. Thus, selection of DAEC-Unit 1 as the reference BWR is expected to provide a somewhat conservative upper bound for conditional blockage probability.

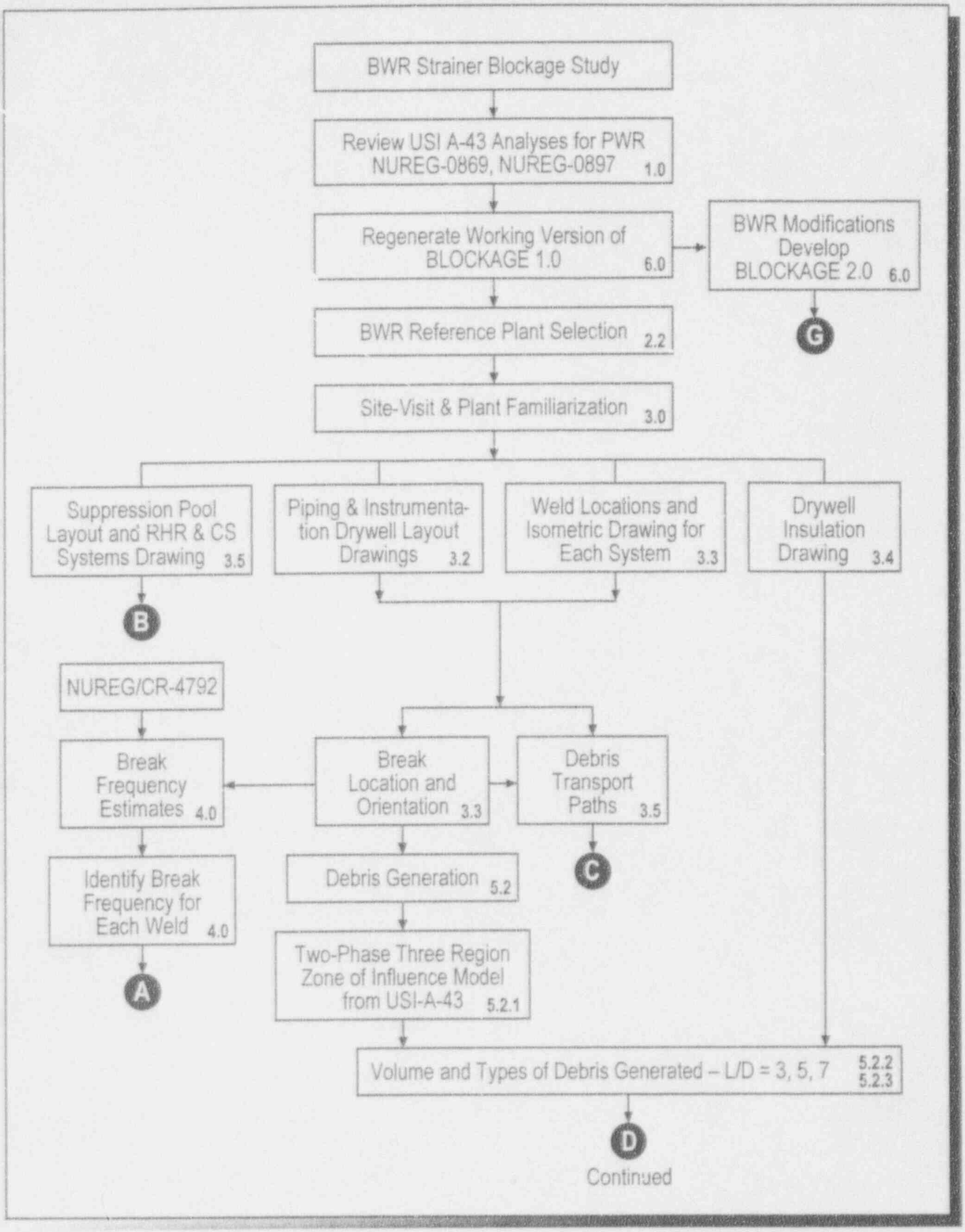

Figure 2-1. Overall Methodology Used for Estimating Potential for BWR ECCS Blockage Due to LOCA Generated Debris

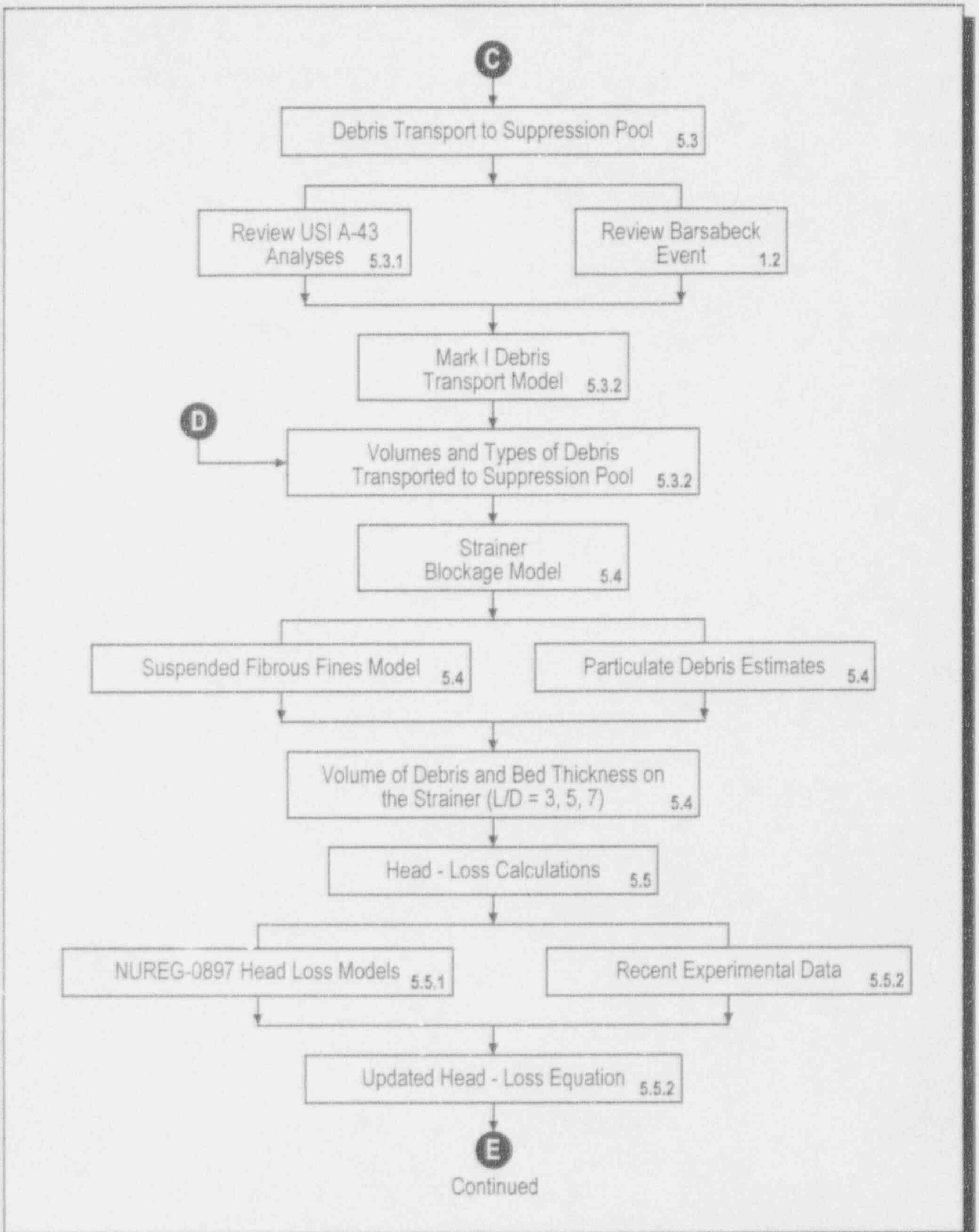

Figure 2-1. Overall Methodology Used for Estimating Potential for BWR ECCS Blockage Due to LOCA Generated Debris (Continued)

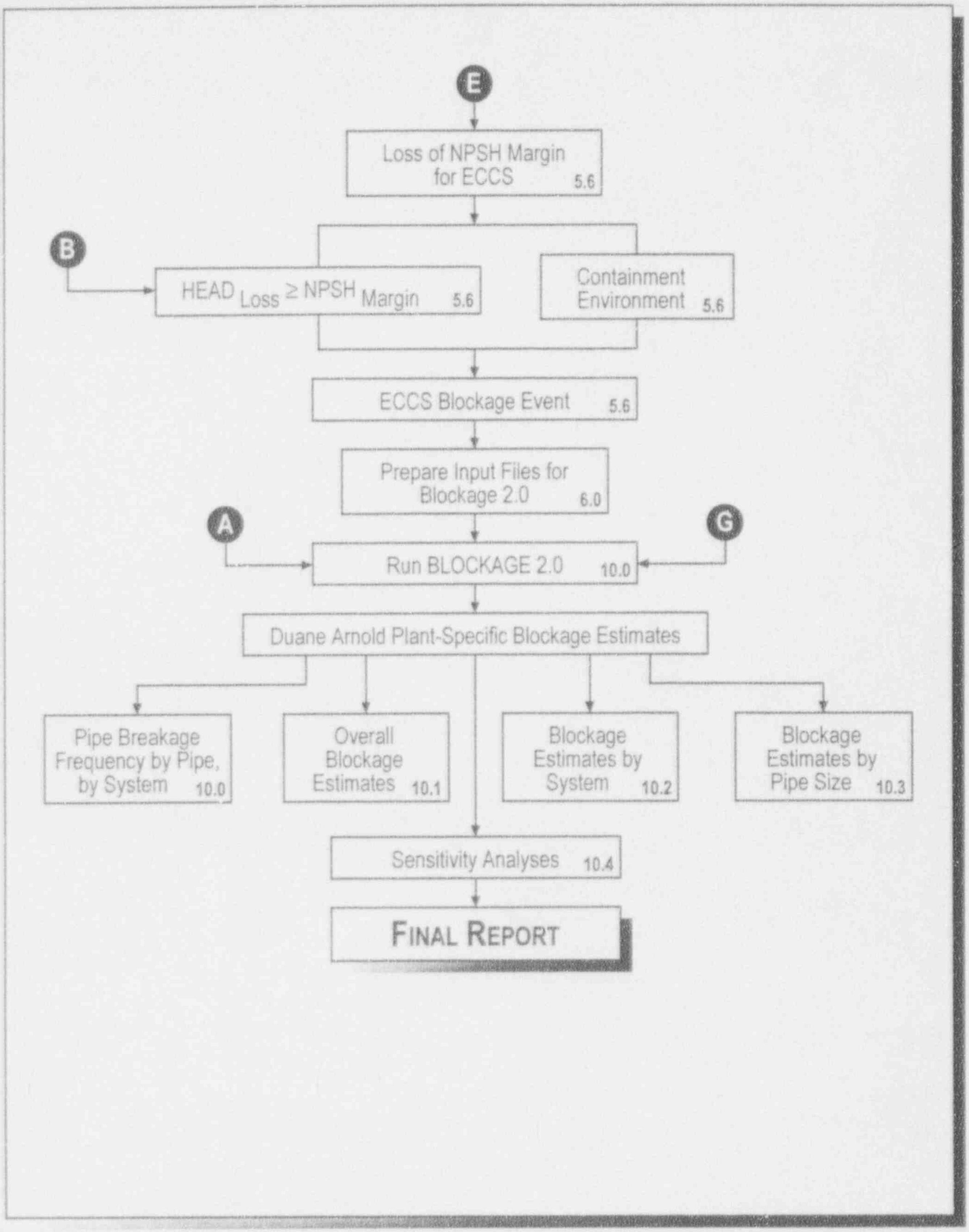

Figure 2-1. Overall Methodology Used for Estimating Potential for BWR ECCS Blockage Due to LOCA Generated Debris (Continued)

During the reference plant selection process questions were raised regarding applicability of DAEC-Unit 1 results to other BWR plants. The discussions regarding generic applicability ranged from the variability of piping layouts in the drywell, differences in Mark I, II and III containment designs, to the RHR intake strainer design, location in the suppression pool and RHR/HPCI flow rates and suppression pool flow velocities. In the present analysis some of these issues were addressed by performing sensitivity analyses that will envelop plants with different piping configurations, transport properties, and strainer sizes. An existing NRC survey of US BWR plants (Ref. 2.4), performed by the NRC/NRR staff, was used to set bounds for the limited parametric variation performed in this study.

2.3 Pipe Break Frequency Considerations

Break location(s) and insulation(s) targeted by the break jet are the key factors in estimating debris generation. NUREG-0897, Rev. 1 (Ref. 2.2) provided key insights on break evaluation for a reference PWR (Salem Unit 1). A similar break evaluation analysis was performed for the reference plant. This analysis identified all the welds in the piping subjected to high pressure during regular operation. Based on this analysis, it was concluded that debris generation in BWRs is dominated by breaks postulated in BWR feed water and recirculation system piping and postulated breaks in BWR main steam lines (MSLs). This analysis focused on estimating the pipe break frequency for the reference BWR in a manner similar to that presented in NUREG/CR-3394 (Ref. 2.5) and Volume 1 of NUREG/CR-4792 (Ref 2.6). Section 4.0 briefly describes the methodology used to estimate pipe break frequencies for various primary system pipes. Appendix A provides further detail insights on the derivation of the break frequencies.

2.4 Debris Generation Considerations

Jet impingement forces are the dominant insulation debris generator following a LOCA. Other contributors, such as pipe whip and pipe impact, have been studied and shown to be of secondary importance. Pertinent details are given in NUREG/CR-2791 (Ref. 2.7). Previous studies, summarized in NUREG-0897, Rev. 1 (Ref. 2.1), clearly demonstrated that the volume of debris generated by jet impingement is strongly influenced by the type of insulation and whether or not it is jacketed. Since DAEC-Unit 1 employs metallic-jacketed NUKON™, present calculations made use of key insights relevant to this type of insulation. However, the methodology developed for this study is sufficiently flexible to be extended to other types of insulation.

A three-region two-phase jet expansion model, described in NUREG-0869, Revision 1, Appendix D (Ref. 2.1) and NUREG-0897, Revision 1 (Ref. 2.2), was used to define a zone of influence over which the insulation will be destroyed and dislodged from the surrounding pipes[4]. Also, presented in that

[4] Refer to Section 3.3.3 and 3.3.4, and Figures 3.26 and 3.27 of NUREG-0897, Revision 1 (Ref. 2.2).

report were the variation of debris sizes and relative quantities of debris generated in the three regions. This study adapted the same model for BWRs, although it was slightly modified to account for the lower operating pressure of BWRs (80 vs 150 bars). However, the zone of influence was assumed to extend from the location of the break to a distance of 7 times the pipe diameter (i.e., L/D = 7) in the shape of a right-angle cone. Initial studies were performed with a rather conservative assumption that all the insulation within this zone of influence is dislodged; i.e., debris volume was set equal to the available insulation volume in this zone. This study, however, opted to vary the fraction of debris that would be dislodged from the pipes for each region: 3 L/D, 5 L/D and 7 L/D. Section 5.2 provides further insights on debris generation.

2.5 Debris Transport Considerations

Debris transport from the drywell, where it is generated, to the suppression pool and subsequently to the strainer is strongly influenced by factors such as tortuosity of the channels available for transport, flow velocities and debris sizes. It has been known that in BWRs separation of the drywell and wetwell tends to inhibit insulation debris transport compared to an equivalent PWR. At Barsebäck[5] only about 50% of the debris generated in the drywell was reported to have reached the suppression pool. The remaining debris was found to have been retained by the intervening containment structures. In other BWRs, the fraction of transported debris may be lower or higher, depending on the containment type[6], location of the break, and type and size of debris produced. This study opted to assign a transport factor to each of three elevations inside the drywell. Section 5.3 provides further insights on debris transport within the drywell.

Recirculation patterns in the suppression pool represent another phenomenon of significance pertinent to debris transport to the strainer. In a non-LOCA situation, suppression pool flow patterns are established by RHR/CS pump flows and make-up flow from the dry-well. In this case two- or three-dimensional potential flow equations can be solved to determine recirculation patterns within the suppression pool. According to such calculations, in a typical non-LOCA scenario, global suppression pool velocities (far field velocities with respect to the strainer) would be low ($\leq$ 0.2 ft/sec) and will result in:

1. sedimentation of a large fraction of the debris on the suppression pool floor, and
2. no further disintegration of the debris.

---

[5] The Barsebäck plant is similar to a BWR/4 with Mark II containment. However, unlike many US Mark II plants, downcomers in Barsebäck are flush with the drywell floor.

[6] Our review of various containments revealed that this fraction may vary for individual containments due to unique lay-outs.

Such assumptions, however, can not be justified following a LOCA event because suppression pool patterns following LOCA events are known to be dominated by thermal-hydraulic instabilities, ranging from swirling to chugging, introduced by steam condensing and intermixing of hot and cold liquids. Suspension and further disintegration of the debris when subjected to these flow instabilities is a complex phenomenon, and its modeling is beyond the scope of the present analysis[7]. Instead, the present analysis assumed that all of the fines (i.e., fiber-size debris and shreds) will remain suspended in the suppression pool for prolonged periods of time and will be deposited on the strainer as a function of the concentration in the flow. The remaining large pieces were assumed to have undergone further shredding and ultimately reach the strainer similar to the fines. This approach is expected to provide a conservative prediction for debris cake thickness.

2.6 Strainer Blockage Considerations

Accumulation of fibrous debris on the strainer will result in head-loss and may lead to loss of NPSH margin. NUREG-0897, Rev. 1 (Ref. 2.2) suggested usage of experimental correlations to predict head-loss across the strainer as a function of strainer flow velocity and thickness of the debris bed. However, such a simple model may not be able to address various factors that strongly influence head loss characteristics, which include:

1. *Uniform vs. non-uniform deposition*: Non-uniform distribution of debris on the screen will result in partial blockage of the strainers. Preliminary analyses revealed that the worst-case scenario is represented by uniform deposition of the debris on the strainer. This also represents most credible means of deposition in the initial stages when strainer blockage is expected to be dominated by fines.

2. *Insulation material type*: A survey of US BWR plants (Ref. 2.4) revealed that fibrous insulation used consists mostly of mineral wool, high density fiber glass or low density NUKON™. Previous experiments reported in NUREG/CR-2982, Rev. 1 (Ref. 2.8) and NUREG-0897, Rev. (Ref. 2.2) clearly demonstrated strong dependence of head-loss on the insulation material type.

3. *Particulate debris*: It is expected that presence of particulate debris in the suppression pool will result in their filtration and retention by the filter-bed formed on the strainer due to fibrous debris accumulation. These particulates, consisting mostly of flakes of rust, paint

[7] It is not clear that extensive modeling will actually reduce uncertainties in their prediction of the fraction of debris transported to the strainer.

or crushed mirror type insulation, may be already present in the suppression pool or swept into the pool along with the fibrous insulation debris. Clearly, retention of particulates by the debris bed will contribute to higher pressure drop across the filter.

The present analysis addressed these three concerns through a combination of hydraulics modeling and parametric variations. The hydraulics modeling focused on deriving applicable head-loss equations for each material, based on up-to-date experimental data, as a function of bed-porosity, flow velocity and bed thickness. A parametric analysis was performed to account for 'filter-cake' effects introduced by particulate filtration by the bed.

2.7 Pump Performance Considerations

For the DAEC-Unit 1 plant-specific analysis, RHR/CS pump performance under adverse conditions was analyzed as described in section 3.2 of NUREG-0897, Rev. 1 (Ref. 2.2); ECCS failure was assumed when head-loss due to strainer plugging was estimated to be larger than NPSH margin per design. Implicitly, the present analysis does not account for pressurization of the suppression pool during blowdown phase or reduction in available NPSH due to increase of pool water temperature. These concerns may be addressed in the future analyses.

2.8 BLOCKAGE 2.0 Overview

USI A-43 study used two main-frame computer codes, PRA and TABLE, to perform strainer blockage frequency calculations for PWRs. These exact functions of PRA and TABLE were reproduced by BLOCKAGE 1.0, which is a PC-based software developed as part of this study. BLOCKAGE 2.0 was then obtained by modifying BLOCKAGE 1.0 to accommodate special characteristics of a representative BWR. The code calculates the frequency, per reactor-yr, of a sequence involving a LOCA followed by inadequate NPSH in the recirculation cooling system due to insulation debris generated by the LOCA.

The user provides the following inputs to BLOCKAGE 2.0:

1. A list of location and size welds whose failure can initiate a LOCA,
2. Weld break frequency for each weld,
3. A list of number, diameter and length of target pipes influenced by each weld,
4. Type and thickness of insulation on each target pipe, and
5. Other parametric input such as strainer area, ECCS flow rate, and head loss equation.

BLOCKAGE 2.0 then follows each weld and determines whether or not it results in a ECCS strainer blockage event. Chapter 5.0 describes various equations used by BLOCKAGE 2.0 to evaluate potential blockage. After completing the analysis BLOCKAGE 2.0 generates six output report files:

- Weld summary report
- Target summary report
- Sequence frequencies reports
- Unavailabilities reports
- Summary reports
- Error messages.

A complete description of input files and their format is presented in Section 6.0.

References for Section 2

2.1 A. W. Serkiz, "USI A-43 Regulatory Analysis," US Nuclear Regulatory Commission, NUREG-0869, Rev. 1, October 1985.

2.2 A. W. Serkiz, "Containment Emergency Sump Performance," US Nuclear Regulatory Commission, NUREG-0897, Rev. 1, October 1985.

2.3 P. Lobner et al., "Overview and Comparison of U. S. Commercial Nuclear Power Plants," published as Science Applications International Corporation Report No. SAIC-89/1541, NUREG/CR-5640, September 1990.

2.4 A. W. Serkiz, Meeting Minutes, "Meeting to Discuss Potential for Loss of ECCS in BWRs Due to LOCA Generated Debris," Sept. 21, 1993.

2.5 J. J. Wysocki, "Probabilistic Assessment of Recirculation Sump Blockage Due to Loss of Coolant Accidents, Containment Emergency Sump Performance USI A-43," Vols. 1 and 2, NUREG/CR-3394, July 1983.

2.6 C. S. Holman and C. K. Chou, "Probability of Failure in BWR Reactor Coolant Piping," published as Lawrence Livermore National Laboratory Report UCID-20914, NUREG/CR-4792, March 1989.

2.7 J. Wysocki and R. Kolbe, "Methodology for Evaluation of Insulation Debris Effects," Burns and Roe, Inc., published as Sandia National Laboratories Report No. SAND82-7067, NUREG/CR-2791, September 1982.

2.8 D. N. Brocard, "Buoyancy, Transport, and Head Loss of Fibrous Reactor Insulation," Alden Research Laboratory, published as Sandia National Laboratories report No. SAND82-7205, Rev. 1, NUREG/CR-2982, Rev. 1, July 1983.

2.9 USNRC, "Water Sources for Long-Term Recirculation Cooling Following a Loss-of-Coolant Accident," Regulatory Guide 1.82, Rev. 1, November 1985.

3.0 REFERENCE BWR PLANT DATA

3.1. Introduction

The DAEC-Unit 1 was selected as the reference plant. This unit is a BWR/4 with a Mark I containment. Important characteristics of this plant include: (a) the plant is equipped with one of the smallest ECCS strainers resulting in one of the highest strainer flow velocities; (b) almost 100% of the primary piping in the drywell is insulated using NUKON™, which is a low density fiber glass material; and (c) recirculation loops are constructed of 304SS which is susceptible to corrosion cracking. Thus, estimation of ECCS strainer blockage frequency for DAEC-Unit 1 was expected to provide a conservative upper bound.

The following sections describe the data development process used for DAEC-Unit 1. The data described below were obtained from: (a) a plant visit and discussion with the systems engineers, (b) Piping and Instrumentation Drawings (P&IDs) of the drywell, (c) isometric drawings of the individual systems, (d) NUKON™ blanket insulation installment drawings for each system, (e) a suppression chamber penetration schematic, and (f) plant engineering calculations. The information presented below has been provided by the utility as being the most recent, and it has been confirmed at different stages through follow-up discussions with the plant systems engineers.

3.2 Piping Layout in the Drywell

Figure 3-1 is a pictorial description of the primary systems piping layout in the reference plant drywell. These piping net-works include: (a) recirculation lines, (b) main steam lines, (c) feedwater lines, (d) residual heat removal (RHR) injection lines, (e) high pressure core injection (HPCI) lines, (f) core spray (CS) lines, (g) reactor core isolation cooling (RCIC) line, (h) reactor water cleanup system (RWCU) piping, and (i) safety relief valve (SRV) drain pipes. All the pipes, except for the RCIC line, RWCU pipe, SRV drain pipes and recirculation drain lines, are insulated using 304SS jacketed NUKON™ insulating material. The RCIC and RWCU lines are insulated with calcium silicate material. The SRV drain pipes are not insulated, and hence, were eliminated from further analysis.

Insulation mats on all primary system piping can be blown off if subjected to energetic jets; thus, all these pipes qualify as targets. However, energetic jets capable of debris generation occur primarily for breaks postulated in the recirculation and feedwater piping and those occurring in main steam lines. A total of 300 possible break locations were identified in these three loops combined.

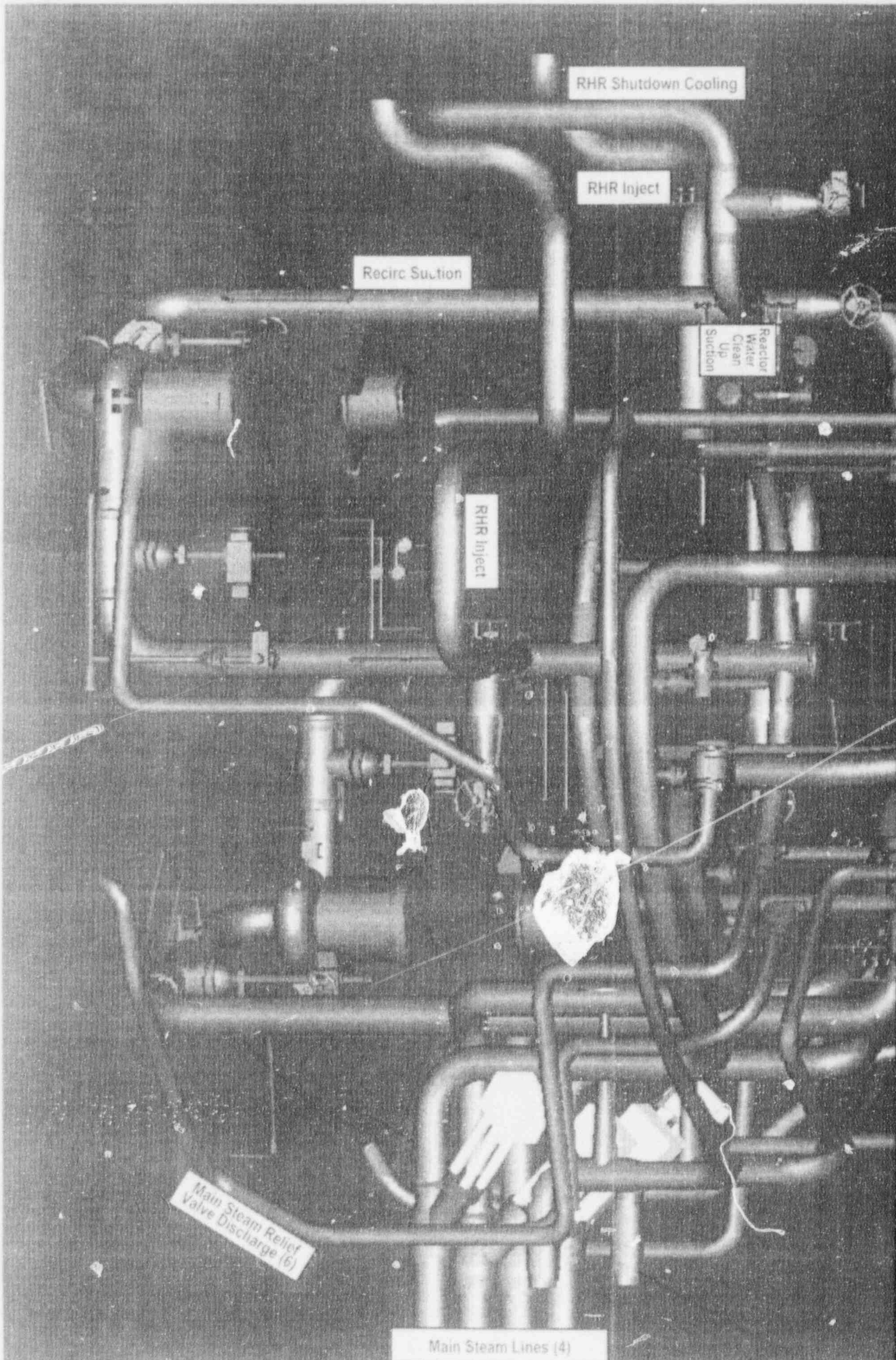
RHR Shutdown Cooling
RHR Inject
Recirc Suction
Reactor Water Clean Up Suction
RHR Inject
Main Steam Relief Valve Discharge (6)
Main Steam Lines (4)

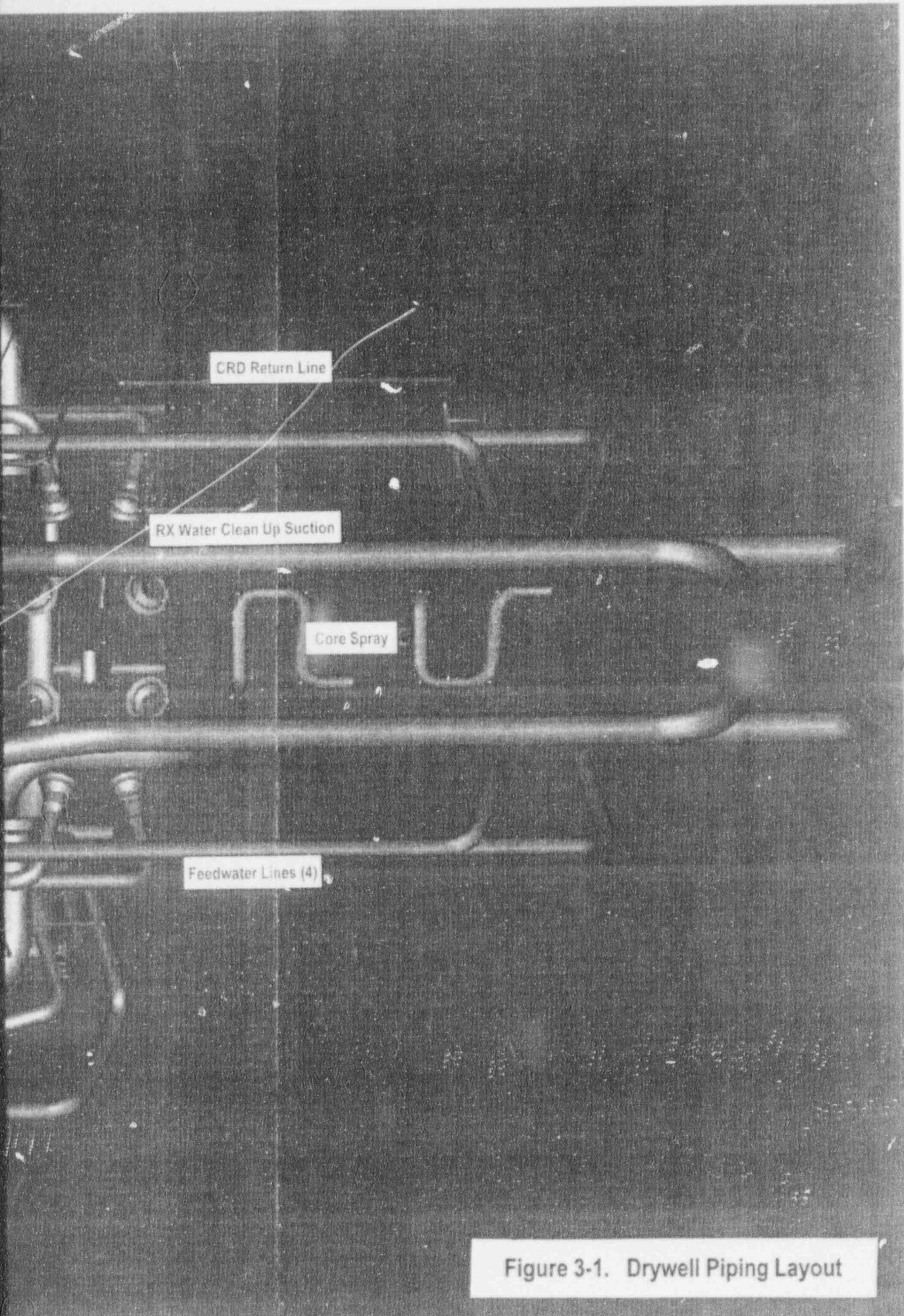

Figure 3-1. Drywell Piping Layout

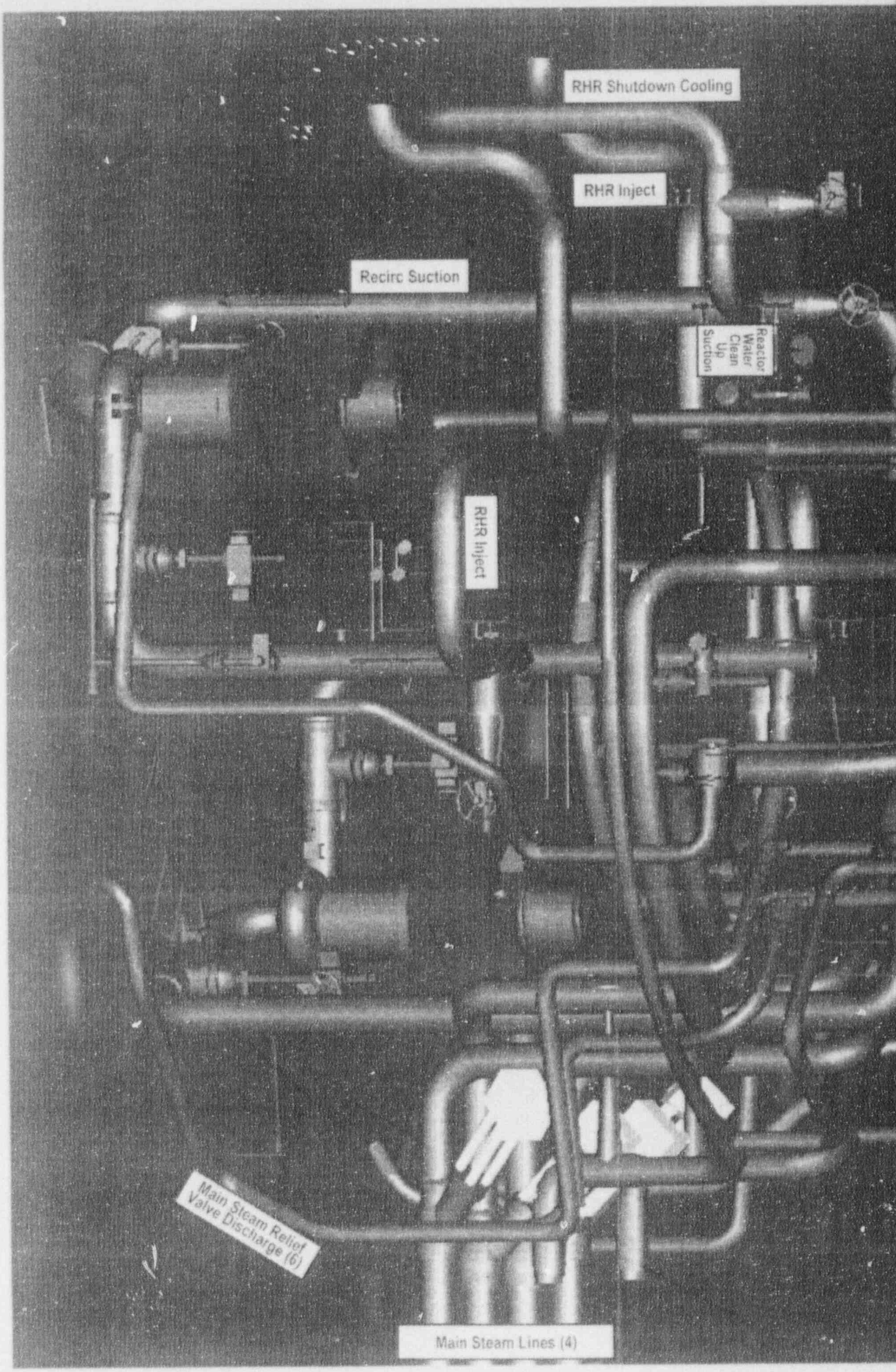

RHR Shutdown Cooling
RHR Inject
Recirc Suction
Reactor Water Clean Up Suction
RHR Inject
Main Steam Relief Valve Discharge (6)
Main Steam Lines (4)

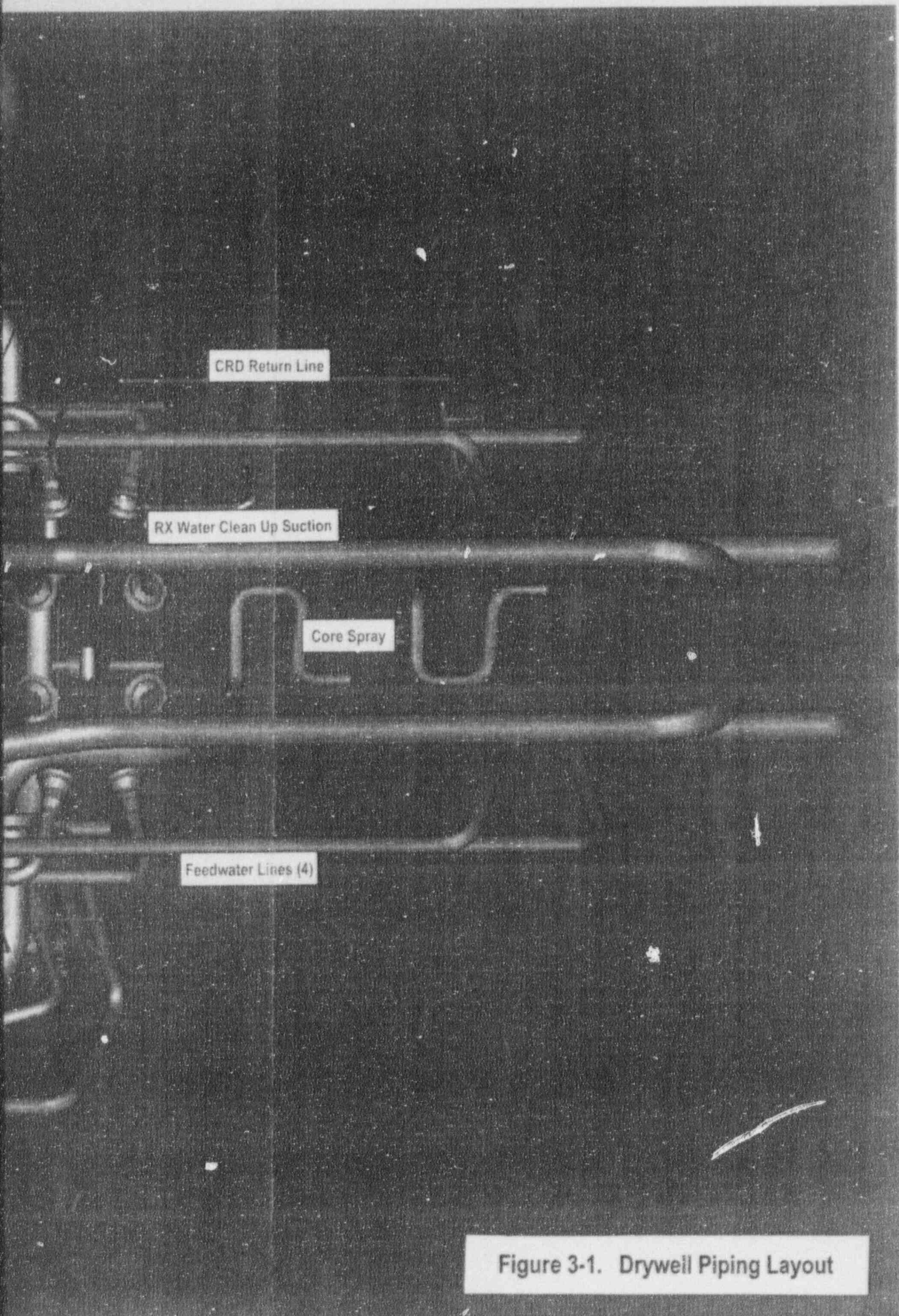

Figure 3-1. Drywell Piping Layout

9402100230-01

An additional 20 welds[8] were identified in the pressurized portions (upstream of isolation valves closed during normal operation) of the remaining systems piping (HPCI, RHR, and CS). A description of the weld locations in HPCI, RHR, and CS systems piping are provided below:

1. *HPCI Lines*: The HPCI system is designed to flood the core from the top of the core. The HPCI system is actuated on a Level 2 signal and commences operation within 30 seconds and starts injection into MSL-Loop B through a 10" line (10"-DBA-B). During normal operation most of this line is not pressurized and the HPCI pump is turned off. The only segment of HPCI exposed to high pressure conditions during normal operation is the piping downstream of motor operated isolation valve MO-2238. This segment is less than 3 ft in length and has three circumferential welds (J1, J4 and J6) and three 1" T-welds[9] (J2, J3 and J5). These six welds were not modeled.

2. *RHR Injection Lines:* The RHR system is designed to provide adequate coolant injection to the core for a large break LOCA. This system receives an actuation signal on Level 1 and injects into the core through the recirculation lines, approximately 30-50 seconds into an accident. During normal operation the RHR piping is not pressurized and is isolated from the recirculation piping by motor operated valves ZS-1907 and ZS-2008 and check valves V19-0149 and V20-0082. The total segment of RHR injection lines subjected to high pressure during normal operation is approximately 5 ft (i.e., loops A and B together). The total number of welds subjected to high pressure is six. As with HPCI, these six welds were not modeled.

3. *Core Spray Lines:* CS system piping (Loops A and B) enters the drywell at elevation 800' and injects directly into the core at approximately 811'-6". During normal operation the CS is isolated from the core by motor operated valves ZS-2142 and ZS-2143, and check valves V21-0072 and V21-0073. The total length of high pressure piping per loop downstream of the motor operated valves is less than 2 ft, and it has one circumferential weld (J6) and one 1" T-weld (J5). These two welds were not modeled.

---

[8] Welds in RWCU and RCIC are not included in this analysis since they are insulated using calcium silicate.

[9] 1" T-welds are instrumentation piping connections.

This initial scoping study did not include these additional welds[10] and was based primarily on the breaks in the recirculation and feedwater systems piping and those in the main steam lines. Future studies can include other systems in the analysis.

3.3 Primary Piping Weld Locations

The primary source for the number and location of the welds in each primary pipe were a set of DAEC Inservice Inspection ASME Section XI Isometric Drawings. These drawings were cross-referenced with various P&IDs and NUKON™ Blanket Insulation Installation Drawings to determine weld orientation and location in the drywell. Also, several tables of data were examined to determine other relevant information such as pipe type and composition, and the type, class and characteristics of the weld. The following sections present weld data for recirculation, feedwater and main steam lines.

3.3.1 Recirculation Loops A and B

Recirculation loops A and B are very similar and the discussions presented below are applicable to both loops. Figure 3-2 is an isometric drawing of the recirculation loop A, reproduced from set of isometric drawings provided by DAEC. Figure 3-3 is a schematic representation of the welds in recirculation loop mapped on to the P&ID of recirculation loop A. Figure 3-3, however, may not include some of the T-welds used to connect smaller diameter instrumentation and pressure equalizer penetrations, or 2"-drain or 4"-bypass lines. The drain line itself is not important since manual valve V16-30 (see Figure 3-2) is closed during normal operation. The 4" bypass line is used during start up as part of the Induction Heating Stress Improvement Program. However, motor operated valve MO-4629 is closed during normal operation. Although the bypass loop is not shown in Figure 3-3, all the welds in this loop were included in this analysis. The only welds not modeled in this analysis were the vessel weld RCA-D001, and vessel nozzle weld RCA-F002. These welds are of special type and their failure frequency may be substantially different from other welds. A complete listing of the welds in recirculation loops A and B is presented in Table 5-1, which is discussed in later sections.

---

[10] Inclusion of these twenty welds will increase the ECCS strainer blockage frequency by 10% at the most.

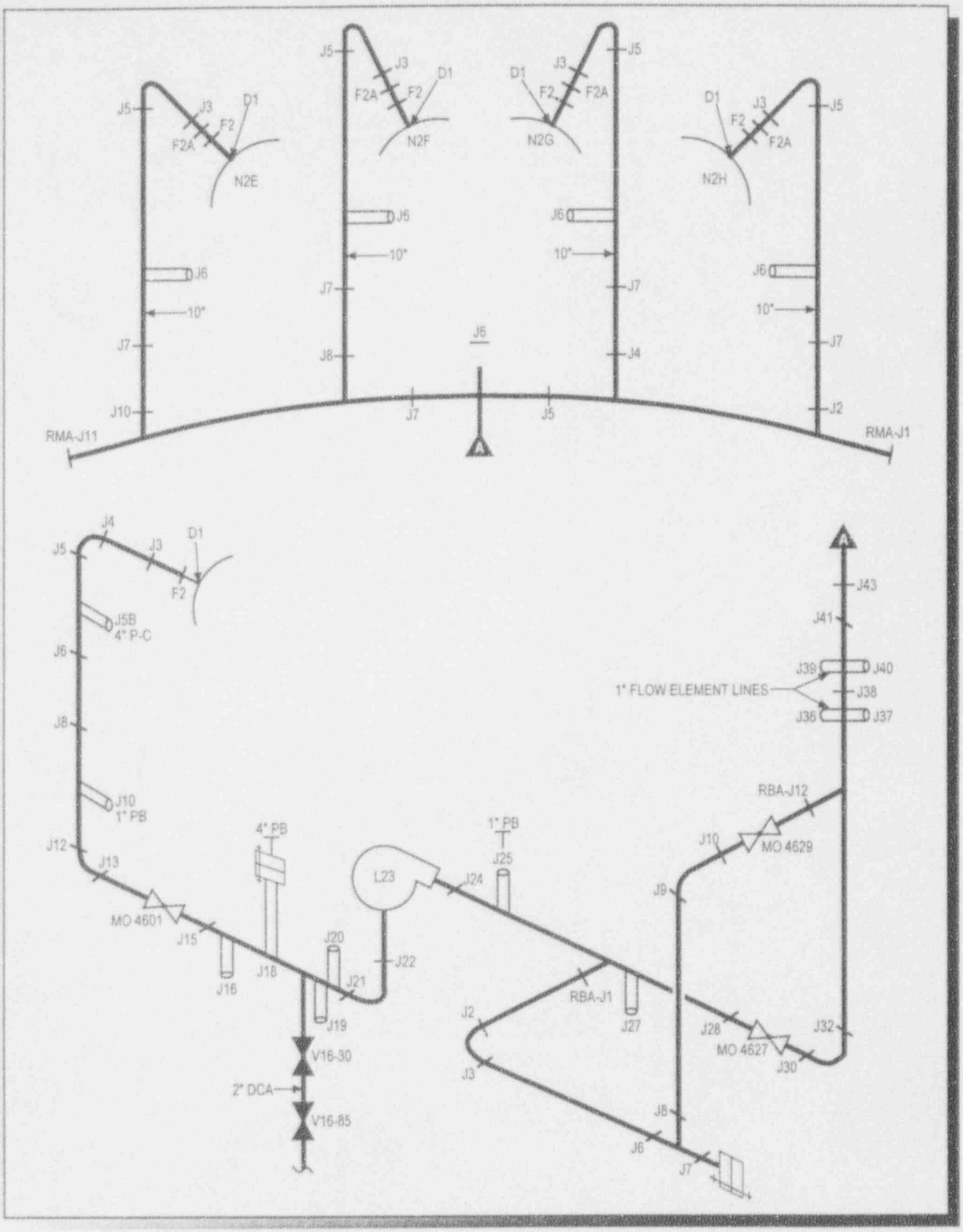

Figure 3-2. Isometric Drawing of Recirculation Loop A, Including Manifold & Risers E, F, G, H

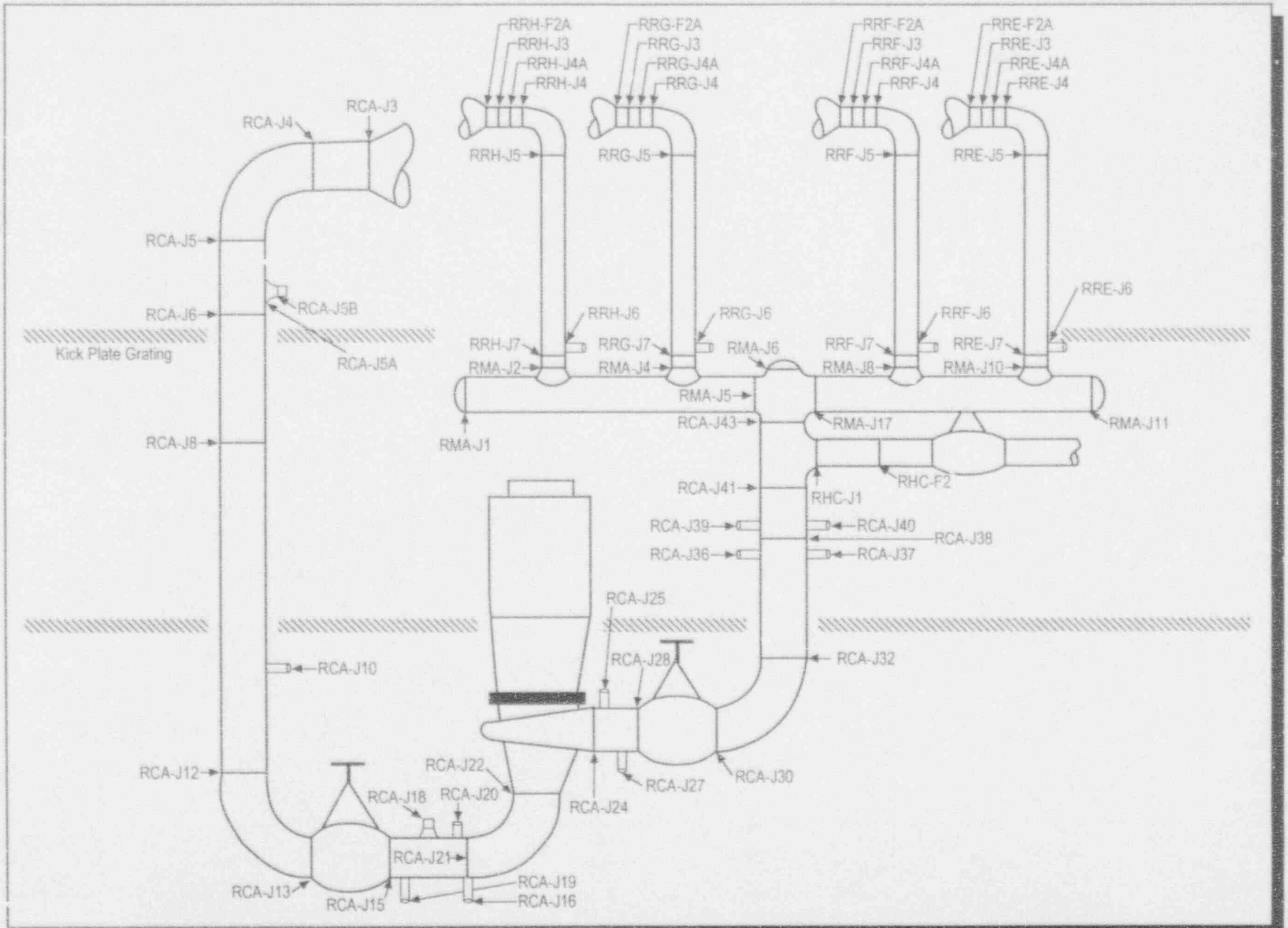

Figure 3-3. Weld Locations in Recirculation Loop A

Preliminary Draft Report

3.3.2 Feedwater Loops A, B and C, D

Feedwater enters the drywell through two 16" 304SS lines at elevation mark 766'. Flow from each 16" pipe is split into two 10" lines at elevation mark 783'-3". Feedwater finally enters the vessel at an elevation of approximately 811"-6". Due to minor differences in pipe routing, the fee l water loops differ from each other (i.e. number and orientation of welds). Figure 3-4 is the isometric drawing for feedwater loops A and B. Figure 3-5 maps these welds on to the P&IDs for these loops. Similarly, Figure 3-6 is an isometric drawing of feedwater loops C and D. The only welds on these loops screened out from this analysis are vessel welds FWA-D001, FWB-D001, FWC-D001, and FWD-D001, for the reasons described above. All the rest of the welds together with their locations and types are listed in Table 5-2.

3.3.3 Main Steam Lines A, B, C and D

The DAEC Unit 1 has four main steam lines, each slightly different from the other due to drywell arrangement. Figures 3-7 and 3-8 present the main steam line arrangement in the drywell. Figures 3-9 through 3-12 are the isometric drawings of the steam lines. In Figure 3-13 all the welds are mapped on to the P&ID of main steam line A. Welds screened out in those lines are vessel welds (D1) and nozzle welds (J2). A complete listing of the welds in MSL A, B, C and D is presented in Table 5-3.

3.4 Drywell Piping Insulation

All the primary lines in the containment are insulated using steel jacketed NUKON™ insulating material. The RCIC, RWCU and recirculation drain lines are insulated with calcium silicate material. In addition, the reactor vessel is insulated using mirror type insulators. The insulation of primary concern for this study is NUKON™ - a fibrous low-density fiber glass wool blanket. The DAEC staff provided detailed P&ID drawings for each primary pipe, and of the type and thickness of the insulating material used. Also presented were the drawings of special designs used to insulate complex parts, such as T-welds, valves, and so on.

The NUKON™ blankets used for insulating primary piping at DAEC Unit 1 are very similar to those described in Section 3.3.2 of NUREG-0897, Rev. 1, (Ref 3.1). The NUKON™ blanket consists of fiberglass insulating wool reinforced with fiberglass scrim (burlap-like covering cloth) and sewn with fiberglass thread. The blankets have a low density (2 to 3 lb/ft^3). The blanket is completely jacketed by 22 gauge 304SS covers.

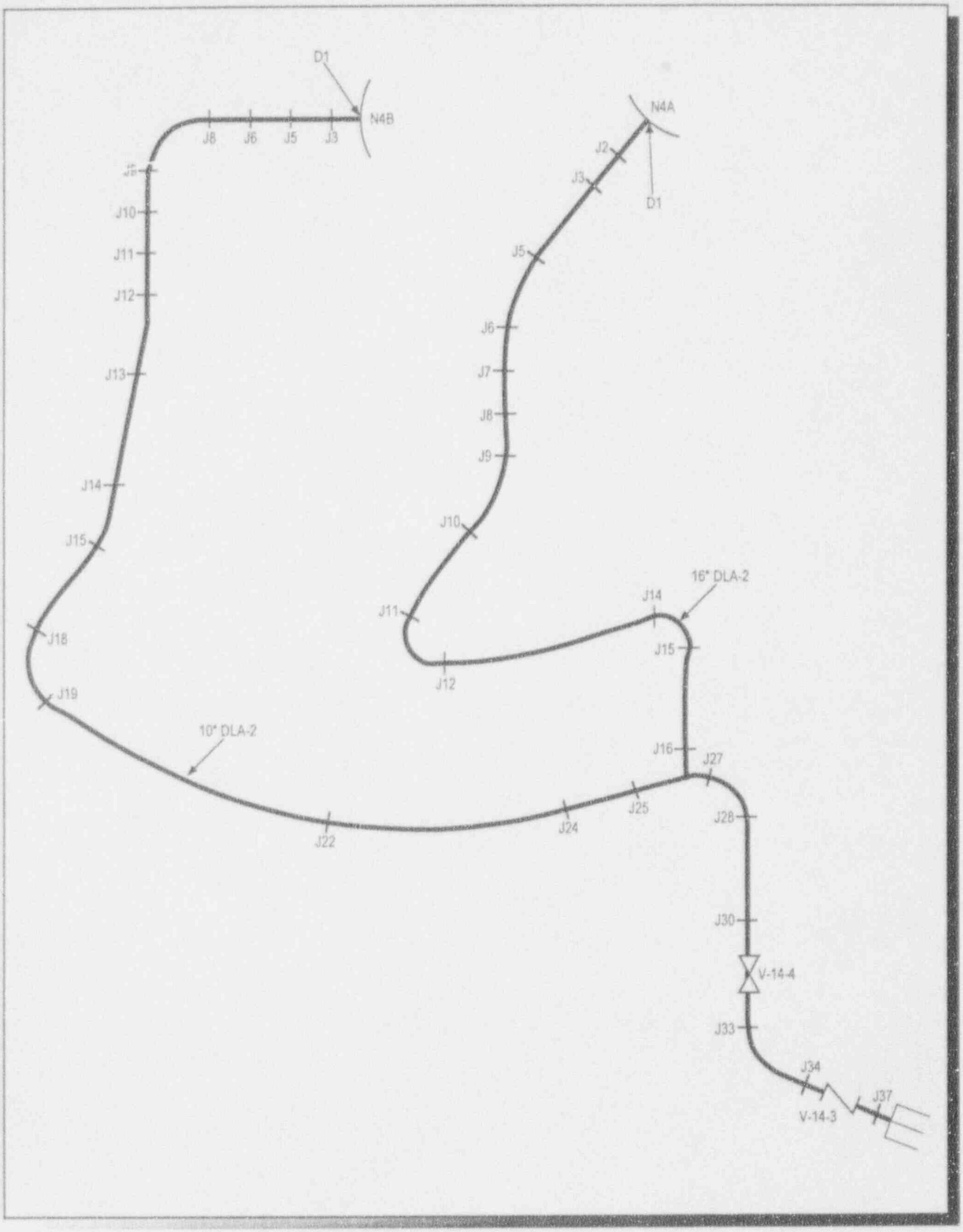

Figure 3-4. Isometric Drawing of Welds in Feedwater Loops A & B

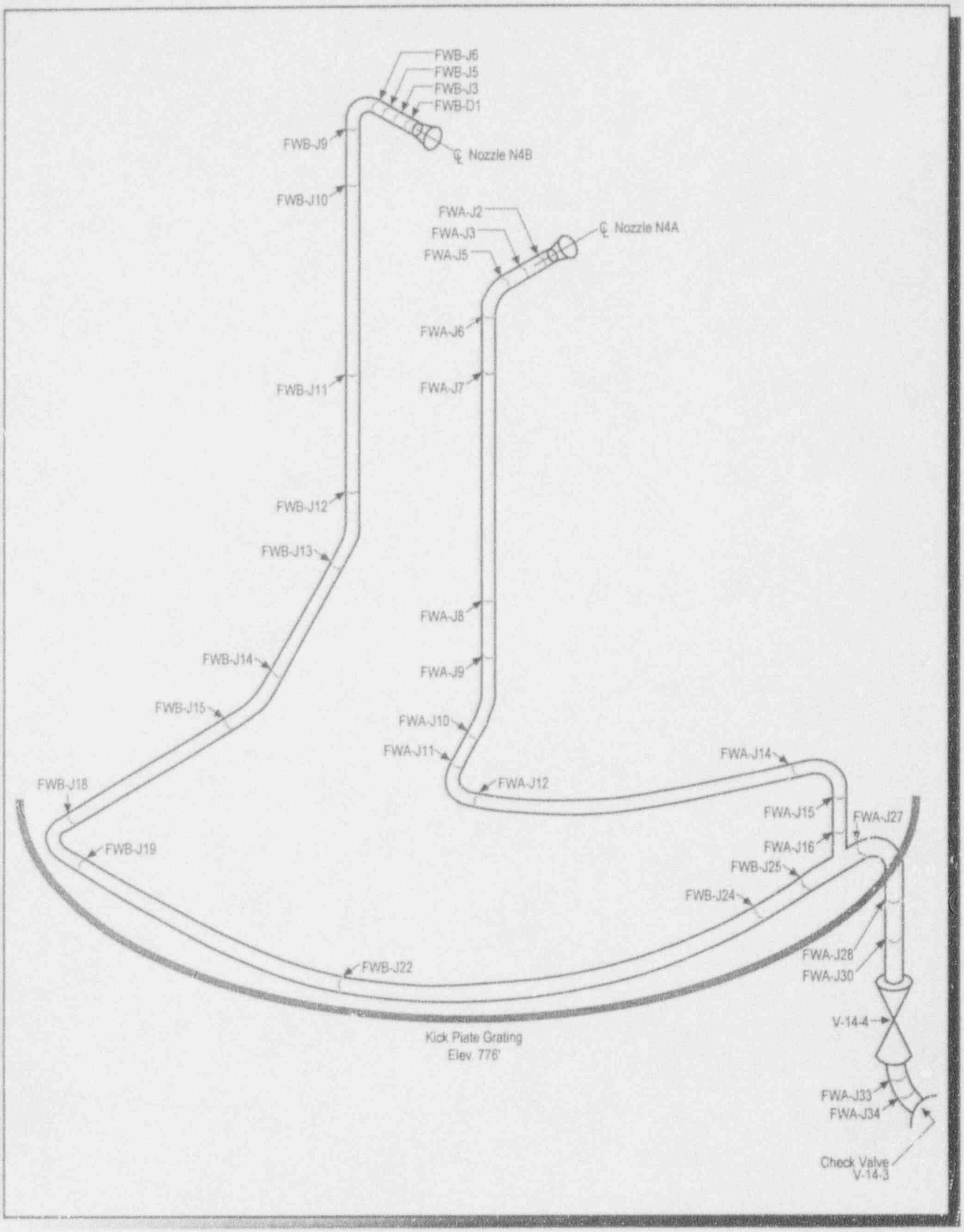

Figure 3-5. Locations of Welds in Feedwater Loops A & B

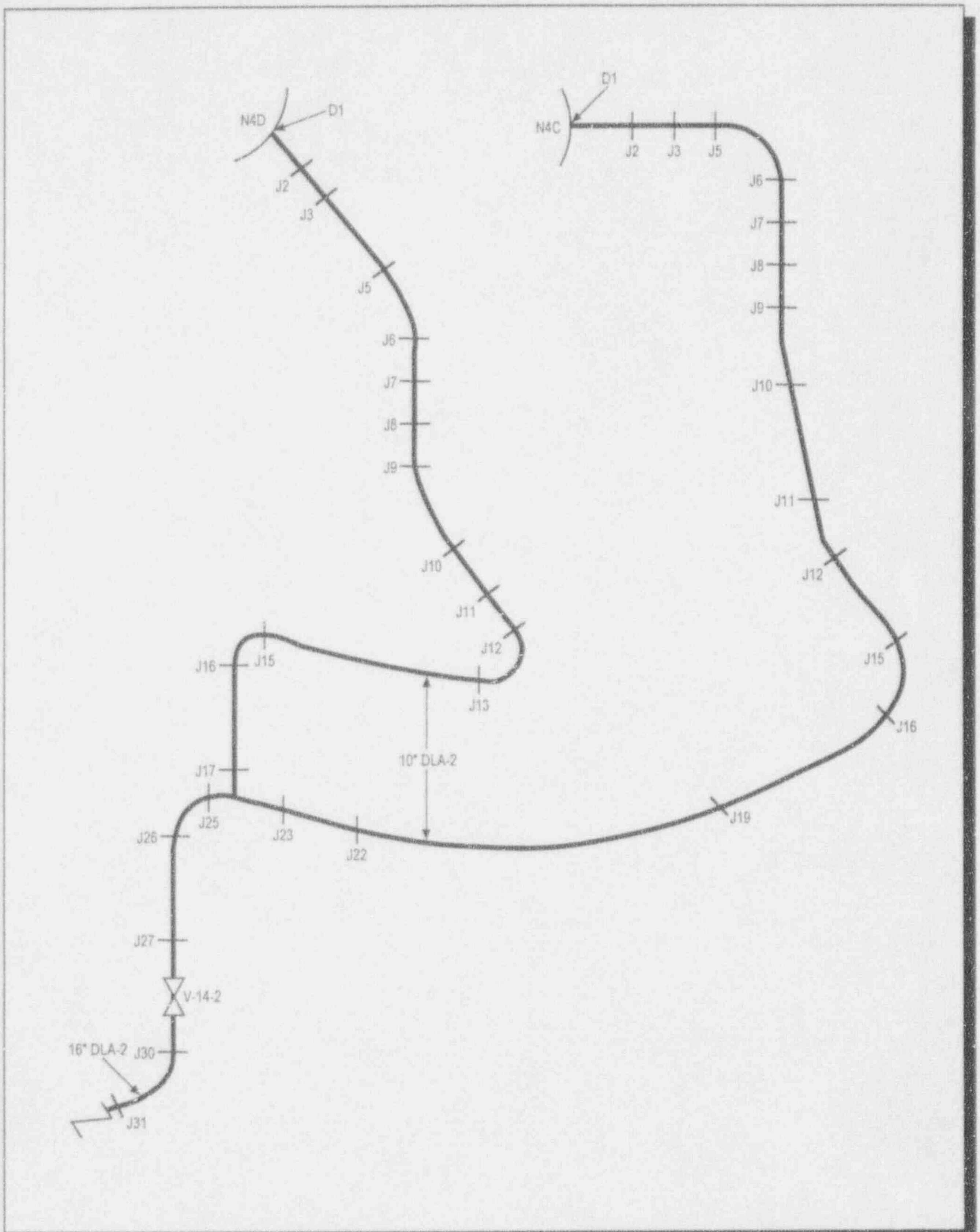

Figure 3-6. Isometric Drawing of Welds in Feedwater Loops C & D

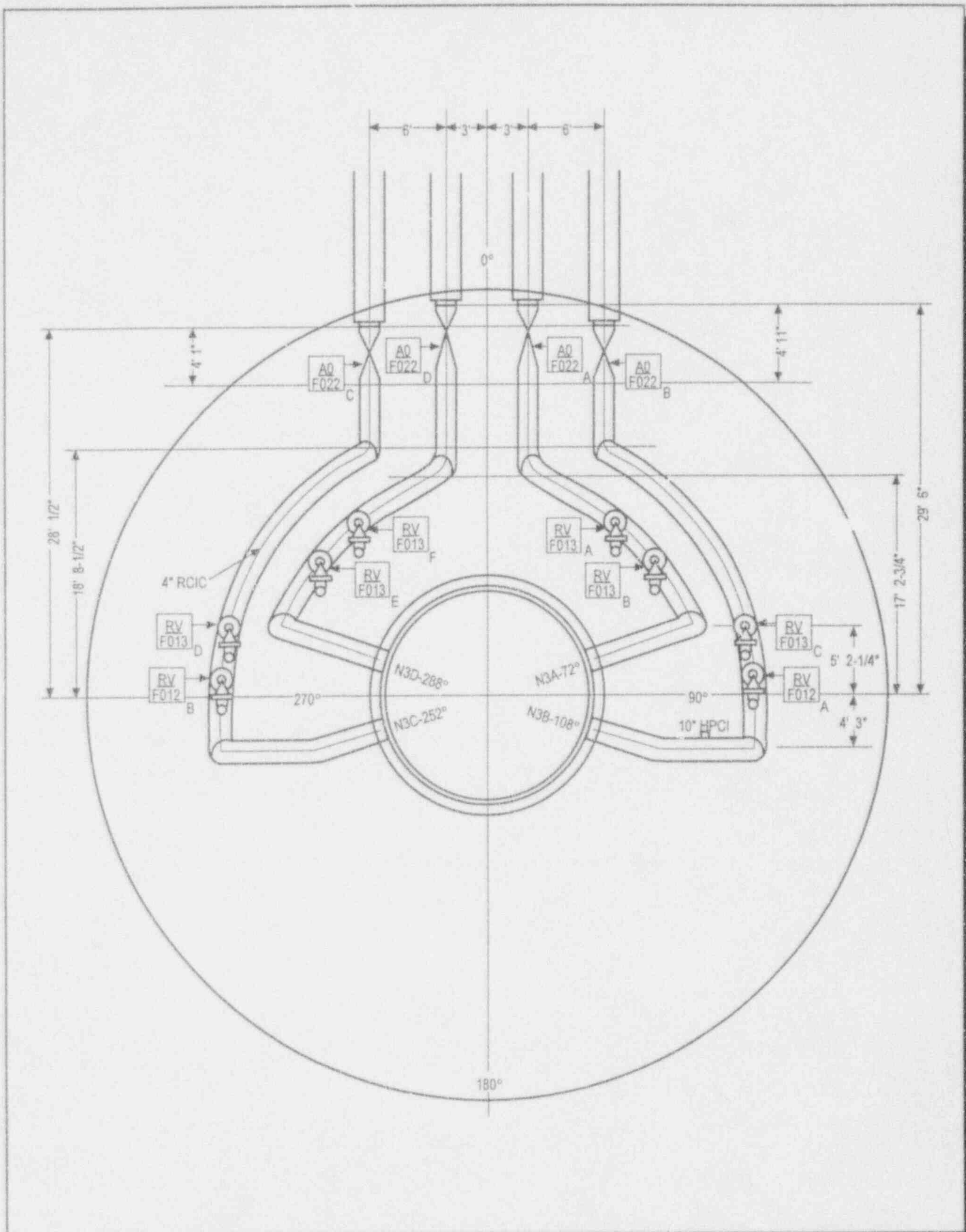

Figure 3-7. Planview of Main Steam Line Arrangement in Drywell

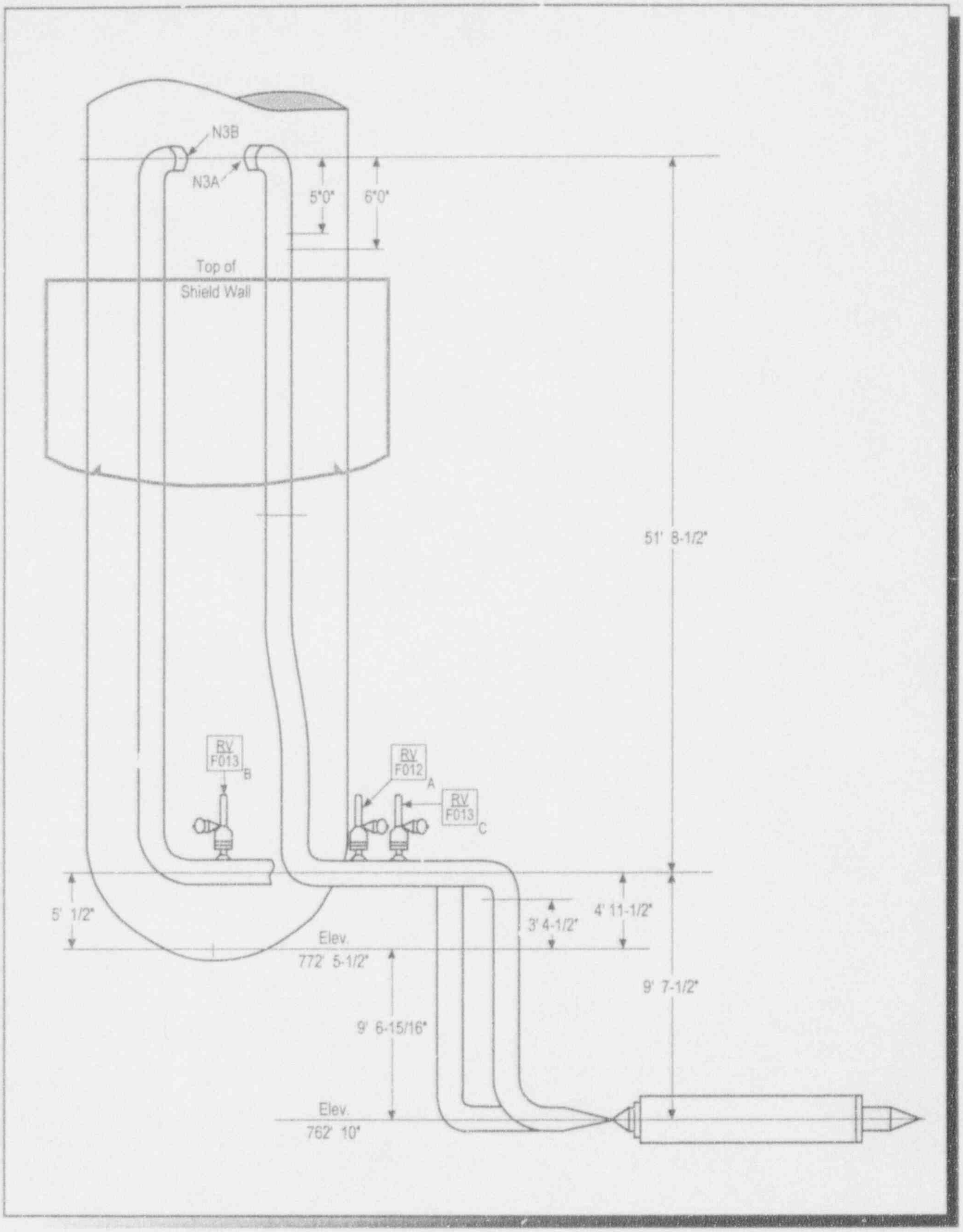

Figure 3-8. Vertical Cross-Section of Main Steam Line Arrangement in Drywell

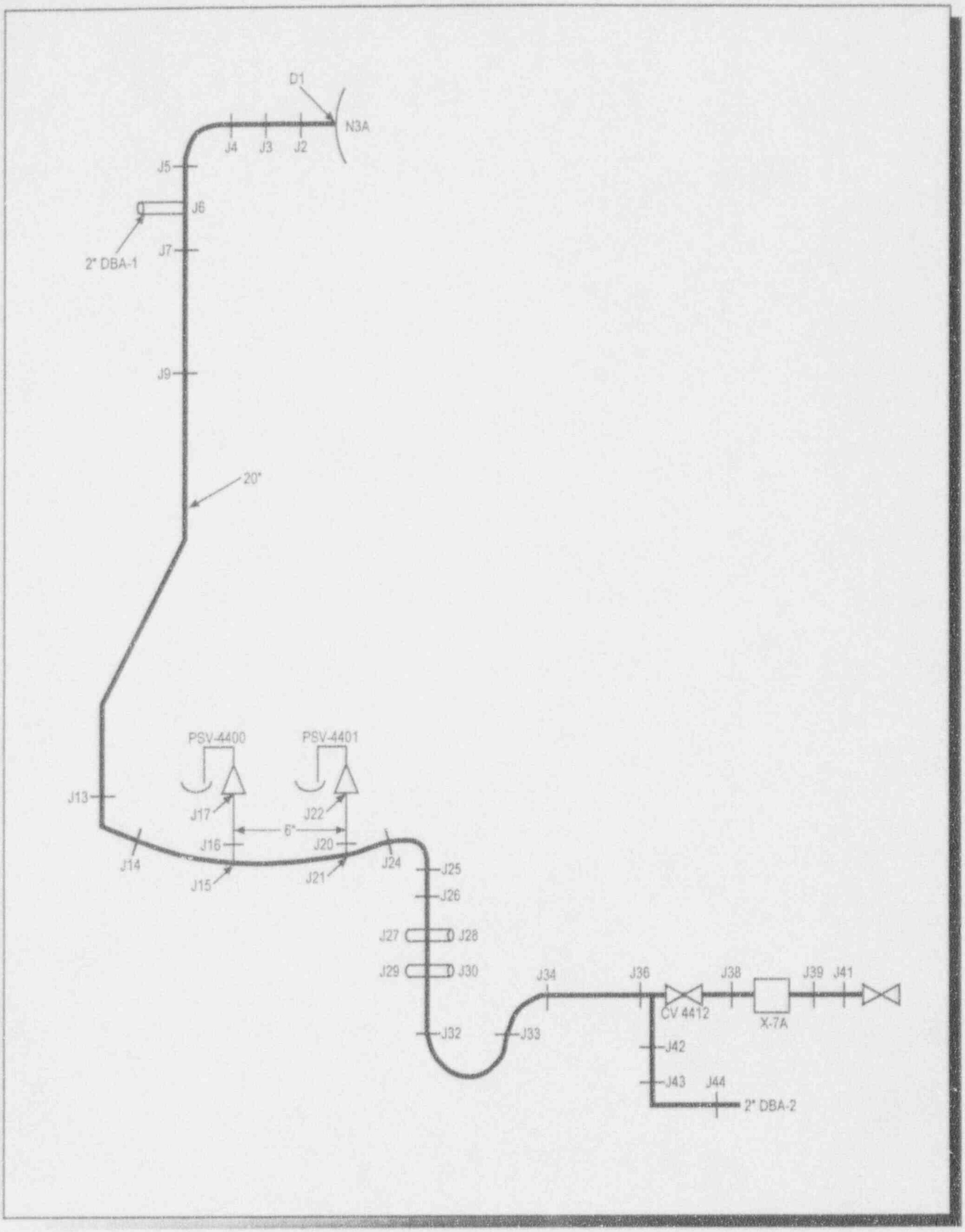

Figure 3-9. Isometric Drawing of Mainsteam Steam Line A

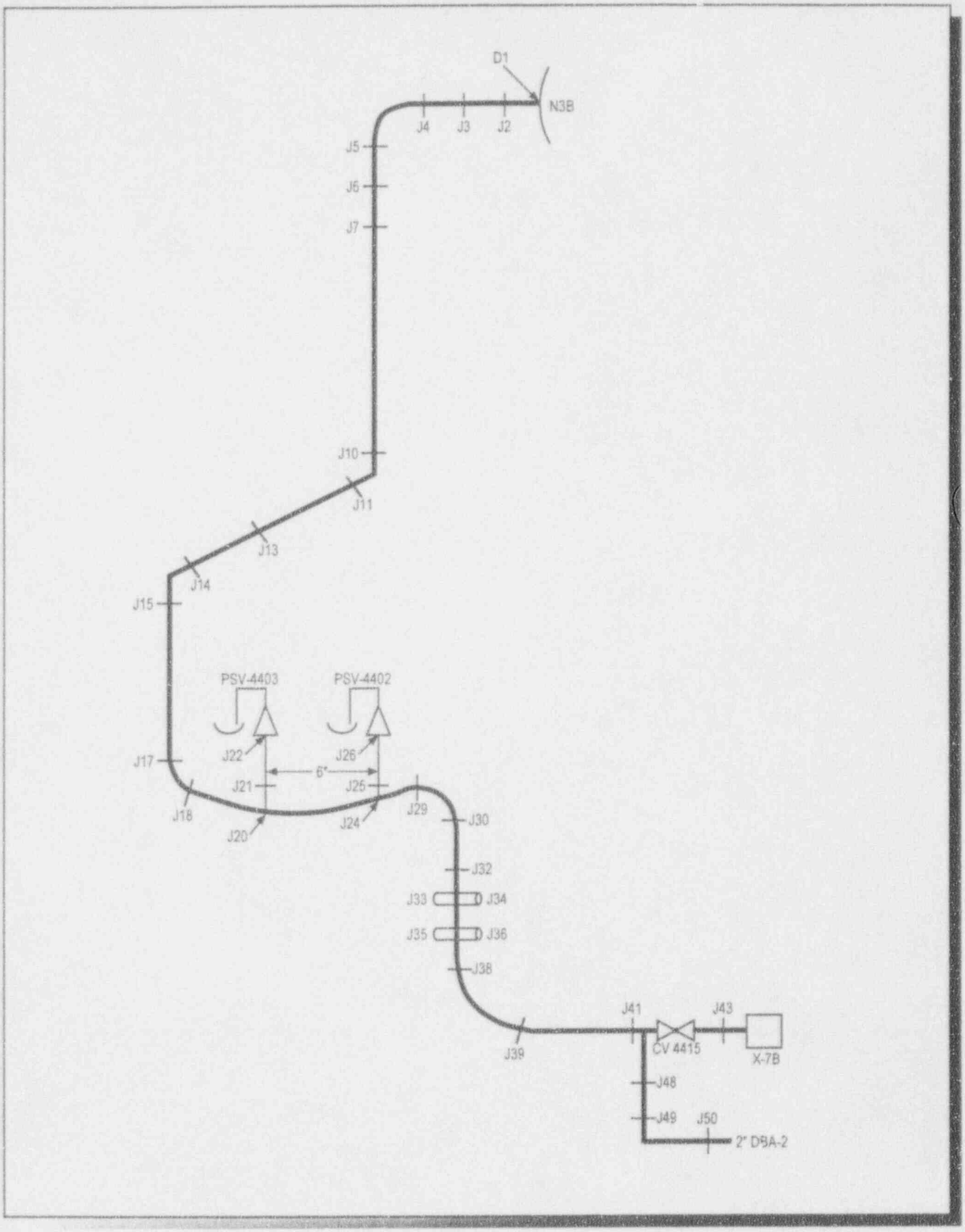

Figure 3-10. Isometric Drawing of Mainsteam Steam Line B

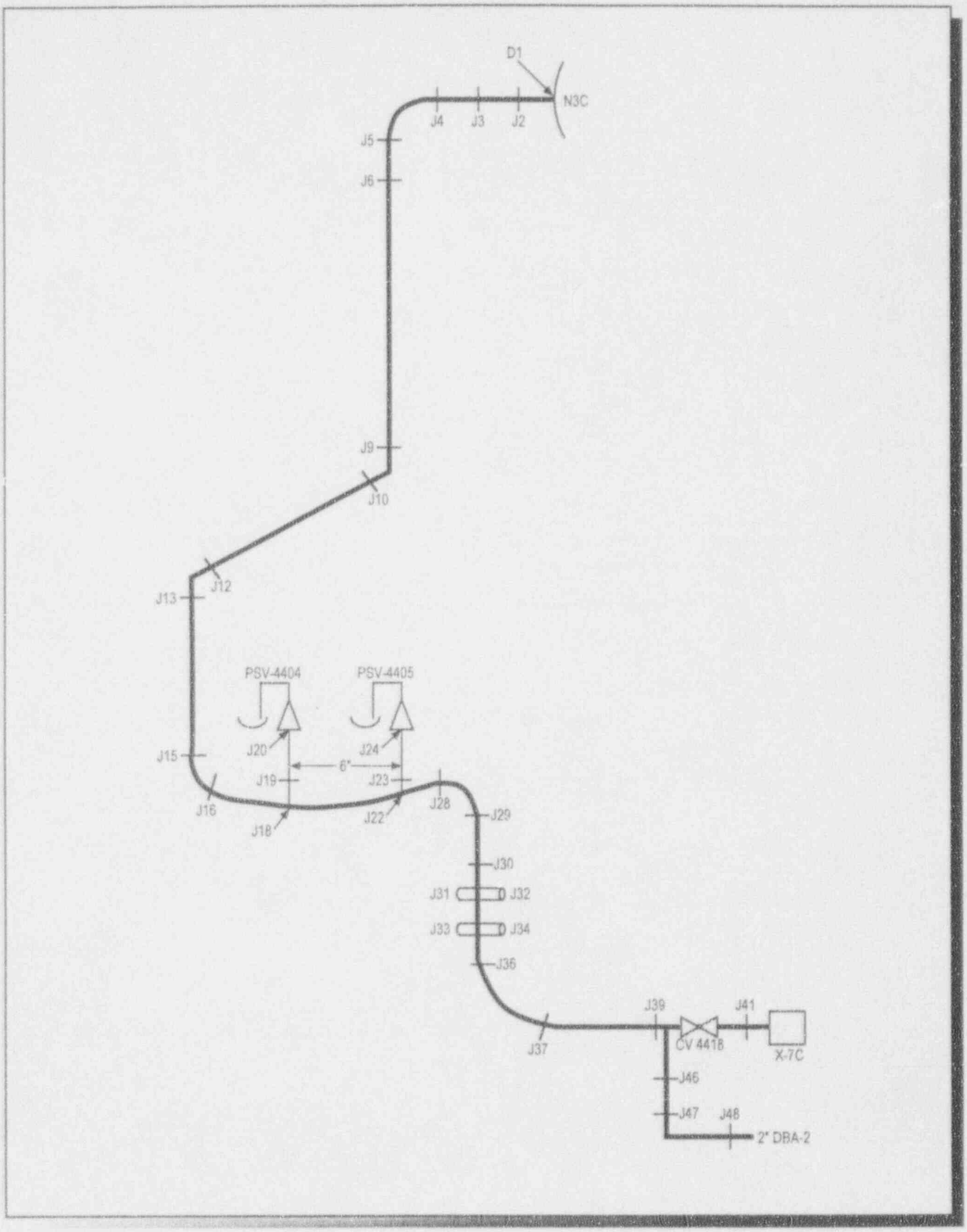

Figure 3-11. Isometric Drawing of Mainsteam Steam Line C

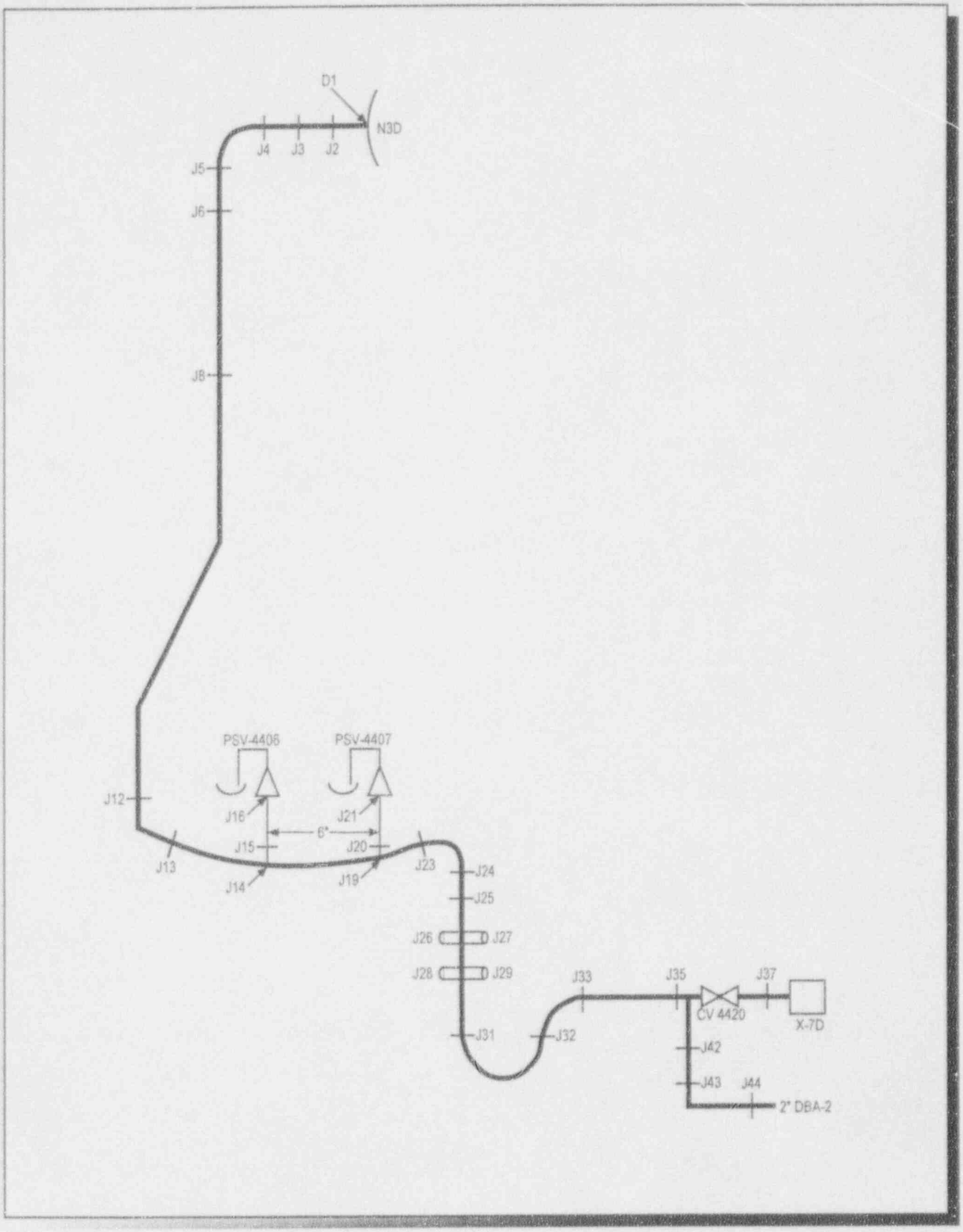

Figure 3-12. Isometric Drawing of Mainsteam Steam Line D

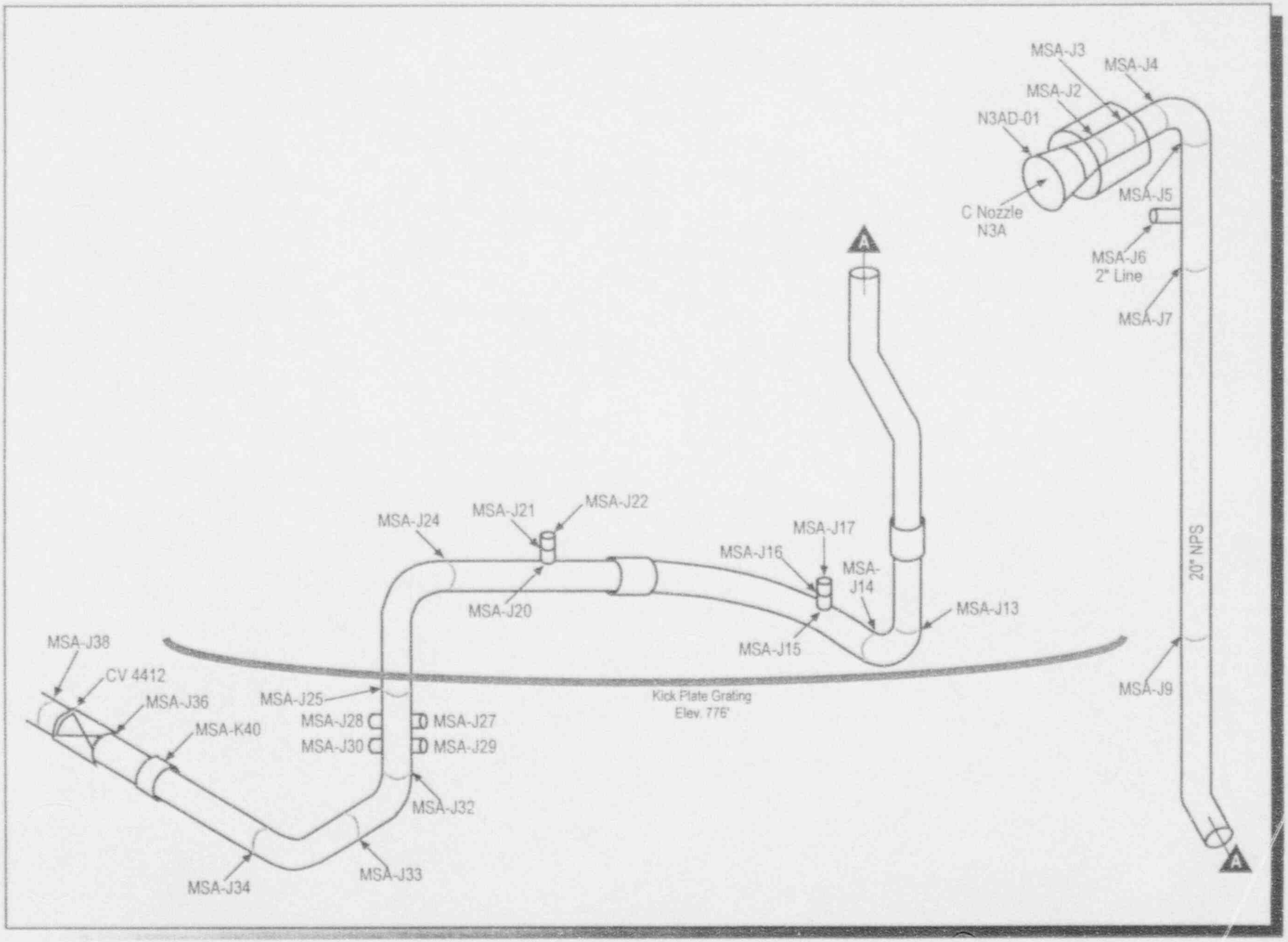

Figure 3-13. Weld Locations in Main Steam Line A

3.5 Drywell and Suppression Pool Layout

A schematic of the drywell layout is presented as Figure 3-14. As shown in this figure, the drywell is closely packed with primary and safety system piping, pipe restraints, piping supports and other related components. The drywell is characterized by three coarse gratings at elevations 805′, 776′, and 757′. These gratings and their related structures were designed to provide structural support to the pipes, and also act as work platforms. Examination of these gratings reveals that:

1. the gratings and the associated structures block jet expansion in certain directions, and may result in reducing the total volume of insulation debris generated by a LOCA, and
2. the gratings also act as impediments for transport of debris to lower elevations.

The effects of these gratings on debris generation and transport was not explicitly modeled. These structures will, however, result in lower volumes of debris transported to the suppression pool. Their effect on debris transport was enveloped by parametric analysis.

The drywell vent pipe (pipes connecting the drywell to the suppression pool) inlets are located at elevation mark 744′. The Mark I suppression pool consists of a torus shaped wetwell, which contains a large quantity of water. The DAEC torus is about 9.25′ in diameter with the center line at elevation mark 732′-3″. Water is drawn from suppression pool for injection into the reactor core by the RHR, CS, RCIC, and HPCI system pumps. For an assumed large LOCA, the RHR and CS are the only adequate mitigating systems. The RHR and CS systems each have two penetrations into the torus; N225A&B for RHR and N227A&B for CS. Each of the system inlets is equipped with a suction strainer, semi-conical in shape. Figure 3-15 is an engineering drawing of the strainer reproduced from utility supplied P&IDs. The strainers are made of 14 gauge perforated (1/8″ holes and 30 holes per square inch) steel sheet, with an open flow area of approximately 40% of the total strainer surface area. Figure 3-15 summarizes the strainer geometrical data, along with the calculated total surface and total flow areas for each strainer.

3.6 RHR and CS Systems Description

The RHR and CS systems are designed to provide low pressure core flooding following a LOCA. These systems take suction from the suppression pool and inject water into the reactor core, which then flows out the break. In this mode of operation, these systems are commonly referred to as low pressure core injection (LPCI) and low pressure core spray (LPCS) systems. Both LPCI and LPCS systems are actuated on either low core water level 1 or high drywell pressure signals. The system becomes operational and is capable of injection within a minute of the initiating event. The LPCI injects into the

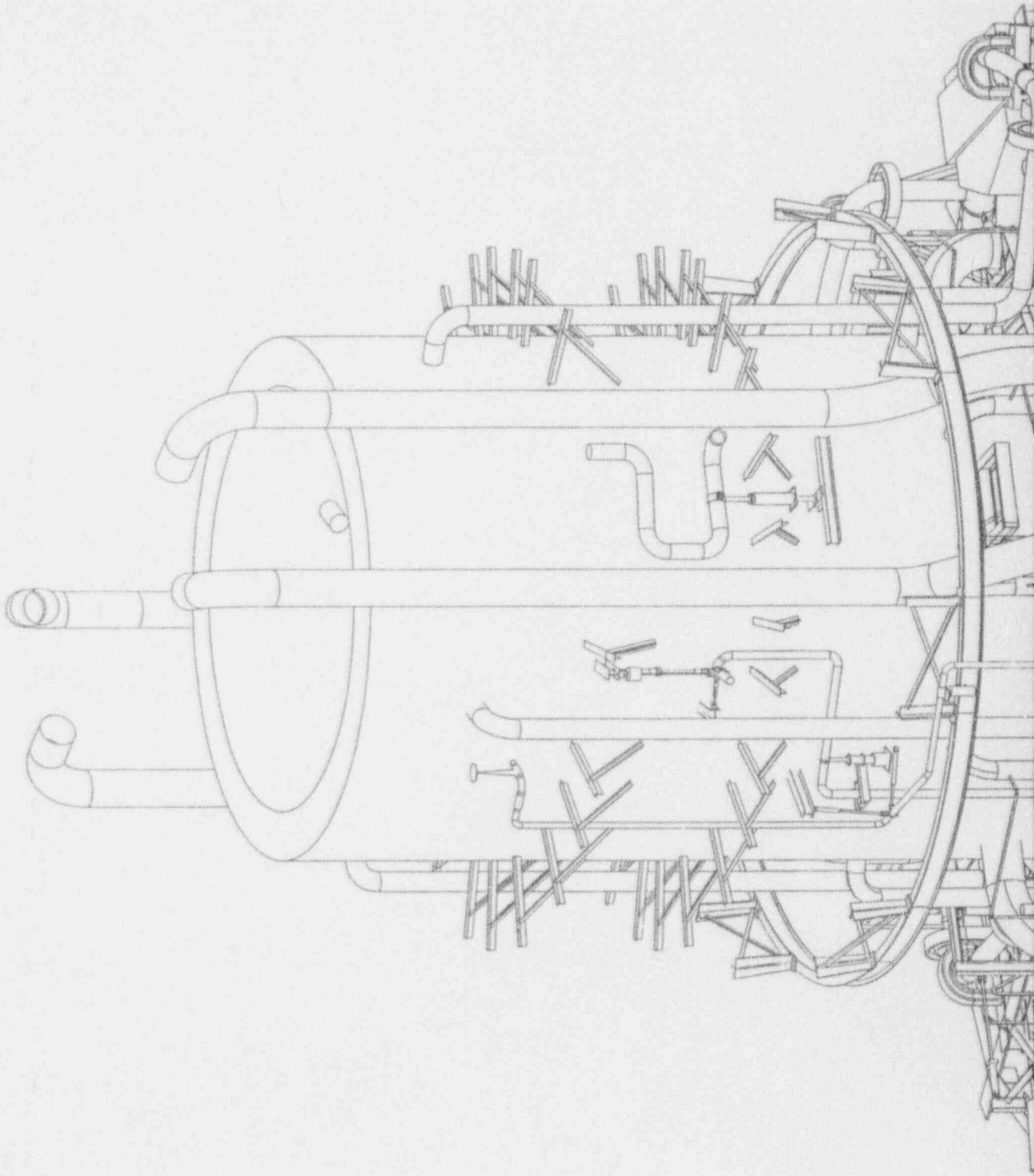

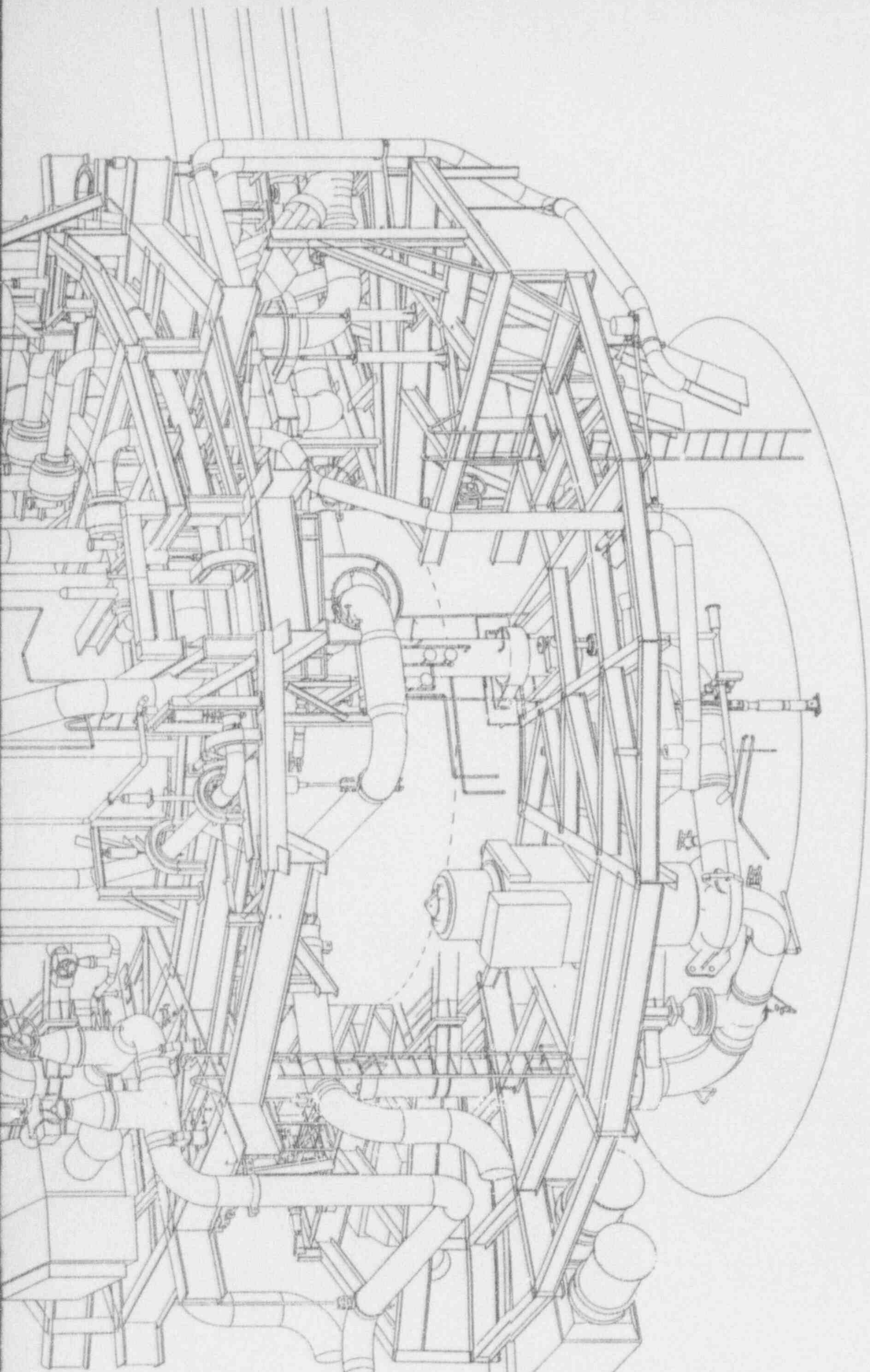

Figure 3-14. Drywell Layout

9402100230-02

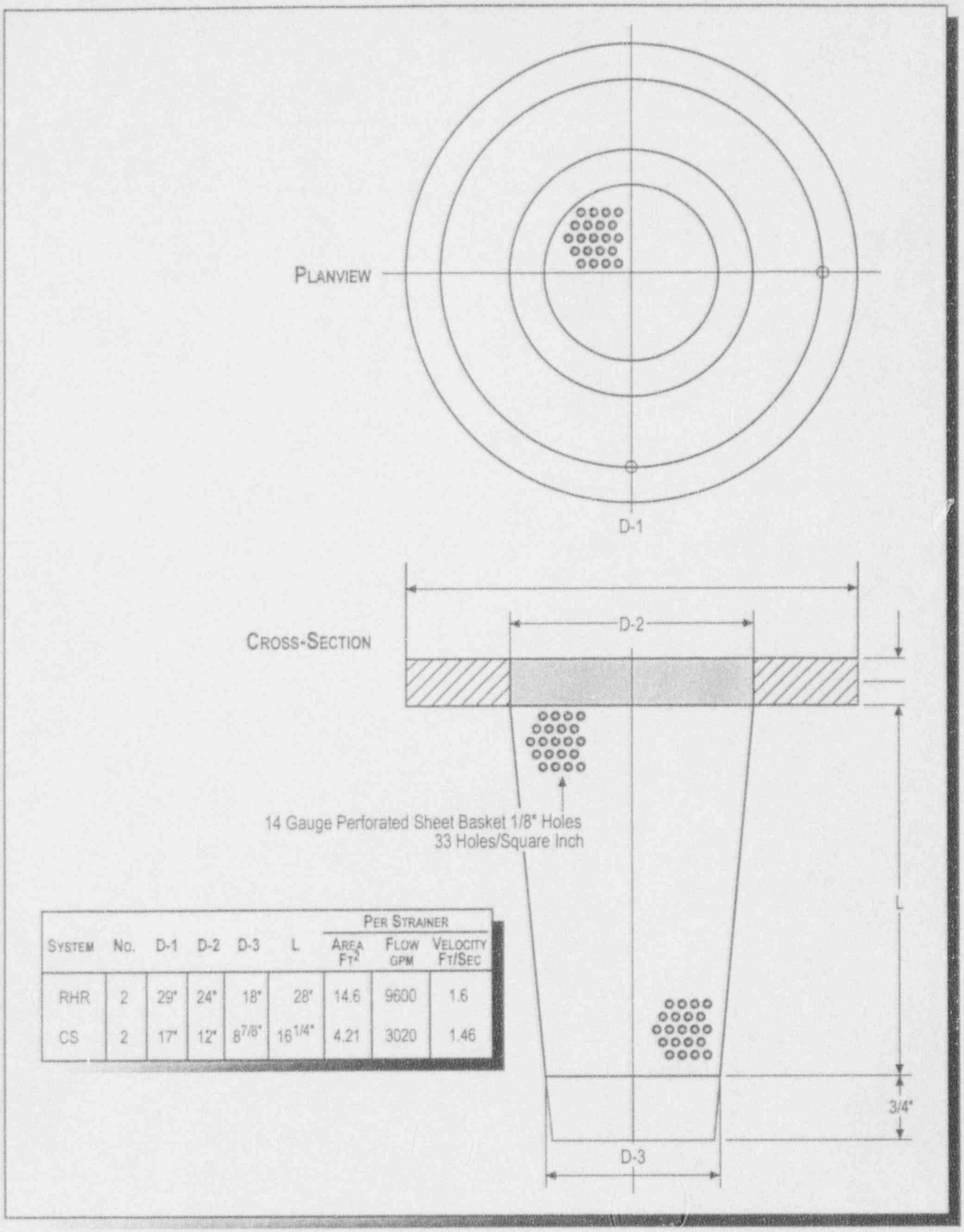

System	No.	D-1	D-2	D-3	L	Per Strainer: Area Ft^2	Flow GPM	Velocity Ft/Sec
RHR	2	29"	24"	18"	28"	14.6	9600	1.6
CS	2	17"	12"	8 7/8"	16 1/4"	4.21	3020	1.46

Figure 3-15. Planview & Cross-Section of Strainer

recirculation suction lines and the LPCS injects directly into the core through dedicated nozzles in the reactor vessel. For the present analysis it is assumed that the functioning of both of these systems is essential to mitigate a LOCA.[11]

The LPCI system consists of a total of four Byron Jackson centrifugal pumps (RHR-A, B, C, and D), each with a rated flow of 4800 GPM at a discharge head of 400 ft of water. Figure 3-16 presents pump curves for these pumps. As shown in this figure, the net positive suction head (NPSH) required for these pumps at the rated flow is about 10 ft of water. The pumps are located at an elevation mark of 718', or about 14 ft below the suppression pool center-line. Pumps RHR-A and C take suction from strainer N225A, and pumps RHR-B and D take suction from strainer N225B. NPSH available at the RHR suction is approximately 24 ft. of water. It results in a NPSH-margin of about 14 ft. of water. The estimated flow through each strainer (N225A and N225B) is 9600 GPM, and the corresponding strainer flow velocity is 1.46 ft./sec.

The CS system consists of two Byron Jackson centrifugal pumps (CS-A and B), each rated to provide 3100 GPM, at a discharge head of 700 ft of water. Figure 3-17 presents pump curves for these pumps. As shown in this figure, the NPSH required for these pumps at rated flow is about 15 ft of water. NPSH available at the CS pump suction is approximately 32 ft. of water. Therefore, NPSH margin available for CS is about 17 ft. of water. Each pump has a dedicated suction strainer. The estimated flow through the CS suction strainers during expected operating conditions is 3100 GPM, and the corresponding strainer flow velocity is 1.60 ft./sec.

In the present analysis, both RHR and CS strainers were combined together to form a single strainer of area equal to the total areas of the individual strainers. Available NPSH margin was assumed to be 14 ft. of water for the following reasons:

1. Although CS pumps have a NPSH margin of 17 ft. of water, it is not clear if CS alone can provide adequate cooling, and
2. Results are expected to be slightly conservative when 14 ft. of water is used.

Additionally, this value was varied over a range of 1 to 20 ft of water to examine the impact of NPSH margin on the ECCS strainer blockage frequency. Finally, net flow through the strainers was assumed to be 25,000 GPM resulting in an average flow velocity of 1.5 ft./sec.

---

[11] Note that this assumption is consistent with DAEC IPE model for large break LOCA.

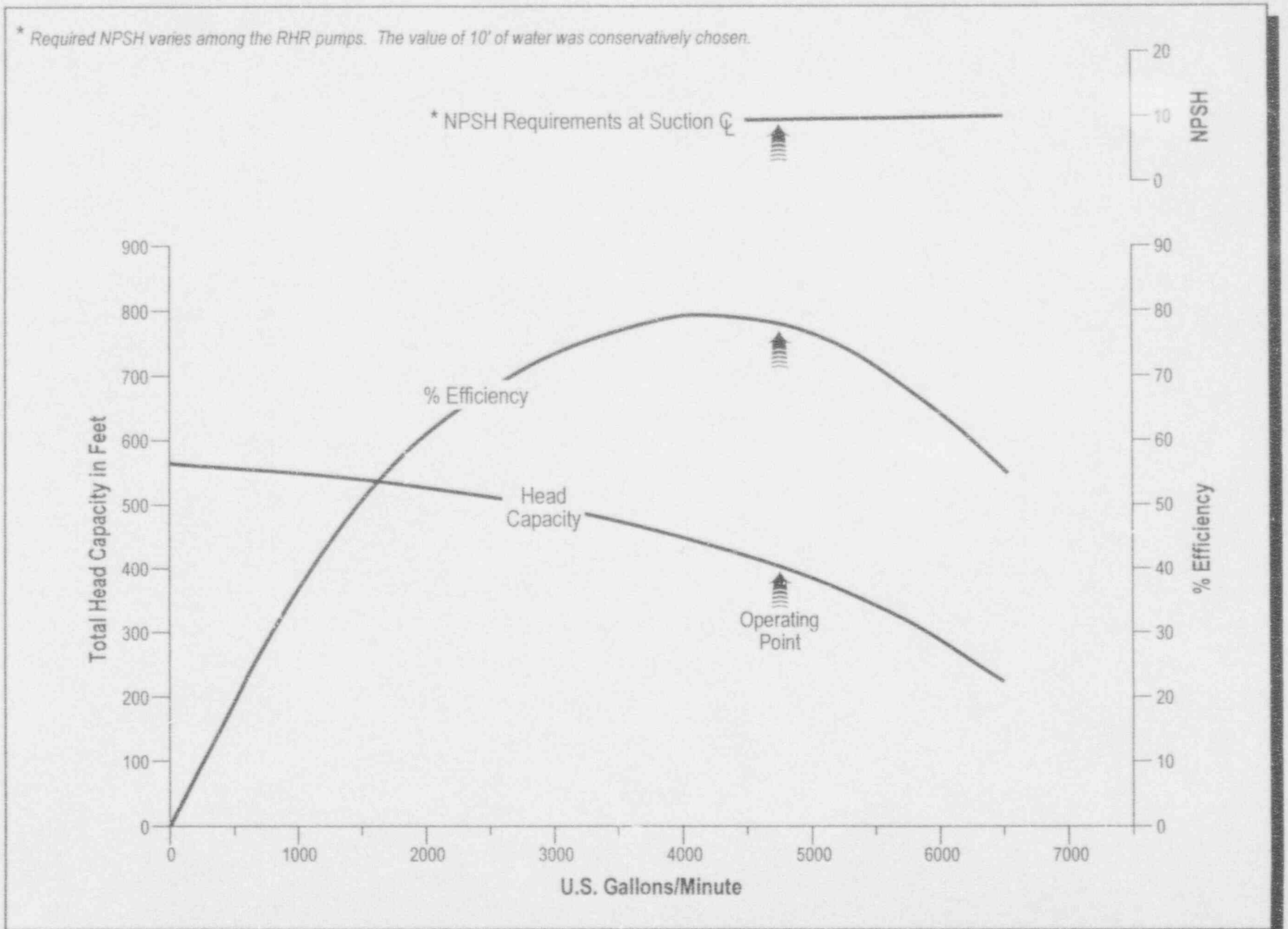

Figure 3-16. Low Pressure Core Injection Pump Curves

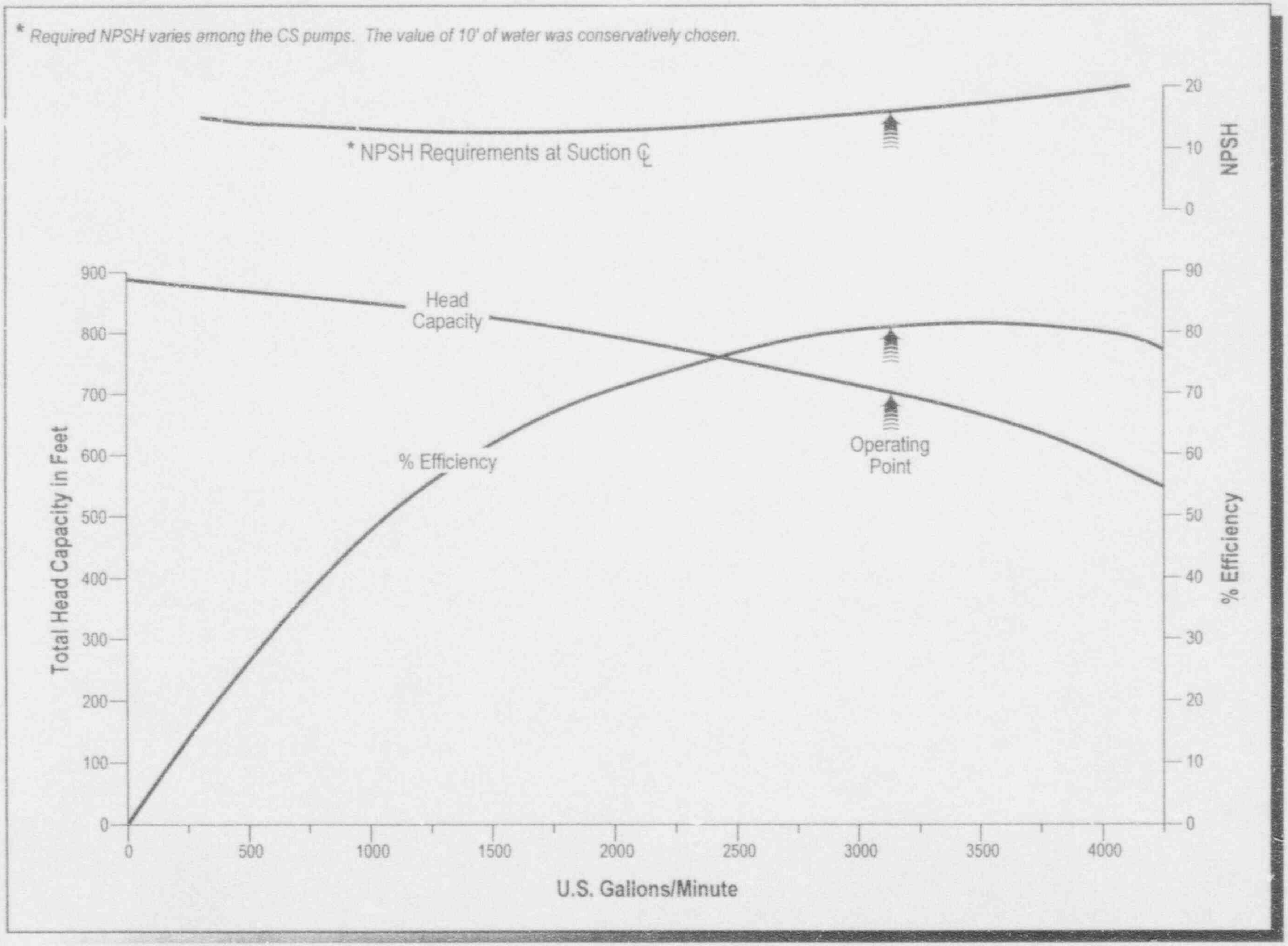

Figure 3-17. Core Spray Pump Curves

References for Section 3

3.1 A. W. Serkiz, "Containment Emergency Sump Perfonnance," US Nuclear Regulatory Commission, NUREG-0897, Rev. 1, October 1985.

4.0 PRIMARY PIPE BREAK FREQUENCIES

This section summarizes the approach used to estimate break frequencies of reactor coolant piping welds. Additionally, a brief overview is given of the approach used in BLOCKAGE 2.0 to derive pipe break frequencies from the weld break frequency data.

4.1 Approach Used to Estimate Weld Break Frequencies

Of the reactor equipment items generally considered in probabilistic safety assessments, piping is generally among the most difficult to treat in regard to failure quantification. This situation exists because of the scarcity of incidents involving actual pipe failures and the difficulties associated with developing detailed analytical predictive models. Actual pipe breaks of significant size have been limited to non-LOCA sensitive systems. Several methods have been applied to estimate pipe failure rates given the limited available data. These methods include Bayesian predictions, analytical models, and expert elicitation.

In making a decision on an approach to quantify pipe break frequencies, particular attention was given to recently-published cautionary information in an ASME document (Ref. 4.1) that contains ASME-sponsored work related to risk-based inspection guidelines for light water reactor components. In particular, p. 15 of Ref. 4.1 notes that conservative design practices have made it very unlikely that pipe failures would occur for a number of anticipated modes of failure, including excessive elastic or plastic deformation, brittle fracture, stress rupture/creep deformation (inelastic), and plastic instability. This document goes on to state that "it is generally believed within the nuclear industry that other causes not addressed in design, by ASME BPVC calculations or otherwise, are most likely to cause structural failures. Two common examples are intergranular stress corrosion cracking (IGSCC) of stainless steel piping and erosion-corrosion wall thinning of carbon steel piping." Note that stainless steel piping is used in BWR recirculation piping system.

Given the ASME cautionary note about potential IGSCC degradation and the relative lack of suitable historical data for pipe failures, it was decided that an analytical approach should be used as the foundation for generating our pipe break frequency estimates. The analytical model chosen for this study was developed by Lawrence Livermore National Laboratory (LLNL) and is described in NUREG/CR-4792, (Ref. 4.2). The LLNL model was chosen because it is comprehensive in nature. This model addresses both indirect and direct causes of failures, including IGSCC.

4.1.1 Brief Description of LLNL Analysis Method

The LLNL analysis combined probabilistic and deterministic techniques to estimate the chances that weld breaks will occur in reactor coolant piping at a representative BWR 4/Mark I plant. The following categories of weld breaks were considered by LLNL:

a) Breaks due to direct causes, specifically:

i) Crack growth at welded joints related to the combined effects of thermal, pressure, seismic, and other loads, and

ii) Crack growth at welded joints related to IGSCC.

b) Breaks due to indirect causes, specifically the seismically-induced failure of equipment, including piping and component supports, that could lead to the break of a reactor coolant pipe.

The LLNL analysis considered three major piping systems: the recirculation, main steam and feedwater systems. However, the evaluation of IGSCC effects was limited to the recirculation system. The LLNL analysis provided results both in terms of "leaks" and Double Ended Guillotine Breaks (DEGBs). As will be explained later, it was assumed that of these two break categories, only the DEGBs would be of concern for later use in the debris blockage analysis. The overwhelming contribution to the overall frequency of DEGB LOCA events at the LLNL reference BWR4/Mark I plant was predicted to be related to IGSCC effects on recirculation piping.

To address potential IGSCC effects, it is useful to consider the LLNL analysis data contained in Figure 4-1. This figure presents the cumulative system probability that a BWR 4/Mark 1 recirculation loop made from 304SS and a (fictitious) 316NG replacement loop with the same configuration will experience a DEGB given IGSCC effects. Note that LLNL has not provided a corresponding uncertainty analysis for these results. Over a 40 year plant lifetime, these probability data predict that a recirculation loop made from 304SS will experience a DEGB event with a frequency of approximately 5E-04/yr. In contrast, the fictitious 316NG replacement loop was predicted to fail with a frequency of approximately 4E-05/yr. These data indicate that the susceptible (304SS) material is over 10 times more likely to experience a DEGB over a 40 yr plant life than the resistant (316NG) material.

The LLNL study also presented the IGSCC DEGB frequency data in terms of specific weld categories. As is shown in Figure 4-2, about 80% of the postulated 304SS recirculation piping DEGBs were associated with 12" riser welds, while about 20% of the 304SS DEGBs were associated with 4" bypass line welds. The header (22"), discharge (28"), and suction (28") welds were each judged to contribute less than 10% to the recirculation loop DEGB frequency, based on the statistical accuracy of the LLNL calculations.

4.1.2 Limitations of the LLNL Analysis

There were a number of limitations associated with the LLNL analysis. Because of the overwhelming contribution of IGSCC to the predicted weld break frequencies, efforts were focused on

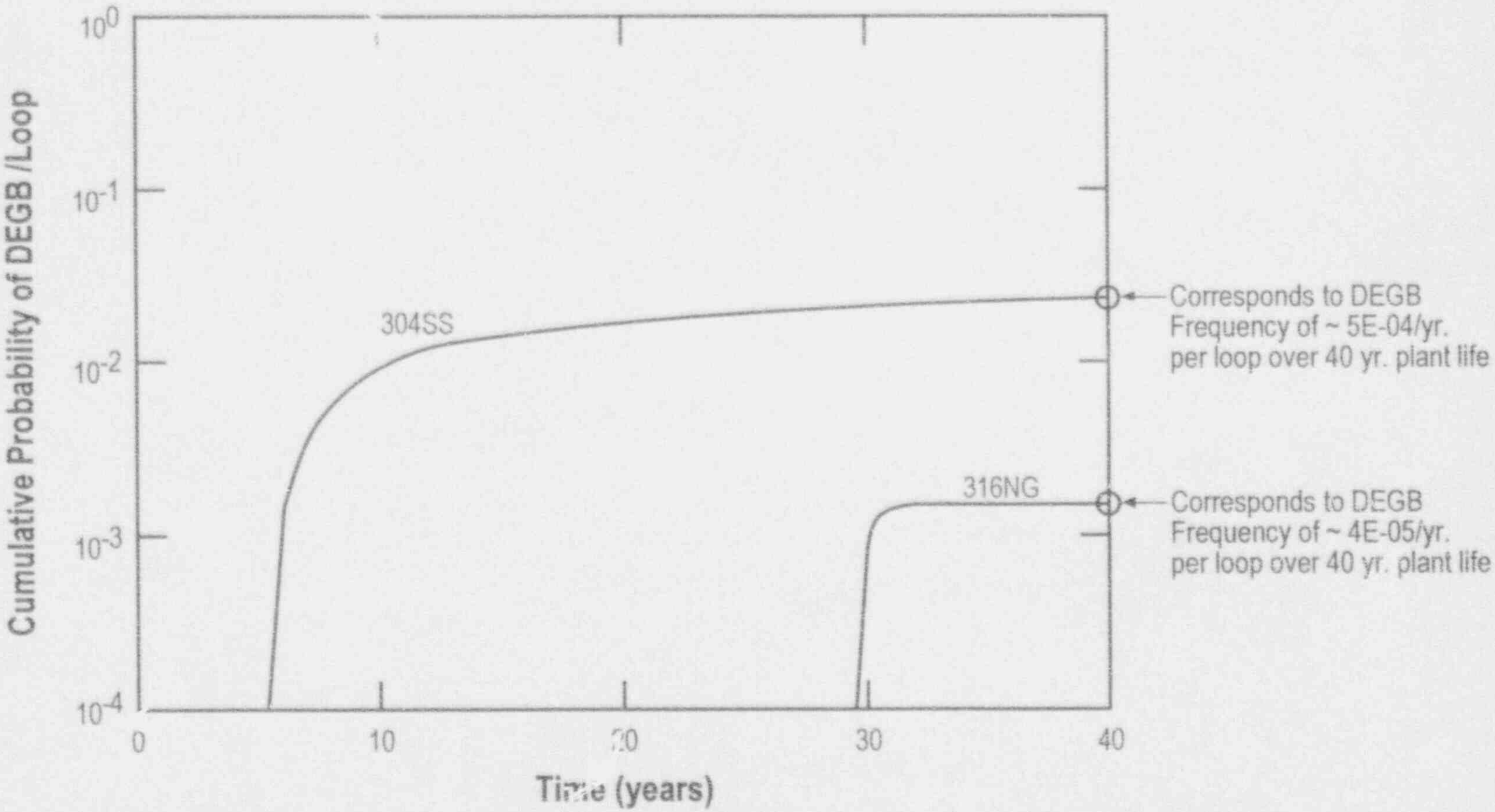

Reproduced from Fig. 4.9(a), Vol. 1 of NUREG/CR-4792

Figure 4-1. Cumulative System Probabilities of DEGB in One Recirculation Loop

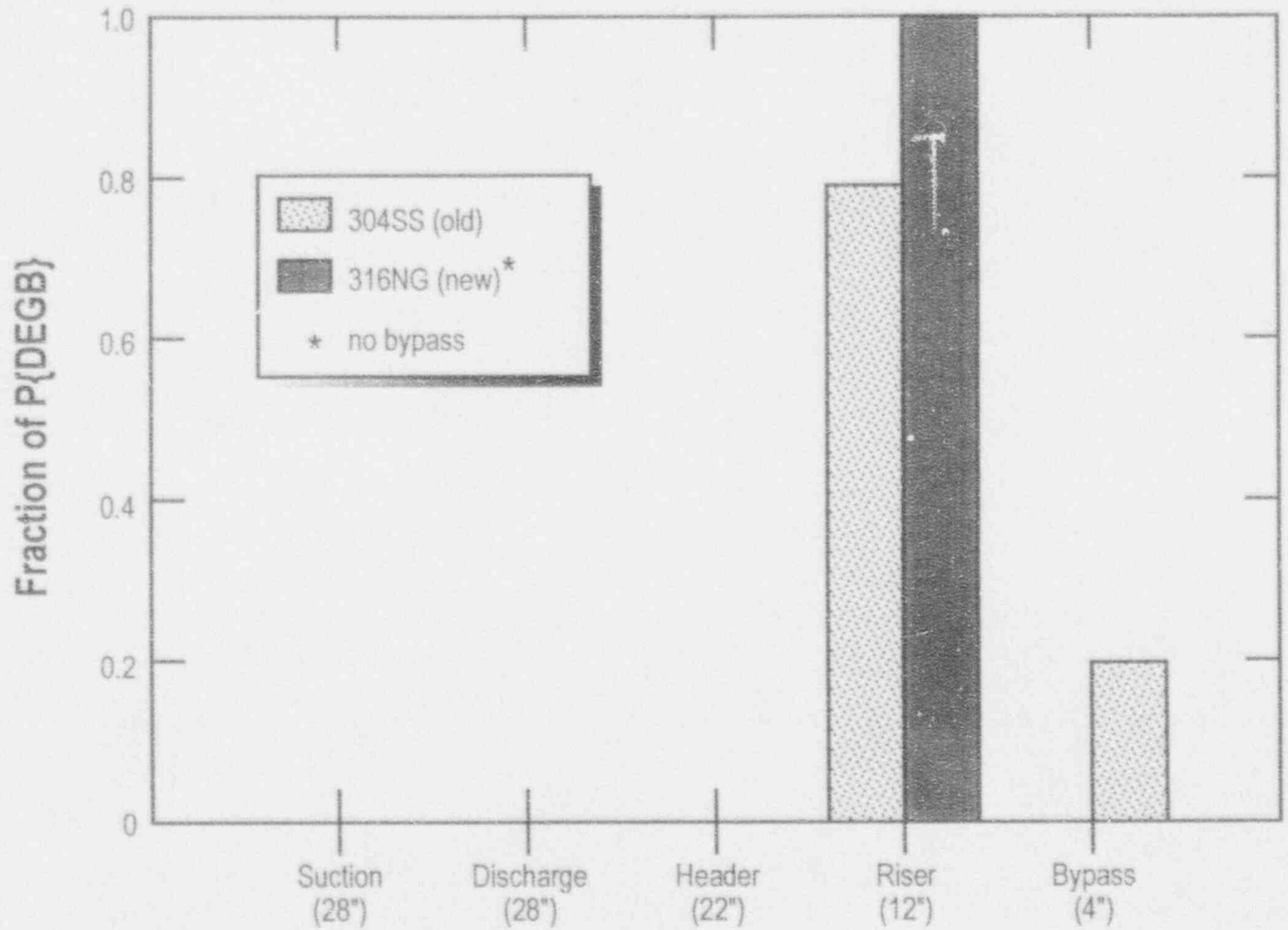

Reproduced from Fig. 4.11(b), Vol. 1 of NUREG/CR-4792

Figure 4-2. Relative Contribution of Various Welds to DEGB in Recirculation Loop

identifying the most significant limitations associated with the IGSCC portion of the analysis. Some of the limitations of the LLNL IGSCC analysis tha. were identified include:

1) Certain local phenomena were not considered in the LLNL analysis, for example the effect of coolant flow velocity on possible flushing of impurities that otherwise could aggravate the susceptibility to IGSCC.

2) The model used "harsh" laboratory conditions to predict growth rates and times-to-initiation. It is conservative to extrapolate the "harsh" laboratory data to the relatively benign conditions that exist in reactor facilities.

3) The failure probability is very sensitive to the type of residual stress assumed in the analysis. Consequently, plant-to-plant experiences could vary significantly depending on residual stresses that remain following pipe assembly welding and "fit up". Worst case stress assumptions were used in the analysis.

4) The analysis did not give credit for actions to mitigate the effects of IGSCC, specifically in-service inspections, weld overlay, or inductive heating stress improvement (IHSI). In addition, the analysis did not address the mitigating effects of corrosion control programs.

5) The main objective of the analysis was to compare the behavior of different types of materials to IGSCC. This emphasis may introduce additional uncertainties in the absolute value of the break frequencies.

6) There were discrepancies between the LLNL predictions and a field test done at a BWR site. As noted in NUREG/CR-5486 (Ref. 4.3), these discrepancies most likely are the result of field variations in various pertinent phenomena and analytical assumptions needed to model these phenomena. However, it is important to note that both the LLNL analysis and field results give highest priority to riser and bypass welds.

7) The LLNL analysis assumed that IGSCC effects could be ignored regarding pipe breaks of the main steam and feedwater piping.

8) Pipe breaks caused by water hammer or a projectile from pump failures were not considered.

9) The analysis did not consider scenarios that involved IGSCC-weakened piping coupled with other pipe challenges (i.e., water hammer, seismic events).

4.2 Recommended Weld Break Frequency Data

The IGSCC-induced DEGB data generated by LLNL were used as a starting point in deriving estimates of weld break frequencies for use in the debris blockage analysis. In using the LLNL predictions of IGSCC-induced DEGB frequency for this analysis, adjustments were made to give credit for in-service inspection activities. Subsection 4.2.1 discusses the assumptions made in the use and refinement of the LLNL IGSCC data. Subsection 4.2.2 presents point estimates of the weld frequencies.

4.2.1 Assumptions Made in the Use and Refinement of LLNL IGSCC Data

In applying the LLNL data to this study, the following assumptions were made:

1) Of the two categories of breaks evaluated in the LLNL analysis (leaks and DEGBs), only breaks in the DEGB category were considered. It was assumed that the predicted breaks in the "leak" category would either represent mathematically-predicted flaws that do not actually pass coolant, or would only allow the passage of coolant at a rate less than needed for ECCS actuation. If either of these two conditions were to exist, sump blockage would not be of concern.

2) Susceptible material (304SS) was assumed to be the material of interest.

3) Welds associated with main steam and feedwater piping would have the same break frequencies as the 22"-28" recirculation welds.

4) Only one IGSCC mitigating action would be in place, namely an in-service inspection program. In adjusting the data for an in-service inspection program, use was made of a discussion of risk-based inspection activities contained in CRTD-Vol. 20-2 (Ref. 4.1). In particular, it was noted on p. 81 of this document that "a high level of inspection can significantly reduce the failure probabilities of BWR piping systems (by a factor of 10 or more)." Supporting data and analyses are contained in this reference. For the purpose of the strainer blockage analysis, it was decided that the LLNL frequency estimates would be reduced by a factor of 10 to account for in-service inspection. The effect of this in-service inspection adjustment is to lower the 304SS DEGB frequency to a value slightly above that predicted for the non-susceptible material (316NG). This situation is illustrated in Figure 4-1.

4.2.2 Recommended Frequency Estimates for Weld Breaks

By using the LLNL IGSCC data for the DEGB category and the assumptions discussed above in Subsection 4.2.1, estimates for weld break frequencies were generated. The recommended weld break point-estimate frequencies are given in Table 4-1. The data in Table 4-1 were generated by applying the in-service inspection reduction factor of 10 discussed above to the LLNL IGSCC DEGB data as described more thoroughly in Appendix A. The data in Table 4-1 were applied to specific categories of DAEC-Unit 1 piping as shown in Table 4-2.

It is important to recognize that there are large uncertainties associated with the recommended point-value frequency estimates. Because an uncertainty analysis has not been performed, it is not possible to further interpret the statistical significance of the point-value estimates given in Table 4-1 or 4-2.

4.3 BLOCKAGE 2.0 Pipe Break Frequency Estimates

The per-weld break frequencies given in Table 4-2 were used as input for BLOCKAGE 2.0 pipe break frequency calculations. BLOCKAGE 2.0 then assigned appropriate weld break frequencies for each weld depending on the weld diameter and piping system in which that weld is located. The overall pipe break frequency was subsequently obtained by simply summing the break frequencies of all the welds included in the analysis.

The per-weld break frequencies given in Table 4-2 were used as input for BLOCKAGE 2.0 pipe break frequency calculations. In applying the Table 4-2 data to generate pipe break frequencies, appropriate summations were made of all individual weld break frequencies in three separate categories, specifically:

- Pipe system,
- Pipe diameter, and
- Pipe location.

For example, the break frequency F_s of a given pipe system was calculated to be:

$$F_s = \sum_{1}^{n} f_i^s ,$$

where,

f_i^s represents the frequency of the ith weld on the selected system category s, and n is the total number of welds in that system.

Table 4-1

Recommended Weld DEGB Frequency Estimates

Pipe Category	Per-weld DEGB Frequency (1/Rx-yr)
4" Recirculation (304SS)	1E-06
12" Recirculation (304SS)	2E-06
22 - 28" Recirculation (304SS)	2E-07
Main Steam	2E-07
Feedwater	2E-07

Table 4-2

Weld DEGB Frequency Data for DAEC-Unit 1

Pipe Category	Per-weld DEGB Frequency (1/Rx-yr)
1" - 10" Recirculation	1E-06
16" Recirculation	2E-06
22" Recirculation	2E-07
All Main Steam	2E-07
All Feedwater	2E-07

The break frequency F_d of a given diameter piping was calculated to be:

$$F_d = \sum_{1}^{n} f_i^d,$$

where,

f_i^d represents the frequency of the i^{th} weld in the selected pipe diameter category d, and n is the total number of welds.

Finally, the break frequency F_L of co-located piping was calculated to be:

$$F_L = \sum_{1}^{n} f_i^L,$$

where,

f_i^L represents the frequency of the i^{th} weld in a selected location category L, and n is the total number of welds in the category.

Tables 4-3, 4-4, and 4-5 summarize the calculations of pipe break frequencies.

Table 4-3

Pipe Break frequency Estimates Categorized by System

Pipe Diameter	Total No. of Welds	Per-Weld DEGB Frequency (1/Rx-yr)[1]	Pipe Break Frequency Estimate (1/Rx-yr)[2] Individual Pipe Size Category	Total[3]
		a) Recirculation System		
1"	25	1E-06	2.5E-05	
1.25"	2	1E-06	2E-06	
2"	2	1E-06	2E-06	
4"	26	1E-06	2.6E-05	
10"	40	1E-06	4E-05	
16"	8	2E-06	1.6E-05	
22"	37	2E-07	7.4E-06	
				1.2E-04
		b) Main Steam System		
1"	16	2E-07	3.2E-06	
2"	12	2E-07	2.4E-06	
6"	1	2E-07	2E-07	
20"	63	2E-07	1.3E-05	
				1.8E-04
		c) Feedwater System		
10"	58	2E-07	1.2E-05	
16"	10	2E-07	2E-06	
				1.4E-05
			Total for All Three Systems	1.5E-04

Notes:
1) Data extracted from Table 4-2.
2) Pipe break frequency estimates generated by multiplying total no. of welds and corresponding per-weld DEGB frequency.
3) Total pipe break frequency for a given system.

Table 4-4
Pipe Break Estimates Categorized by Pipe Diameter

System	Total No. of Welds	Per-Weld DEGB Frequency (1/Rx-yr)[1]	Pipe Break Frequency Estimate (1/Rx-yr)[2] Individual System	Total[3]
		a) 1" Pipe Diameter		
Recirculation	25	1E-06	2.5E-05	2.8E-05
Main Steam	16	2E-07	3.2E-06	
		b) 1.25" Pipe Diameter		
Recirculation	2	1E-06	2E-06	2E-06
		c) 2" Pipe Diameter		
Recirculation	2	1E-06	2E-06	4.4E-06
Main Steam	12	2E-07	2.4E-06	
		d) 4" Pipe diameter		
Recirculation	26	1E-06	2.6E-05	2.6E-05
		e) 6" Pipe Diameter		
Main Steam	1	2E-07	2E-07	2E-07
		f) 10" Pipe Diameter		
Recirculation	40	1E-06	4E-05	5.2E-05
Feedwater	58	2E-07	1.2E-05	
		g) 16" Pipe Diameter		
Recirculation	8	2E-06	1.6E-05	1.8E-05
Feedwater	10	2E-07	2E-06	
		h) 20" Pipe Diameter		
Main Steam	63	2E-07	1.3E-05	1.3E-05
		i) 22" Pipe Diameter		
Recirculation	37	2E-07	7.4E-06	7.4E-06
			Overall Total	1.5E-04

Notes:
1) Data extracted from Table 4-2.
2) Pipe break frequency estimates generated by multiplying total n . of welds and corresponding per-weld DEGB frequency.
3) Total pipe break frequency for a given pipe diameter class.

Table 4-5
Pipe Break frequency Estimates Categorized by Pipe Location

System	Pipe Diameter	Total No. of Welds	Per-Weld DEGB Frequency (1/Rx-yr)[1]	Pipe Break Frequency Estimate (1/Rx-yr)[2] Individual System Category	Total[3]
			a) Above 776′ Grating (H)		
Recirculation	1"	8	1E-06	8E-06	
Recirculation	4"	2	1E-06	2E-06	
Recirculation	10"	24	1E-06	2.4E-05	
Recirculation	22"	7	2E-07	1.4E-06	
Feedwater	10"	58	2E-07	1.2E-05	
Feedwater	16"	2	2E-07	4E-07	
Main Steam	6"	1	2E-07	2E-07	
Main Steam	20"	40	2E-07	8E-06	
					5.6E-05
			b) Between Gratings (M)		
Recirculation	1"	9	1E-06	9E-06	
Recirculation	4"	4	1E-06	4E-06	
Recirculation	10"	16	1E-06	1.6E-05	
Recirculation	16"	8	2E-06	1.6E-05	
Recirculation	22"	11	2E-07	2.2E-06	
Feedwater	16"	8	2E-07	1.6E-06	
Main Steam	1"	16	2E-07	3.2E-06	
Main Steam	20"	23	2E-07	4.6E-06	
					5.7E-05
			c) Below 757′ Grating (L)		
Recirculation	1"	8	1E-06	8E-06	
Recirculation	1.25"	2	1E-06	2E-06	
Recirculation	2"	2	1E-06	2E-06	
Recirculation	4"	20	1E-06	2E-05	
Recirculation	22"	19	2E-07	3.8E-06	
Main Steam	2"	12	2E-07	2.4E-06	
					3.8E-05
				Total for All Three Locations	1.5E-04

Notes:
1) Data extracted from Table 4-2.
2) Pipe break frequency estimates generated by multiplying total no. of welds and corresponding per-weld DEGB frequency.
3) Total pipe break frequency for a given pipe location.

References for Section 4

4.1 The American Society of Mechanical Engineers, "Risk-Based Inspection -- Development of Guidelines, Volume 2 - Part 1, Light Water Reactor (LWR) Nuclear Power Plant Components," CRTD-Vol. 20-2, 1992.

4.2 G. S. Holman and C. K. Chou, "Probability of Failure in BWR Reactor Coolant Piping," published as Lawrence Livermore National Laboratory report UCID-20914, NUREG/CR-4792, March 1989.

4.3 G.S. Holman, "Application of Reliability Techniques to Prioritize BWR Recirculation Loop Welds for In-Service Inspection," published as Lawrence Livermore National Laboratory report UCID-21838, NUREG/CR-5486, December 1989.

5.0 SCREE BLOCKAGE MODELS

5.1 Introduction

Debris generation, their transport to the suppression pool and ultimately to the strainer, and strainer blockage by the debris is a complex process. As part of USI A-43 study, NUREG/CR-2791 (Ref. 5.1) attempted to develop analytical models for each stage of accident progression in PWRs. However, these attempts were abandoned and a more empirical approach was adopted as described in NUREG-0897, Rev. 1 (Ref 5.2). These later empirical models were in most cases based on experimental data, obtained as part of the USI A-43 study. NUREG-0897, Rev. 1, discussed various models, their applicability to BWRs and their limitations. The present study closely adhered to the recommendations of NUREG-0897, Rev. 1 (Ref. 5.2). Various models were, however, slightly modified to account for differences in BWR and PWR containment layouts and to incorporate key insights gained from more recent experiments.

5.2 Debris Generation Model

Following the evaluation of break locations and their orientations (Section 3.0), the amount and type of insulation debris generated by postulated breaks must be calculated. This section summarizes the model used to estimate types and quantities of debris generated by each weld break.

5.2.1 Review of USI A-43 Debris Generation Model

Initially, USI A-43 postulated three mechanisms (pipe whip, pipe impact and jet impingement) for insulation debris generation. However, initial analyses summarized in NUREG/CR-2791 (Ref 5.1) showed that contributions of pipe whip and pipe impact are of secondary importance. Consequently, NUREG-0897, Rev. 1 (Ref. 5.2), focused on estimating debris generated by jet impingement, and ignored contribution by other two mechanisms.

Determination of the extent of potential damage to the insulation caused by an expanding high energy two-phase jet from a double ended guillotine break is extremely complicated. As a result, USI A-43 adapted a two prong approach: Heissdampfreaktor (HDR) jet impingement experiments and Sandia National Laboratories (SNL) two-phase jet expansion modeling.

The destructive nature of high pressure jets has been experimentally investigated at the HDR facility. In these blowdown tests (blowdown from 110 bars and 280-315 °C), all glass fiber insulation was destroyed within two meters of the break nozzle[12] and distributed throughout the HDR containment in the shape of very fine particles. In addition, iron wrappers were thrown away from the piping within 4 to 6 meters of the break with the fiber untouched. With the fibrous insulation encapsulated in steel

[12] Break nozzles 200-mm, 350-mm and 430-mm in diameter were investigated.

sheets, the damage was considerably reduced (See Appendix-F of Ref. 5.2). Based on these experiments the following conclusions were reached:

1. The pressure wave mainly destroys the covers around the fibrous insulation. Then, the impact of the fluid jet peels off the unprotected fibrous layer.

2. The jet forces act only in a diameter of 2-5 m around the nozzle, depending on the break diameter and break geometry.

The jet expansion model proposed in NUREG-0897, Rev. 1 (Ref. 5.2), is a result of the SNL study of the HDR data. This study calculated two-dimensional pressure distributions in space for expanding jets representative of PWR and BWR blowdown conditions. These jet expansion models are documented in NUREG/CR-2913 (Ref. 5.3). Significant findings of the SNL study are as follows:

1. Target pressure loadings increase asymptotically at L/D's less than 3.0 to the break exit pressures. At L/D's less than 3, survivability of insulation materials is highly unlikely.

2. At L/D's from 5 to 7, the centerline stagnation pressure becomes essentially constant at approximately 2 ± 1 bars.

3. The multidimension pressure field loads the target over a large region which can be approximated by a 90° jet cone expansion model. The hemisphere geometry can be another approximation for this expanding pressure field.

The two-phase jet modeling results and the levels of insulation damage evidenced by the HDR experiments led NUREG-0897, Rev. 1 (Ref. 5.2), to the development of a three-region jet-debris generation model. Figure 5-1, reproduced from Ref. 5.2, illustrates these regions together with the isobar contours for a break pressure of 150 bars and a subcooling of 35 K. In Region I ($0 \leq L/D \leq 3$), extremely high levels of destruction would occur due to very high jet pressures, exceeding 10 bars. Region II ($3 \leq L/D \leq 7$) is characterized by moderate jet pressures in the range of 10 to 3 bars. In this region high levels of damage are possible, but factors such as type of insulation and whether insulation is encapsulated should be considered to estimate the volume of debris generated. Finally, Region III (L/D's > 7 from the break) is a zone where destruction is likely to be dislodgement of insulation and may be in the worst case result in large shreds. This third region is assumed to extend until the length where the jet thrust would

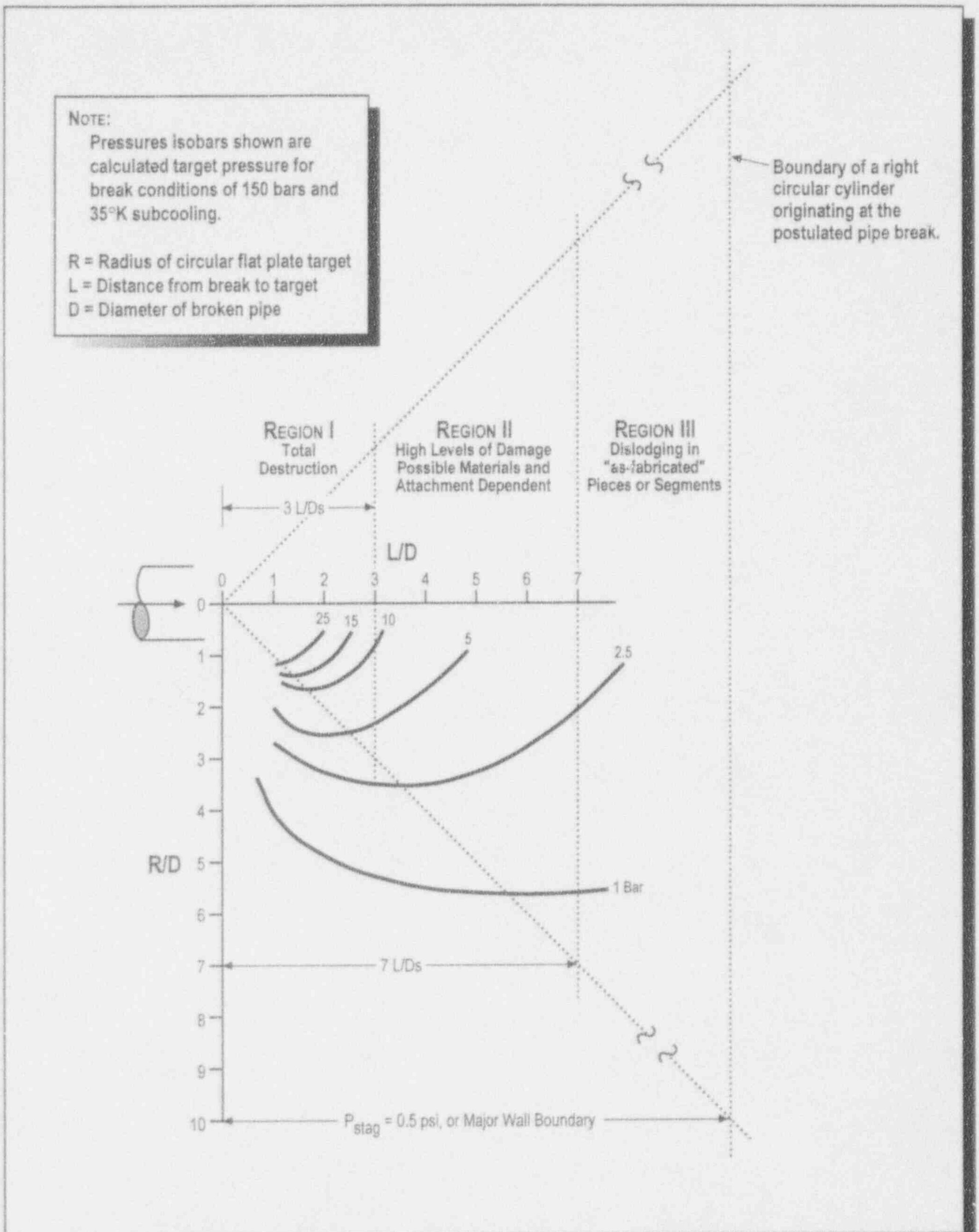

Figure 5-1. Multiple Region Insulation Debris Generation Model

be equal to 0.5 psig[13]. The USI A-43 study recognized that lengths of these regions would be different for BWRs where the break pressures are expected to be no larger than 80 bars, compared to 150 bars for a typical PWR. The study also pointed out that the extent of damage to the unjacketed fibrous insulation is near total, whereas the same blankets encapsulated in steel jackets would be damaged only partially.

5.2.2 BWR Debris Generation Model

The USI A-43 model was modified for BWRs, characterized by saturated fluid at the break and stagnation pressures on the order of 80 bars. Constant pressure contours for this case are calculated using the SNL two-phase model described in NUREG/CR-2913 (Ref. 5.3) and displayed in Figure 3.42 of NUREG-0897 (Ref. 5.2), Rev. 1, which are reproduced here as Figure 5-2. As is evident from this figure, the jet pressure fields for a BWR break decay rapidly with distance from the break. If total destruction is assumed for pressures above 10 bars as in USI A-43, the Region I extends from the break only up to a L/D slightly larger than 2. Similarly, Region II, characterized by moderate pressures (2.5-10 bars), is bounded by $2 \leq L/D \leq 5$. Finally, Region III extends from an axial length of 5D to a length where the pressure would be equal to 0.5 psig. The upper bound for Region III can be established using Moody's two-phase jet model, or through usage of experimental data. This adaption of the USI A-43 approach constitutes the basic debris generation model used in this study for BWRs.

In order to ensure that the debris generation model predictions provide a conservative upper bound in all cases, the following region boundaries were redefined for this study, and are shown in Figure 5-2, along with the isobar contours predicted by the SNL two-phase jet model.

Region I Outer bound: Region I extends up to a length of 3 L/D, similar to USI A-43. This extension accounts for uncertainties associated with possible extensive damage for pressures down to 5 bars, instead of 10 bars assumed in USI A-43.

Region III Outer bound: It is assumed that the outer bound for Region III is 7 L/D based on two sets of experimental data: original HDR tests for NUKON™ pillows (Appendix-F of Ref. 5.2) and more recent NUKON™ tests at Colorado Engineering Experiment Station Inc. (CEESI) by Performance Contracting, Inc. (Ref. 5.5). It should also be noted that the predicted jet pressure field at L/D of 7 is only slightly larger than 0.5 psig. Finally, this 7D limit is also consistent with 1982 and 1983 Alden research Laboratories (ARL) experiments sponsored by the NRC (Ref. 5.2 and 5.6).

---

[13] NUREG-0897, Rev. 1 (Ref. 5.2), conservatively assumed that damage is possible for jet pressures larger than 0.5 psig. In reality, this value is probably material dependent.

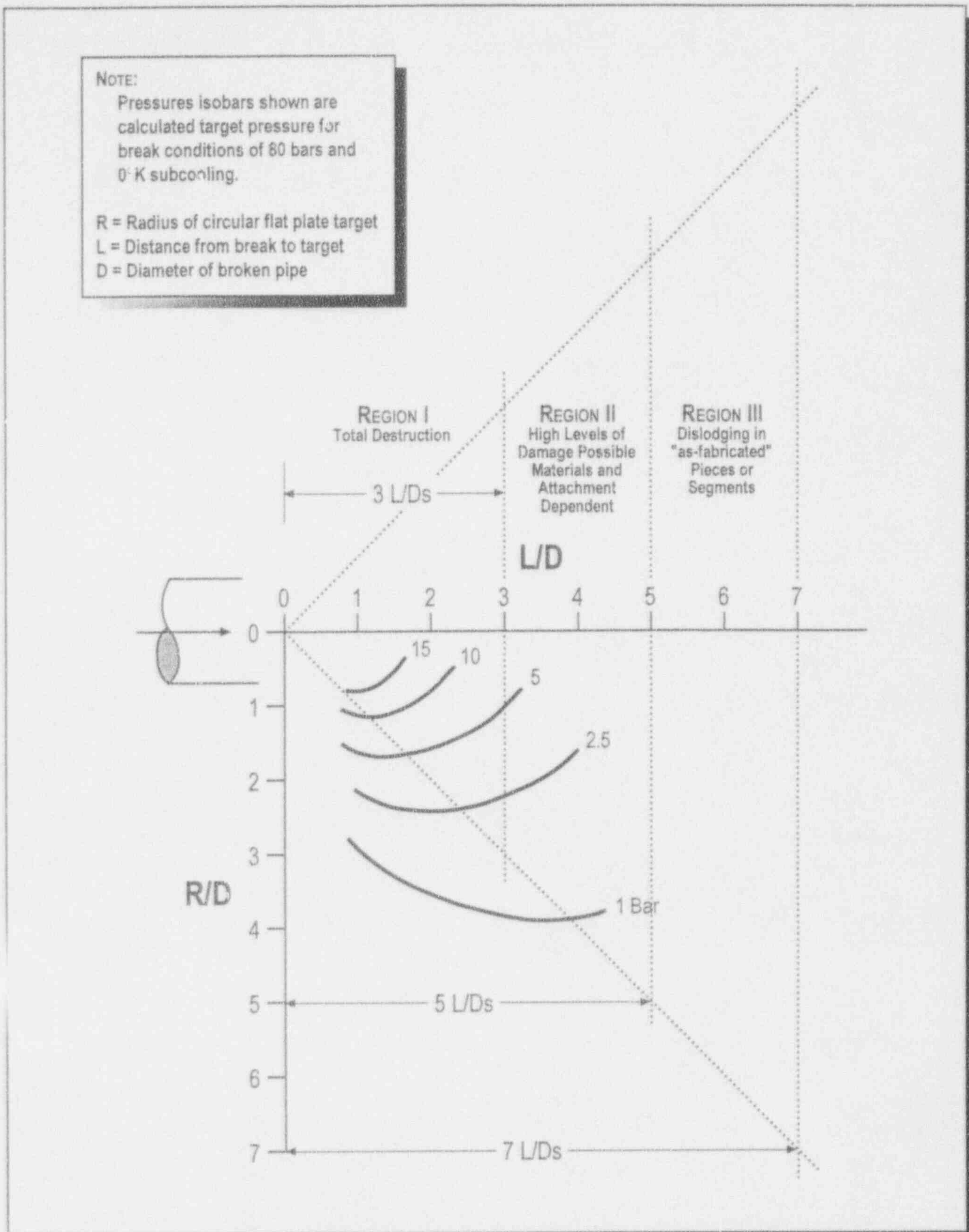

Figure 5-2. Three Region Model Used in the Present Study

As discussed in Section 5.2.1, the fraction of debris in each region shredded into transportable sizes[14] varies with the type of insulation and mode of encapsulation. The HDR tests revealed that steel jacketed insulation is less susceptible to destruction as compared to non-jacketed insulation. Also, factors such as pressure wave reflection by the surrounding structures influence the quantity and type of debris generated. As a result, no generic values can be assigned for these fractions. Initial studies assigned a rather unrealistic fraction of 1.0 for all regions, implying that all insulation in all three regions is dislodged. This study opted to vary the fraction of debris generated over a range obtained through engineering judgement based on experimental data for steel jacketed NUKON™ blankets. HDR experiments with a stagnation pressure of 110 bars, demonstrated that up to a maximum of 75% of the steel jacketed insulation can be damaged in Region I (i.e., $0 \leq L/D \leq 3$). Considering that BWR stagnation pressures are about 80 bars, the fraction of insulation damaged would probably be in the order of 50%. Thus, the volume of debris generated in Region I was conservatively estimated to be 0.75 times the total volume of insulation present in this region. Similarly, destruction fractions in Regions II and III was assumed to be 0.6, and 0.4, respectively. As noted above, these values were established based on engineering judgement. Nevertheless, it is highly unlikely that for steel jacketed NUKON™ insulation the fraction of transportable debris would exceed the base case values of 0.75, 0.6, and 0.4 for Regions I, II and III respectively. A parametric study was performed to examine the impact of the value of the destruction factor on ECCS strainer blockage frequency.

5.2.3 Application to DAEC Unit 1

The BWR debris generation model described above was applied to DAEC Unit 1 to estimate the volume and type of debris generated by each weld. For each weld, the plant drawings (P&ID and Isometric drawings) were utilized (a) to identify the number of pipes that fall within the zone of influence (i.e. number of target pipes), and (b) to determine diameter, length, and orientation with respect to the weld of each target pipe. The target pipes were selected using the following criteria:

1. The only target pipe of concern is the pipe in which the break occurred. Other primary piping sections in the surrounding areas are eliminated from consideration.

2. In most cases, the jet is assumed to discharge from both ends of the DEGB, since blowdown is expected from both directions. In selected cases, such as MSLs and recirculation discharge bypass lines, the target pipe length is calculated assuming a unidirectional jet.

---

[14] Transportable size is defined in this study as small to medium shreds and fines.

3. The shadowing effect of containment structures, such as gratings and pipe restraints, was neglected.

Figure 5-3 illustrates the debris generation model used in this study. The zone of influence was divided into three regions (Regions I, II, and III) defined by L/D = 3, 5, and 7, respectively. The target pipe length for each region is the total length of the target pipe that falls in that region. Tables 5-1, 5-2 and 5-3 present break diameter and location, insulation type and thickness, and target pipe diameter and length for each of the postulated breaks in the recirculation, feedwater and main steam lines, respectively. These tables essentially constitute the 'WELD.INP' file provided as input to BLOCKAGE 2.0, which uses the following equation to calculate the total volume of available insulation in each region, V_R (ft^3), for each weld:

$$V_R = \sum_{i=1}^{N_{target}} [C\ \pi/4\ ((D+2I)^2 - D^2)_i\ L_{iR}] \qquad 5.1$$

where,

R is the Region (I, II and III),
i is the target number (1 to total no. of targets),
D is the target pipe diameter (in.),
I is the thickness of the insulation blanket (in.),
L_{iR} is the length of i^{th} target in R^{th} Region (ft.), and
C is a unit-conversion factor.

The debris generation model of BLOCKAGE 2.0 is based on the consideration that <u>not</u> all the volume of debris within the zone of influence is destructed into transportable shreds and dislodged from the target pipe. As such, the volume of insulation which is in the form of fines or shreds capable of being transported to the suppression pool can be estimated as:

$$V_g = \sum_{R=I,\ II,\ III} V_R * F_R \qquad 5.2$$

where,

V_g is the volume of insulation generated by a break,
V_R is the volume of available insulation in R^{th} Region (Equation 5.1),
F_R is the fraction of that insulation that was actually destructed into shreds and fines by the expanding jet.

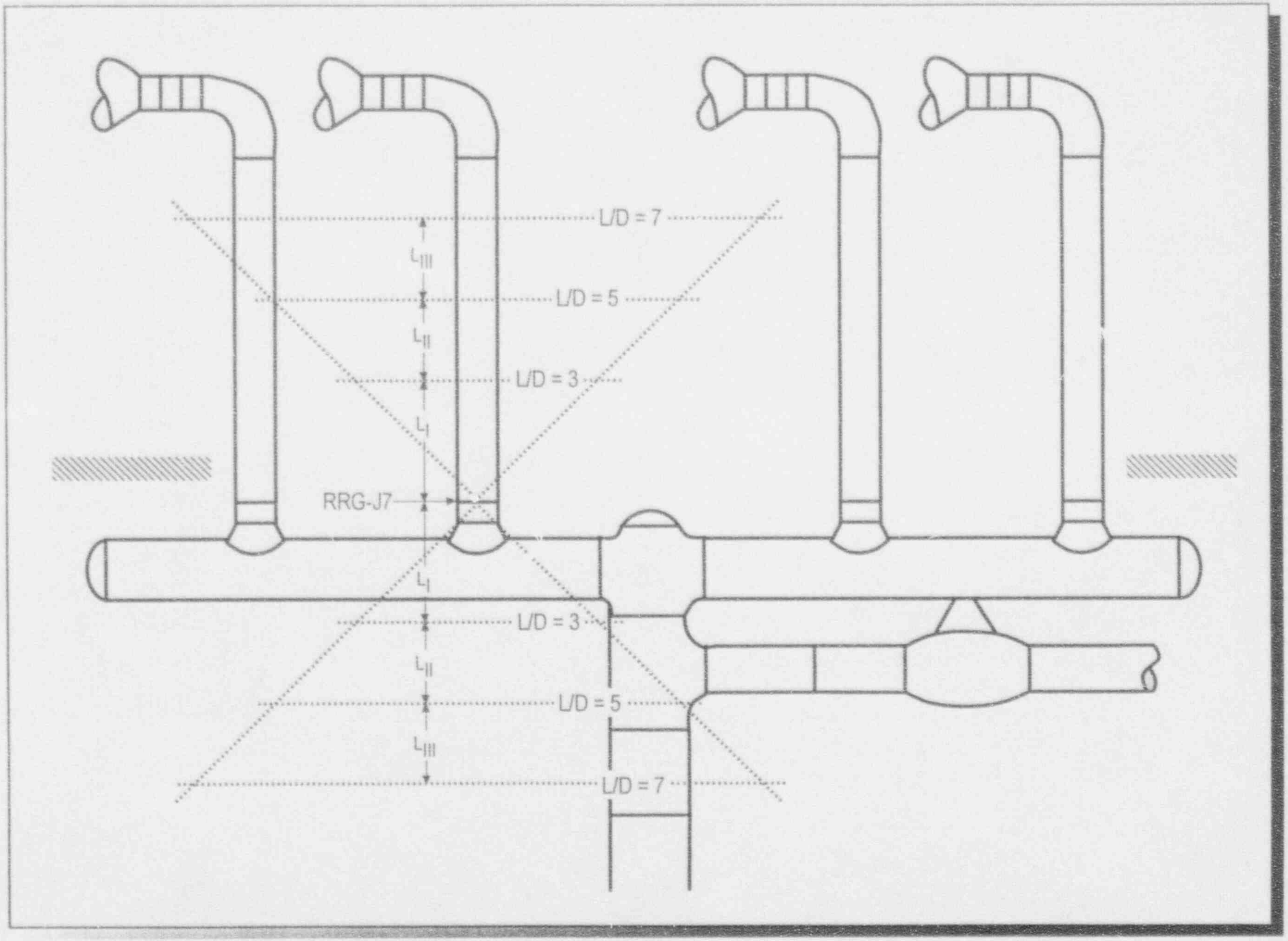

Figure 5-3. Debris Generation Model Used to Estimate Total Insulation Volume in Regions I, II, III for Break Postulated in Riser Pipe G

Table 5-1. Listing of Welds in Recirculation Loops A and B. Welds in Suction Bypass and Riser lines are included.

WELD ID	Sys ID #	WELD INFORMATION Dia. (inch)	WELD INFORMATION Type	WELD INFORMATION Location‡ H,M,L	TARGET INFORMATION Total No.	TARGET INFORMATION #	TARGET INFORMATION Dia. (inch)	INSULATION Sys.	INSULATION Type	INSULATION Thick (inch)	TARGET LENGTH L/D=3 (ft)	TARGET LENGTH L/D=5 (ft)	TARGET LENGTH L/D=7 (ft)
RCA-J003	1	22.00	S1	H	1	1	22.00	RCA	NK	3.00	7.33	11.00	14.67
RCA-J004	1	22.00	S1	H	1	1	22.00	RCA	NK	3.00	8.25	12.00	15.60
RCA-J005	1	22.00	S1	H	1	1	22.00	RCA	NK	3.00	11.00	18.33	25.67
RCA-J006	1	22.00	S1	H	1	1	22.00	RCA	NK	3.00	11.00	18.33	25.67
RCA-J008	1	22.00	S1	M	1	1	22.00	RCA	NK	3.00	11.00	18.33	25.67
RCA-J012	1	22.00	S1	L	1	1	22.00	RCA	NK	3.00	11.00	18.33	25.67
RCA-J013	1	22.00	S1	L	1	1	22.00	RCA	NK	3.00	11.00	18.33	25.67
RCA-J015	1	22.00	S1	L	1	1	22.00	RCA	NK	3.00	11.00	18.33	25.67
RCA-J021	1	22.00	S1	L	1	1	22.00	RCA	NK	3.00	11.00	18.33	25.67
RCA-J022	1	22.00	S1	L	1	1	22.00	RCA	NK	3.00	11.00	18.33	25.67
RCA-J05A	1	4.00	S2	H	1	1	4.00	RCA	NK	3.00	1.00	1.67	2.33
RCA-J05B	1	4.00	S2	H	1	1	4.00	RCA	NK	3.00	1.00	1.67	2.33
RCA-J010	1	1.00	S1	L	1	1	1.00	RCA	NK	2.00	0.25	0.42	0.58
RCA-J016	1	1.25	S1	L	1	1	1.25	RCA	NK	2.00	0.31	0.52	0.73
RCA-J018	1	4.00	S2	L	1	1	4.00	RCA	NK	3.00	1.00	1.67	2.33
RCA-J019	1	2.00	S1	L	1	1	2.00	RCA	NK	2.50	0.50	0.83	1.17
RCA-J020	1	1.00	S1	L	1	1	1.00	RCA	NK	2.00	0.25	0.42	0.58
RCA-J024	1	22.00	S1	L	1	1	22.00	RCA	NK	3.00	5.50	9.16	12.85
RCA-J028	1	22.00	S1	L	1	1	22.00	RCA	NK	3.00	11.00	18.33	25.67
RCA-J030	1	22.00	S1	L	1	1	22.00	RCA	NK	3.00	11.00	18.33	25.67
RCA-J032	1	22.00	S1	L	1	1	22.00	RCA	NK	3.00	11.00	18.33	25.67
RCA-J038	1	22.00	S1	L	1	1	22.00	RCA	NK	3.00	11.00	18.33	25.67
RCA-J041	1	22.00	S1	M	1	1	22.00	RCA	NK	3.00	11.00	18.33	25.67
RCA-J043	1	22.00	S1	M	1	1	22.00	RCA	NK	3.00	11.00	18.33	25.67
RCA-J025	1	1.00	S1	L	1	1	1.00	RCA	NK	2.00	0.25	0.42	0.58
RCA-J036	1	1.00	S1	M	1	1	1.00	RCA	NK	2.00	0.25	0.42	0.58
RCA-J037	1	1.00	S1	M	1	1	1.00	RCA	NK	2.00	0.25	0.42	0.58
RCA-J039	1	1.00	S1	M	1	1	1.00	RCA	NK	2.00	0.25	0.42	0.58
RCA-J040	1	1.00	S1	M	1	1	1.00	RCA	NK	2.00	0.25	0.42	0.58
RCA-J027	1	4.00	S2	L	1	1	4.00	RCA	NK	3.00	1.00	1.67	2.33
RBA-J001	1	4.00	S3	L	1	1	4.00	RBA	NK	3.00	1.00	1.67	2.33
RBA-J002	1	4.00	S3	L	1	1	4.00	RBA	NK	3.00	2.00	3.33	4.67
RBA-J003	1	4.00	S3	L	1	1	4.00	RBA	NK	3.00	2.00	3.33	4.67
RBA-J006	1	4.00	S3	L	1	1	4.00	RBA	NK	3.00	2.00	3.33	4.67
RBA-J007	1	4.00	S3	L	1	1	4.00	RBA	NK	3.00	2.00	3.33	4.67
RBA-J008	1	4.00	S3	L	1	1	4.00	RBA	NK	3.00	2.00	3.33	4.67
RBA-J009	1	4.00	S3	L	1	1	4.00	RBA	NK	3.00	2.00	3.33	4.67
RBA-J010	1	4.00	S3	L	1	1	4.00	RBA	NK	3.00	2.00	3.33	4.67
RBA-J012	1	4.00	S3	M	1	1	4.00	RBA	NK	3.00	2.00	3.33	4.67
RCA-J034	1	4.00	S2	M	1	1	4.00	RBA	NK	3.00	1.00	1.67	2.33
RMA-J006	1	22.00	S1	M	1	1	22.00	RMA	NK	3.00	0.90	0.90	0.90
RMA-J005	1	16.00	S1	M	1	1	16.00	RMA	NK	3.00	8.00	13.33	18.67
RMA-J007	1	16.00	S1	M	1	1	16.00	RMA	NK	3.00	8.00	13.33	18.67
RMA-J001	1	16.00	S1	M	1	1	16.00	RMA	NK	3.00	0.90	0.90	0.90
RMA-J011	1	16.00	S1	M	1	1	16.00	RMA	NK	3.00	0.90	0.90	0.90
RMA-J010	1	10.00	S1	M	2	1	10.00	RRE	NK	2.50	2.50	4.17	5.83
						2	16.00	RMA	NK	3.00	5.00	8.33	11.67
RMA-J008	1	10.00	S1	M	2	1	10.00	RRF	NK	2.50	2.50	4.17	5.83
						2	16.00	RMA	NK	3.00	5.00	8.33	11.67
RMA-J004	1	10.00	S1	M	2	1	10.00	RRG	NK	2.50	2.50	4.17	5.83
						2	16.00	RMA	NK	3.00	5.00	8.33	11.67
RMA-J002	1	10.00	S1	M	2	1	10.00	RRH	NK	2.50	2.50	4.17	5.83
						2	16.00	RMA	NK	3.00	5.00	8.33	11.67
RRE-J007	1	10.00	S1	M	1	1	10.00	RRE	NK	2.50	5.00	8.33	11.67
RRE-J005	1	10.00	S1	H	1	1	10.00	RRE	NK	2.50	5.00	8.33	11.67
RRE-J004	1	10.00	S1	H	1	1	10.00	RRE	NK	2.50	5.00	8.33	11.67
RRE-J003	1	10.00	S1	H	1	1	10.00	RRE	NK	2.50	5.00	8.33	11.67
RRE-J006	1	1.00	S1	H	1	1	1.00	RRE	NK	2.50	0.25	0.42	0.58
RRF-J007	1	10.00	S1	M	1	1	10.00	RRF	NK	2.50	5.00	8.33	11.67
RRF-J005	1	10.00	S1	H	1	1	10.00	RRF	NK	2.50	5.00	8.33	11.67
RRF-J004	1	10.00	S1	H	1	1	10.00	RRF	NK	2.50	5.00	8.33	11.67
RRF-J003	1	10.00	S1	H	1	1	10.00	RRF	NK	2.50	5.00	8.33	11.67
RRF-J006	1	1.00	S1	H	1	1	1.00	RRF	NK	2.00	0.25	0.42	0.58
RRG-J007	1	10.00	S1	M	1	1	10.00	RRG	NK	2.50	5.00	8.33	11.67
RRG-J005	1	10.00	S1	H	1	1	10.00	RRG	NK	2.50	5.00	8.33	11.67
RRG-J004	1	10.00	S1	H	1	1	10.00	RRG	NK	2.50	5.00	8.33	11.67
RRG-J003	1	10.00	S1	H	1	1	10.00	RRG	NK	2.50	5.00	8.33	11.67
RRG-J006	1	1.00	S1	H	1	1	1.00	RRG	NK	2.00	0.25	0.42	0.58
RRH-J007	1	10.00	S1	M	1	1	10.00	RRH	NK	2.50	5.00	8.33	11.67

Table 5-1. Listing of Welds in Recirculation Loops A and B. (Cont).

WELD ID	Sys ID #	WELD INFORMATION Dia. (inch)	Type	Location H,M,L	TARGET INFORMATION Total No.	#	Dia. (inch)	INSULATION Sys.	Type	Thick (inch)	TARGET LENGTH L/D=3 (ft)	L/D=5 (ft)	L/D=7 (ft)
RRH-J005	1	10.00	S1	H	1	1	10.00	RRH	NK	2.50	5.00	8.33	11.67
RRH-J004	1	10.00	S1	H	1	1	10.00	RRH	NK	2.50	5.00	8.33	11.67
RRH-J003	1	10.00	S1	H	1	1	10.00	RRH	NK	2.50	5.00	8.33	11.67
RRH-J006	1	1.00	S1	H	1	1	1.00	RRH	NK	2.00	0.25	0.42	0.58
RCB-J003	1	22.00	S1	H	1	1	22.00	RCB	NK	3.00	7.33	11.00	14.67
RCB-J004	1	22.00	S1	H	1	1	22.00	RCB	NK	3.00	8.25	12.00	15.60
RCB-J005	1	22.00	S1	H	1	1	22.00	RCB	NK	3.00	11.00	18.33	25.67
RCB-J006	1	22.00	S1	M	1	1	22.00	RCB	NK	3.00	11.00	18.33	25.67
RCB-J007	1	22.00	S1	M	1	1	22.00	RCB	NK	3.00	11.00	18.33	25.67
RCB-J009	1	22.00	S1	M	1	1	22.00	RCB	NK	3.00	11.00	18.33	25.67
RCB-J015	1	22.00	S1	L	1	1	22.00	RCB	NK	3.00	11.00	18.33	25.67
RCB-J016	1	22.00	S1	L	1	1	22.00	RCB	NK	3.00	11.00	18.33	25.67
RCB-J018	1	22.00	S1	L	1	1	22.00	RCB	NK	3.00	11.00	18.33	25.67
RCB-J024	1	22.00	S1	L	1	1	22.00	RCB	NK	3.00	11.00	18.33	25.67
RCB-J025	1	22.00	S1	L	1	1	22.00	RCB	NK	3.00	11.00	18.33	25.67
RCB-J011	1	1.00	S1	L	1	1	1.00	RCB	NK	2.00	0.25	0.42	0.58
RCB-J012	1	1.00	S1	L	1	1	1.00	RCB	NK	2.00	0.25	0.42	0.58
RCB-J013	1	1.00	S1	L	1	1	1.00	RCB	NK	2.00	0.25	0.42	0.58
RCB-J019	1	1.25	S1	L	1	1	1.25	RCB	NK	3.00	0.31	0.52	0.73
RCB-J021	1	4.00	S2	L	1	1	4.00	RCB	NK	2.50	1.00	1.67	2.33
RCB-J022	1	2.00	S1	L	1	1	2.00	RCB	NK	2.00	0.50	0.83	1.17
RCB-J023	1	1.00	S1	L	1	1	1.00	RCB	NK	2.00	0.25	0.42	0.58
RCB-J027	1	22.00	S1	L	1	1	22.00	RCB	NK	3.00	5.25	9.16	12.89
RCB-J031	1	22.00	S1	L	1	1	22.00	RCB	NK	3.00	11.00	18.33	25.67
RCB-J033	1	22.00	S1	L	1	1	22.00	RCB	NK	3.00	11.00	18.33	25.67
RCB-J035	1	22.00	S1	L	1	1	22.00	RCB	NK	3.00	11.00	18.33	25.67
RCB-J041	1	22.00	S1	M	1	1	22.00	RCB	NK	3.00	11.00	18.33	25.67
RCB-J044	1	22.00	S1	M	1	1	22.00	RCB	NK	3.00	11.00	18.33	25.67
RCB-J046	1	22.00	S1	M	1	1	22.00	RCB	NK	3.00	11.00	18.33	25.67
RCB-J028	1	1.00	S1	L	1	1	1.00	RCB	NK	2.00	0.25	0.42	0.58
RCB-J039	1	1.00	S1	M	1	1	1.00	RCB	NK	2.00	0.25	0.42	0.58
RCB-J040	1	1.00	S1	M	1	1	1.00	RCB	NK	2.00	0.25	0.42	0.58
RCB-J042	1	1.00	S1	M	1	1	1.00	RCB	NK	2.00	0.25	0.42	0.58
RCB-J043	1	1.00	S1	M	1	1	1.00	RCB	NK	2.00	0.25	0.42	0.58
RCB-J030	1	4.00	S2	L	1	1	4.00	RCB	NK	3.00	1.00	1.67	2.33
RBB-JOO1	1	4.00	S3	L	1	1	4.00	RBB	NK	3.00	1.00	1.67	2.33
RBB-J002	1	4.00	S3	L	1	1	4.00	RBB	NK	3.00	1.00	1.67	2.33
RBB-J003	1	4.00	S3	L	1	1	4.00	RBB	NK	3.00	1.00	1.67	2.33
RBB-J006	1	4.00	S3	L	1	1	4.00	RBB	NK	3.00	1.00	1.67	2.33
RBB-J007	1	4.00	S3	L	1	1	4.00	RBB	NK	3.00	1.00	1.67	2.33
RBB-J008	1	4.00	S3	L	1	1	4.00	RBB	NK	3.00	1.00	1.67	2.33
RBB-J009	1	4.00	S3	L	1	1	4.00	RBB	NK	3.00	1.00	1.67	2.33
RBB-J010	1	4.00	S3	L	1	1	4.00	RBB	NK	3.00	1.00	1.67	2.33
RBB-J012	1	4.00	S3	M	1	1	4.00	RBB	NK	3.00	1.00	1.67	2.33
RCB-J037	1	4.00	S2	M	1	1	4.00	RBB	NK	3.00	1.00	1.67	2.33
RMB-J007	1	22.00	S1	M	1	1	22.00	RMB	NK	3.00	0.92	0.92	0.92
RMB-J008	1	16.00	S1	M	1	1	16.00	RMB	NK	3.00	8.00	13.33	18.67
RMB-J006	1	16.00	S1	M	1	1	16.00	RMB	NK	3.00	8.00	13.33	18.67
RMB-J001	1	16.00	S1	M	1	1	16.00	RMB	NK	3.00	0.92	0.92	0.92
RMB-J012	1	16.00	S1	M	1	1	16.00	RMB	NK	3.00	0.92	0.92	0.92
RMB-J011	1	10.00	S1	M	2	1	10.00	RRA	NK	2.50	2.50	4.17	5.83
						2	16.00	RMB	NK	3.00	5.00	8.33	11.67
RMB-J009	1	10.00	S1	M	2	1	10.00	RRB	NK	2.50	2.50	4.17	5.83
						2	16.00	RMB	NK	3.00	5.00	8.33	11.67
RMB-J005	1	10.00	S1	M	2	1	10.00	RRC	NK	2.50	2.50	4.17	5.83
						2	16.00	RMB	NK	3.00	5.00	8.33	11.67
RMB-J002	1	10.00	S1	M	2	1	10.00	RRD	NK	2.50	2.50	4.17	5.83
						2	16.00	RMB	NK	3.00	5.00	8.33	11.67
RMB-J004	1	1.00	S1	M	2	1	1.00	RMB	NK	2.00	0.25	0.42	0.58
						2	16.00	RMB	NK	3.00	0.50	0.83	1.17
RRA-J007	1	10.00	S1	M	1	1	10.00	RRA	NK	2.50	5.00	8.33	11.67
RRA-J005	1	10.00	S1	H	1	1	10.00	RRA	NK	2.50	5.00	8.33	11.67
RRA-J004	1	10.00	S1	H	1	1	10.00	RRA	NK	2.50	5.00	8.33	11.67
RRA-J003	1	10.00	S1	H	1	1	10.00	RRA	NK	2.50	5.00	8.33	11.67
RRA-J006	1	1.00	S1	H	1	1	1.00	RRA	NK	2.00	0.25	0.42	0.58
RRB-J007	1	10.00	S1	M	1	1	10.00	RRB	NK	2.50	5.00	8.33	11.67
RRB-J005	1	10.00	S1	H	1	1	10.00	RRB	NK	2.50	5.00	8.33	11.67
RRB-J004	1	10.00	S1	H	1	1	10.00	RRB	NK	2.50	5.00	8.33	11.67
RRB-J003	1	10.00	S1	H	1	1	10.00	RRB	NK	2.50	5.00	8.33	11.67
RRB-J006	1	1.00	S1	H	1	1	1.00	RRB	NK	2.00	0.25	0.42	0.58

Table 5-1. Listing of Welds in Recirculation Loops A and B. (Cont).

WELD ID	Sys ID #	WELD INFORMATION Dia. (inch)	Type	Location H,M,L	TARGET INFORMATION Total No.	#	Dia. (inch)	INSULATION Sys.	Type	Thick (inch)	TARGET LENGTH L/D=3 (ft)	L/D=5 (ft)	L/D=7 (ft)
RRC-J007	1	10.00	S1	M	1	1	10.00	RRC	NK	2.50	5.00	8.33	11.67
RRC-J005	1	10.00	S1	H	1	1	10.00	RRC	NK	2.50	5.00	8.33	11.67
RRC-J004	1	10.00	S1	H	1	1	10.00	RRC	NK	2.50	5.00	8.33	11.67
RRC-J003	1	10.00	S1	H	1	1	10.00	RRC	NK	2.50	5.00	8.33	11.67
RRC-J006	1	1.00	S1	H	1	1	1.00	RRC	NK	2.00	0.25	0.42	0.58
RRD-J007	1	10.00	S1	M	1	1	10.00	RRD	NK	2.50	5.00	8.33	11.67
RRD-J005	1	10.00	S1	H	1	1	10.00	RRD	NK	2.50	5.00	8.33	11.67
RRD-J004	1	10.00	S1	H	1	1	10.00	RRD	NK	2.50	5.00	8.33	11.67
RRD-J003	1	10.00	S1	H	1	1	10.00	RRD	NK	2.50	5.00	8.33	11.67
RRD-J006	1	1.00	S1	H	1	1	1.00	RRD	NK	2.00	0.25	0.42	0.58

‡ Location classes H, M & L are addressed in Section 5.3.2.

Table 5-2. Listing of Welds in Feedwater Loops A, B, C and D.

WELD ID	Sys ID #	WELD INFORMATION Dia. (inch)	Type	Location H,M,L	TARGET INFORMATION Total No.	#	Dia. (inch)	INSULATION Sys.	Type	Thick (inch)	TARGET LENGTH L/D=3 (ft)	L/D=5 (ft)	L/D=7 (ft)
FWA-J002	3	10.00	C4	H	1	1	10.00	FWA	NK	2.50	3.33	5.00	6.67
FWA-J003	3	10.00	C3	H	1	1	10.00	FWA	NK	2.50	4.17	5.83	7.50
FWA-J005	3	10.00	C3	H	1	1	10.00	FWA	NK	2.50	4.67	6.33	8.00
FWA-J006	3	10.00	C3	H	1	1	10.00	FWA	NK	2.50	5.00	8.33	10.83
FWA-J007	3	10.00	C3	H	1	1	10.00	FWA	NK	2.50	5.00	8.33	11.67
FWA-J008	3	10.00	C3	H	1	1	10.00	FWA	NK	2.50	5.00	8.33	11.67
FWA-J009	3	10.00	C3	H	1	1	10.00	FWA	NK	2.50	5.00	8.33	11.67
FWA-J010	3	10.00	C3	H	1	1	10.00	FWA	NK	2.50	5.00	8.33	11.67
FWA-J011	3	10.00	C3	H	1	1	10.00	FWA	NK	2.50	5.00	8.33	11.67
FWA-J012	3	10.00	C3	H	1	1	10.00	FWA	NK	2.50	5.00	8.33	11.67
FWA-J014	3	10.00	C3	H	1	1	10.00	FWA	NK	2.50	5.00	8.33	11.67
FWA-J015	3	10.00	C3	H	1	1	10.00	FWA	NK	2.50	5.00	8.33	11.67
FWA-J016	3	10.00	C3	H	2	1	10.00	FWA	NK	2.50	2.50	4.17	5.83
						2	16.00	FWA	NK	2.50	5.00	8.33	11.67
FWA-J027	3	16.00	C3	H	1	1	16.00	FWA	NK	2.50	8.00	13.33	18.67
FWA-J028	3	16.00	C3	M	1	1	16.00	FWA	NK	2.50	8.00	13.33	18.67
FWA-J030	3	16.00	C3	M	1	1	16.00	FWA	NK	2.50	8.00	13.33	18.67
FWA-J033	3	16.00	C3	M	1	1	16.00	FWA	NK	2.50	8.00	13.33	18.67
FWA-J034	3	16.00	C3	M	1	1	16.00	FWA	NK	2.50	8.00	13.33	18.67
FWB-J003	3	10.00	C3	H	1	1	10.00	FWB	NK	2.50	3.33	5.00	6.67
FWB-J005	3	10.00	C3	H	1	1	10.00	FWB	NK	2.50	3.83	5.50	7.17
FWB-J006	3	10.00	C3	H	1	1	10.00	FWB	NK	2.50	4.17	5.83	7.50
FWB-J008	3	10.00	C3	H	1	1	10.00	FWB	NK	2.50	4.83	6.50	8.17
FWB-J009	3	10.00	C3	H	1	1	10.00	FWB	NK	2.50	5.00	8.33	10.00
FWB-J010	3	10.00	C3	H	1	1	10.00	FWB	NK	2.50	5.00	8.33	11.33
FWB-J011	3	10.00	C3	H	1	1	10.00	FWB	NK	2.50	5.00	8.33	11.67
FWB-J012	3	10.00	C3	H	1	1	10.00	FWB	NK	2.50	5.00	8.33	11.67
FWB-J013	3	10.00	C3	H	1	1	10.00	FWB	NK	2.50	5.00	8.33	11.67
FWB-J014	3	10.00	C3	H	1	1	10.00	FWB	NK	2.50	5.00	8.33	11.67
FWB-J015	3	10.00	C3	H	1	1	10.00	FWB	NK	2.50	5.00	8.33	11.67
FWB-J016	3	10.00	C3	H	1	1	10.00	FWB	NK	2.50	5.00	8.33	11.67
FWB-J019	3	10.00	C3	H	1	1	10.00	FWB	NK	2.50	5.00	8.33	11.67
FWB-J022	3	10.00	C3	H	1	1	10.00	FWB	NK	2.50	5.00	8.33	11.67
FWB-J024	3	10.00	C3	H	1	1	10.00	FWB	NK	2.50	5.00	8.33	11.67
FWB-J025	3	10.00	C3	H	2	1	10.00	FWB	NK	2.50	2.50	4.17	5.83
						2	16.00	FWB	NK	2.50	5.00	8.33	11.67
FWC-J002	3	10.00	C4	H	1	1	10.00	FWC	NK	2.50	3.33	5.00	6.67
FWC-J003	3	10.00	C3	H	1	1	10.00	FWC	NK	2.50	4.17	5.83	7.50
FWC-J005	3	10.00	C3	H	1	1	10.00	FWC	NK	2.50	4.67	6.33	8.00
FWC-J006	3	10.00	C3	H	1	1	10.00	FWC	NK	2.50	5.00	8.33	10.00
FWC-J007	3	10.00	C3	H	1	1	10.00	FWC	NK	2.50	5.00	8.33	11.67
FWC-J008	3	10.00	C3	H	1	1	10.00	FWC	NK	2.50	5.00	8.33	11.67
FWC-J009	3	10.00	C3	H	1	1	10.00	FWC	NK	2.50	5.00	8.33	11.67
FWC-J010	3	10.00	C3	H	1	1	10.00	FWC	NK	2.50	5.00	8.33	11.67
FWC-J011	3	10.00	C3	H	1	1	10.00	FWC	NK	2.50	5.00	8.33	11.67
FWC-J012	3	10.00	C3	H	1	1	10.00	FWC	NK	2.50	5.00	8.33	11.67
FWC-J015	3	10.00	C3	H	1	1	10.00	FWC	NK	2.50	5.00	8.33	11.67
FWC-J016	3	10.00	C3	H	1	1	10.00	FWC	NK	2.50	5.00	8.33	11.67
FWC-J019	3	10.00	C3	H	1	1	10.00	FWC	NK	2.50	5.00	8.33	11.67
FWC-J022	3	10.00	C3	H	1	1	10.00	FWC	NK	2.50	5.00	8.33	11.67
FWC-J023	3	10.00	C3	H	2	1	16.00	FWC	NK	2.50	4.50	6.67	9.33
						2	10.00	FWC	NK	2.50	2.50	4.17	5.83
FWC-J025	3	16.00	C3	H	1	1	16.00	FWC	NK	2.50	8.00	13.33	18.67
FWC-J026	3	16.00	C3	M	1	1	16.00	FWC	NK	2.50	8.00	13.33	18.67
FWC-J027	3	16.00	C3	M	1	1	16.00	FWC	NK	2.50	8.00	13.33	18.67
FWC-J030	3	16.00	C3	M	1	1	16.00	FWC	NK	2.50	8.00	13.33	18.67
FWC-J031	3	16.00	C3	M	1	1	16.00	FWC	NK	2.50	8.00	13.33	18.67
FWD-J002	3	10.00	C3	H	1	1	10.00	FWD	NK	2.50	3.33	5.00	6.67
FWD-J003	3	10.00	C3	H	1	1	10.00	FWD	NK	2.50	4.17	5.83	7.50
FWD-J005	3	10.00	C3	H	1	1	10.00	FWD	NK	2.50	4.50	6.17	7.83
FWD-J006	3	10.00	C3	H	1	1	10.00	FWD	NK	2.50	5.00	8.33	10.00
FWD-J007	3	10.00	C3	H	1	1	10.00	FWD	NK	2.50	5.00	8.33	11.67
FWD-J008	3	10.00	C3	H	1	1	10.00	FWD	NK	2.50	5.00	8.33	11.67
FWD-J009	3	10.00	C3	H	1	1	10.00	FWD	NK	2.50	5.00	8.33	11.67
FWD-J010	3	10.00	C3	H	1	1	10.00	FWD	NK	2.50	5.00	8.33	11.67
FWD-J011	3	10.00	C3	H	1	1	10.00	FWD	NK	2.50	5.00	8.33	11.67
FWD-J012	3	10.00	C3	H	1	1	10.00	FWD	NK	2.50	5.00	8.33	11.67
FWD-J013	3	10.00	C3	H	1	1	10.00	FWD	NK	2.50	5.00	8.33	11.67
FWD-J015	3	10.00	C3	H	1	1	10.00	FWD	NK	2.50	5.00	8.33	11.67
FWD-J016	3	10.00	C3	H	1	1	10.00	FWD	NK	2.50	5.00	8.33	11.67
FWD-J017	3	10.00	C3	H	2	1	16.00	FWD	NK	2.50	4.00	6.67	9.33

Table 5-3. Listing of Welds in Main Steam Lines A, B, C and D.

WELD ID	Sys ID #	WELD INFORMATION Dia. (inch)	Type	Location H,M,L	TARGET INFORMATION Total No.	#	Dia. (inch)	INSULATION Sys.	Type	Thick. (inch)	TARGET LENGTH L/D=3 (ft)	L/D=5 (ft)	L/D=7 (ft)
MSA-J003	2	20.00	C1	H	1	1	20.00	MSA	NK	3.00	5.00	8.33	11.67
MSA-J004	2	20.00	C1	H	1	1	20.00	MSA	NK	3.00	5.00	8.33	11.67
MSA-J005	2	20.00	C1	H	1	1	20.00	MSA	NK	3.00	5.00	8.33	11.67
MSA-J007	2	20.00	C1	H	1	1	20.00	MSA	NK	3.00	5.00	8.33	11.67
MSA-J009	2	20.00	C1	H	1	1	20.00	MSA	NK	3.00	5.00	8.33	11.67
MSA-J013	2	20.00	C1	H	1	1	20.00	MSA	NK	3.00	5.00	8.33	11.67
MSA-J014	2	20.00	C1	H	1	1	20.00	MSA	NK	3.00	5.00	8.33	11.67
MSA-J024	2	20.00	C1	M	1	1	20.00	MSA	NK	3.00	5.00	8.33	11.67
MSA-J025	2	20.00	C1	M	1	1	20.00	MSA	NK	3.00	5.00	8.33	11.67
MSA-J026	2	20.00	C1	M	1	1	20.00	MSA	NK	3.00	5.00	8.33	11.67
MSA-J032	2	20.00	C1	M	1	1	20.00	MSA	NK	3.00	5.00	8.33	11.67
MSA-J033	2	20.00	C1	M	1	1	20.00	MSA	NK	3.00	5.00	8.33	11.67
MSA-J034	2	20.00	C1	M	1	1	20.00	MSA	NK	3.00	5.00	8.33	11.67
MSA-J036	2	20.00	C1	M	1	1	20.00	MSA	NK	3.00	5.00	8.33	11.67
MSA-J038	2	20.00	C1	M	1	1	20.00	MSA	NK	3.00	5.00	8.33	11.67
MSA-J006	2	6.00	C1	H	1	1	6.00	MSA	NK	3.00	1.50	2.50	3.50
MSA-J027	2	1.00	C1	M	1	1	1.00	MSA	NK	2.00	0.25	0.42	0.58
MSA-J028	2	1.00	C1	M	1	1	1.00	MSA	NK	2.00	0.25	0.42	0.58
MSA-J029	2	1.00	C1	M	1	1	1.00	MSA	NK	2.00	0.25	0.42	0.58
MSA-J030	2	1.00	C1	M	1	1	1.00	MSA	NK	2.00	0.25	0.42	0.58
MSA-J042	2	2.00	C1	L	1	1	2.00	MSA	NK	2.50	0.50	0.83	1.17
MSA-J043	2	2.00	C1	L	1	1	2.00	MSA	NK	2.50	1.00	1.67	2.33
MSA-J044	2	2.00	C1	L	1	1	2.00	MSA	NK	2.50	1.00	1.67	2.33
MSB-J003	2	20.00	C1	H	1	1	20.00	MSB	NK	3.00	5.00	8.33	11.67
MSB-J004	2	20.00	C1	H	1	1	20.00	MSB	NK	3.00	5.00	8.33	11.67
MSB-J005	2	20.00	C1	H	1	1	20.00	MSB	NK	3.00	5.00	8.33	11.67
MSB-J006	2	20.00	C1	H	1	1	20.00	MSB	NK	3.00	5.00	8.33	11.67
MSB-J007	2	20.00	C1	H	1	1	20.00	MSB	NK	3.00	5.00	8.33	11.67
MSB-J010	2	20.00	C1	H	1	1	20.00	MSB	NK	3.00	5.00	8.33	11.67
MSB-J011	2	20.00	C1	H	1	1	20.00	MSB	NK	3.00	5.00	8.33	11.67
MSB-J013	2	20.00	C1	H	1	1	20.00	MSB	NK	3.00	5.00	8.33	11.67
MSB-J014	2	20.00	C1	H	1	1	20.00	MSB	NK	3.00	5.00	8.33	11.67
MSB-J015	2	20.00	C1	H	1	1	20.00	MSB	NK	3.00	5.00	8.33	11.67
MSB-J017	2	20.00	C1	H	1	1	20.00	MSB	NK	3.00	5.00	8.33	11.67
MSB-J018	2	20.00	C1	H	1	1	20.00	MSB	NK	3.00	5.00	8.33	11.67
MSB-J029	2	20.00	C1	H	1	1	20.00	MSB	NK	3.00	5.00	8.33	11.67
MSB-J030	2	20.00	C1	M	1	1	20.00	MSB	NK	3.00	5.00	8.33	11.67
MSB-J032	2	20.00	C1	M	1	1	20.00	MSB	NK	3.00	5.00	8.33	11.67
MSB-J038	2	20.00	C1	L	1	1	20.00	MSB	NK	3.00	5.00	8.33	11.67
MSB-J039	2	20.00	C1	L	1	1	20.00	MSB	NK	3.00	5.00	8.33	11.67
MSB-J041	2	20.00	C1	L	1	1	20.00	MSB	NK	3.00	5.00	8.33	11.67
MSB-J033	2	1.00	C1	M	1	1	1.00	MSB	NK	2.00	0.25	0.42	0.58
MSB-J034	2	1.00	C1	M	1	1	1.00	MSB	NK	2.00	0.25	0.42	0.58
MSB-J035	2	1.00	C1	M	1	1	1.00	MSB	NK	2.00	0.25	0.42	0.58
MSB-J036	2	1.00	C1	M	1	1	1.00	MSB	NK	2.00	0.25	0.42	0.58
MSB-J048	2	2.00	C1	L	1	1	2.00	MSB	CS	2.50	0.50	0.83	1.17
MSB-J049	2	2.00	C1	L	1	1	2.00	MSB	CS	2.50	1.00	1.67	2.33
MSB-J050	2	2.00	C1	L	1	1	2.00	MSB	CS	2.50	1.00	1.67	2.33
MSC-J003	2	20.00	C1	H	1	1	20.00	MSC	NK	3.00	5.00	8.33	11.67
MSC-J004	2	20.00	C1	H	1	1	20.00	MSC	NK	3.00	5.00	8.33	11.67
MSC-J005	2	20.00	C1	H	1	1	20.00	MSC	NK	3.00	5.00	8.33	11.67
MSC-J006	2	20.00	C1	H	1	1	20.00	MSC	NK	3.00	5.00	8.33	11.67
MSC-J009	2	20.00	C1	M	1	1	20.00	MSC	NK	3.00	5.00	8.33	11.67
MSC-J010	2	20.00	C1	M	1	1	20.00	MSC	NK	3.00	5.00	8.33	11.67
MSC-J012	2	20.00	C1	M	1	1	20.00	MSC	NK	3.00	5.00	8.33	11.67
MSC-J013	2	20.00	C1	M	1	1	20.00	MSC	NK	3.00	5.00	8.33	11.67
MSC-J015	2	20.00	C1	M	1	1	20.00	MSC	NK	3.00	5.00	8.33	11.67
MSC-J016	2	20.00	C1	M	1	1	20.00	MSC	NK	3.00	5.00	8.33	11.67
MSC-J028	2	20.00	C1	M	1	1	20.00	MSC	NK	3.00	5.00	8.33	11.67
MSC-J029	2	20.00	C1	M	1	1	20.00	MSC	NK	3.00	5.00	8.33	11.67
MSC-J030	2	20.00	C1	M	1	1	20.00	MSC	NK	3.00	5.00	8.33	11.67
MSC-J036	2	20.00	C1	M	1	1	20.00	MSC	NK	3.00	5.00	8.33	11.67
MSC-J037	2	20.00	C1	M	1	1	20.00	MSC	NK	3.00	5.00	8.33	11.67
MSC-J039	2	20.00	C1	M	1	1	20.00	MSC	NK	3.00	5.00	8.33	11.67
MSC-J031	2	1.00	C1	M	1	1	1.00	MSC	NK	2.00	0.25	0.42	0.58
MSC-J032	2	1.00	C1	M	1	1	1.00	MSC	NK	2.00	0.25	0.42	0.58
MSC-J033	2	1.00	C1	M	1	1	1.00	MSC	NK	2.00	0.25	0.42	0.58
MSC-J034	2	1.00	C1	M	1	1	1.00	MSC	NK	2.00	0.25	0.42	0.58
MSC-J046	2	2.00	C1	L	1	1	2.00	MSC	CS	2.50	0.50	0.83	1.17
MSC-J047	2	2.00	C1	L	1	1	2.00	MSC	CS	2.50	1.00	1.67	2.33
MSC-J048	2	2.00	C1	L	1	1	2.00	MSC	CS	2.50	1.00	1.67	2.33
MSD-J003	2	20.00	C1	H	1	1	20.00	MSD	NK	3.00	5.00	8.33	11.67
MSD-J004	2	20.00	C1	H	1	1	20.00	MSD	NK	3.00	5.00	8.33	11.67

Table 5-3. Listing of Welds in Main Steam Lines A, B, C and D
(Continued)

WELD ID	Sys ID #	WELD INFORMATION Dia. (inch)	Type	Location H,M,L	TARGET INFORMATION Total No.	#	Dia. (inch)	INSULATION Sys.	Type	Thick. (inch)	TARGET LENGTH L/D=3 (ft)	L/D=5 (ft)	L/D=7 (ft)
													MSD-J005
MSD-J005	2	20.00	C1	H	1	1	20.00	MSD	NK	3.00	5.00	8.33	11.67
MSD-J006	2	20.00	C1	H	1	1	20.00	MSD	NK	3.00	5.00	8.33	11.67
MSD-J008	2	20.00	C1	H	1	1	20.00	MSD	NK	3.00	5.00	8.33	11.67
MSD-J012	2	20.00	C1	H	1	1	20.00	MSD	NK	3.00	5.00	8.33	11.67
MSD-J013	2	20.00	C1	H	1	1	20.00	MSD	NK	3.00	5.00	8.33	11.67
MSD-J023	2	20.00	C1	H	1	1	20.00	MSD	NK	3.00	5.00	8.33	11.67
MSD-J024	2	20.00	C1	M	1	1	20.00	MSD	NK	3.00	5.00	8.33	11.67
MSD-J025	2	20.00	C1	M	1	1	20.00	MSD	NK	3.00	5.00	8.33	11.67
MSD-J031	2	20.00	C1	M	1	1	20.00	MSD	NK	3.00	5.00	8.33	11.67
MSD-J032	2	20.00	C1	M	1	1	20.00	MSD	NK	3.00	5.00	8.33	11.67
MSD-J033	2	20.00	C1	M	1	1	20.00	MSD	NK	3.00	5.00	8.33	11.67
MSD-J035	2	20.00	C1	M	1	1	20.00	MSD	NK	3.00	5.00	8.33	11.67
MSD-J026	2	1.00	C1	M	1	1	1.00	MSD	NK	2.00	0.25	0.42	0.58
MSD-J027	2	1.00	C1	M	1	1	1.00	MSD	NK	2.00	0.25	0.42	0.58
MSD-J028	2	1.00	C1	M	1	1	1.00	MSD	NK	2.00	0.25	0.42	0.58
MSD-J029	2	1.00	C1	M	1	1	1.00	MSD	NK	2.00	0.25	0.42	0.58
MSD-J042	2	2.00	C1	L	1	1	2.00	MSD	CS	2.50	0.50	0.83	1.17
MSD-J043	2	2.00	C1	L	1	1	2.00	MSD	CS	2.50	1.00	1.67	2.33
MSD-J044	2	2.00	C1	L	1	1	2.00	MSD	CS	2.50	1.00	1.67	2.33

As discussed above, the base case used point estimates of 0.75, 0.60, and 0.40 for F_I, F_{II} and F_{III}. The parametric study varied these values over a range of ±25%. Results of the sensitivity analyses are presented in Chapter 7.0.

5.3 Debris Transport to the Suppression Pool

The fibrous debris generated in the form of shreds and fines in the drywell due to a LOCA will be transported to the lower elevations by the blowdown/recirculation[15] flow, and then through the drywell vent pipes to the suppression pool. The fraction of total debris transported to the suppression pool depends on the tortousity of the channels available for transport, flow velocities and debris sizes. A limited amount of experimental and theoretical data pertinent to transport characteristics of the fibrous debris during the recirculation phase is reported in NUREG-0897, Rev. 1 (Ref. 5.2). The following section summarizes key findings of that study. Section presents a model adapted for BWRs, specifically for the DAEC-Unit 1.

5.3.1 Review of USI A-43 Debris Transport Model

The NRC sponsored a series of tests at ARL to examine buoyancy and transport characteristics of the fibrous materials (Ref. 5.4). Based on these experiments it is concluded that high density fiber glass insulation readily absorbs water and sinks rapidly. This conclusion was supported by more ARL tests that specifically examined low density NUKON™ material used in DAEC-Unit 1 (Ref. 5.6). Furthermore, these tests revealed that water velocities needed to initiate motion of insulation debris are on the order of 0.2 ft/sec for individual shreds, 0.5 to 0.7 ft/sec for small pieces and 0.9 to 1.5 ft/sec for large pieces. Also, that in the absence of a turbulence generator of any sort, large pieces tend to settle at the bottom of the sump, whereas small shreds tend to remain suspended in the water column until they are collected on the entire screen.

USI A-43 proposed a network resistance model for flow velocities during the long-term ECCS recirculation phase which might occur in PWRs. The recirculation velocities calculated from this model were then used to estimate transportability of the debris to the sump, as well their sedimentation. These models, however, are neither directly applicable to BWRs, nor can they be adapted to BWRs because of major differences in the containment designs. In a typical BWR the break flow goes unimpeded, except for floor gratings, to the bottom of the drywell where it is accumulated until it overflows into the vent pipes and discharges into the suppression pool. In Mark I containments the overflow to the suppression pool is through the vent pipes uniformly spaced around the drywell, whereas in Mark II plants the downcomer vents are used to accomplish the same function. There are several fine variations to these

15 Blowdown is short-term and recirculation is long-term.

arrangements; for example, in some Mark II containments the downcomer vents are arranged so that their inlets are flush with the drywell floor, which prevents water accumulation and debris sedimentation at the bottom of the drywell. In all cases, this recirculation pattern is markedly different from that expected in a typical PWR (see Appendix D of Ref. 5.2). As a result, the transport models proposed in USI A-43 are not applicable to BWRs, and especially for BWRs with Mark I containments.

5.3.2 BWR Debris Transport Model

The BWR debris transport model developed as part of this study is very empirical in nature. It is based on two findings:

1. The HDR test results show that shreds of fibrous debris are carried and deposited in various compartments that are far from the break by the blowdown jets. Considerable quantities of debris were found to have been firmly attached to the containment structures including walls, grids and components. It is highly likely that such attached debris will remain on the structure and may never reach the suppression pool.[16] Although the HDR containment is similar to a PWR containment, this finding is equally applicable to BWRs since initial debris transport in both cases is by blowdown.

2. In the Barsebäck incident more than half of the debris dislodged from the target pipes was left behind in the drywell. The Barsebäck containment is similar to a Mark II containment with less torturous transport channels than are characteristic of Mark I designs and the drywell vent pipes are flush with the drywell floor.

Two important conclusions can be drawn: (a) a fraction of insulation debris would be reduced into fines and shreds that are more likely to be transported to the suppression pool during the blowdown phase, (b) an additional fraction will be washed down by the break flow and containment sprays during the recirculation phase, and (c) a fraction of the fines and shreds will be retained within the drywell. The fraction retained in the containment is expected to be the largest for breaks postulated in high elevations, moderate for breaks in the middle regions of the drywell, and smallest for the breaks occurring in the lower part of the drywell. It can also be stated that no analytical model will be capable of estimating this fraction with a reasonable certainty, since it strongly depends on the containment type and various structures within the drywell.

---

[16] Note that this phenomenon was observed at Barsebäck.

The model used in this study divided the drywell into three regions based on elevation: High, Mid-level, and Low-level. Break locations below an elevation of 757′ are classified as 'low' or L. Debris generated by this LOCA category can be more readily transported to the bottom of the drywell, with only minor impediment. On the other hand, breaks at elevations between 757′ and 776′ are classified as 'Mid-level' or M. Debris from these breaks must be transported through the torturous space between various piping structures and then through the grating at elevation 757′. Finally, break locations higher than the second grating located at elevation 776 ft are classified as 'high' or H. Debris transported from these locations is impeded by the piping network above the 776′ grating, the piping structure between the 776′ and 757′ gratings, and the 757′ grating.

The model uses different transport factors for each region, T_H, T_M, and T_L, to calculate volume of debris actually transported to the sump. The equation used to estimate volume transported to the sump, V_s, is as follows:

$$V_s = T * V_g \qquad 5.3$$

where,

V_g is the volume generated by a break (see Equation 5.2), and

T is the transport factor (= T_H, T_M, or T_L, for breaks in H-, M- and L-elevations).

This equation is used in BLOCKAGE 2.0, to estimate the volume of debris transported to the sump. The base case used the point estimates of 0.25, 0.50, and 0.75 for T_H, T_M, and T_L, based both on the observed nature of debris transport in Barsebäck and on engineering judgement. A parametric analysis was carried out to quantitatively examine the influence of the transport factors on the screen blockage sequence frequency. Results of this sensitivity analysis are summarized in Section 7.0.

5.4 Debris Transport Within the Sump

Debris transport within the suppression pool is considerably influenced by existing recirculation flow fields. This issue was not addressed in USI A-43 in detail. Qualitatively, debris transport within the suppression pool can be described as follows:

1. Debris in the form of fines and shredded pieces (small and large) are introduced into the sump through the drywell vent pipes.

2. Large pieces may either sink to or settle at the bottom of the suppression pool, or may be broken into small pieces which can then be kept afloat by the turbulence.

3. Turbulence introduced by mixing pumps and/or two-phase instabilities will greatly contribute to debris disintegration and resuspension in the suppression pool.

4. Suspended fines and small shreds will be carried to the strainers, where they are assumed to deposit uniformly over the surface of the strainer.

Several BWR strainer blockage studies are reportedly underway to model these phenomena using variations of potential flow equations, with superimposed turbulence. Such modeling may be adequate for small pipe breaks or for safety relief valve rupture events where containment pressures are not expected to increase drastically. Neither these studies nor their findings were reviewed as part of this study. Nevertheless, applicability of such studies to post-LOCA scenarios where pool flow fields are dominated by vigorous chugging and other two-phase instabilities is questionable.

The present analysis addressed this issue in a conservative manner by assuming that all the debris reaching the suppression pool will remain suspended for prolonged periods of time. The debris will ultimately be deposited on the strainer(s) as a function of time. The quantity deposited on each strainer is assumed to be directly proportional to the flow through the strainer. Finally, it is assumed that debris retained by the strainer will form a layer of uniform thickness. The thickness of this layer can be calculated as

$$t = V_s/A_s \qquad 5.4$$

where,

t is thickness of the debris layer on the strainer (ft),

V_s is the volume of fibrous debris reaching the sump (ft^3), and

A_s is the total area of the strainer(s) (ft^2) assumed to be active following the LOCA event.

BLOCKAGE 2.0 uses this equation to estimate thickness of the debris layer on the strainers.

5.5 Strainer Head Loss Model

Head loss models are used to calculate head loss due to clogging of ECCS strainers by the fibrous debris. Considerable effort was expended by USI A-43 study to develop analytical and/or empirical equations that can be used to calculate head-loss as a function of strainer flow rate and debris thickness. The following section summarizes key findings of the USI A-43 study. This section presents new equations used in this study, which are based on more recent sets of experimental data as well as an improved understanding of the blockage process.

5.5.1 Review of USI A-43 Head Loss Model

A series of tests were conducted under NRC sponsorship at ARL to measure head loss for various insulation materials typically used in nuclear power plants. The three materials tested were (a) mineral wool, (b) high density fiber glass, and (c) NUKON™. The results of mineral wool and high density fiber glass are reported in NUREG/CR-2892 (Ref. 5.4), and results for NUKON™ are summarized in NUREG-0897, Rev. 1 (Ref. 5.2). For all these materials head loss was measured as a function of screen approach velocity and theoretical debris thickness[17] for both the 'as-fabricated' insulation blankets, and for insulation shreds of various sizes. The manufacturer of the i ulation provided several blankets of insulation in their original form for testing. These blankets wer ed 'as-is' for head loss measurement for as-fabricated mats. The blankets were then manually shr ed into small pieces, ranging from 1" x 0.5" x 0.125" to 3" x 2" x 0.125", for head loss measurement. Best-fit expressions for the head loss through shredded fibrous insulation, were derived as follows:

for mineral wool:

$$\Delta H = 123\ U^{1.51}\ t^{1.36} \qquad 5.5.1a$$

for fiberglass:

$$\Delta H = 1653\ U^{1.84}\ t^{1.54} \qquad 5.5.2a$$

for NUKON™:

$$\Delta H = 68.3\ U^{1.79}\ t^{1.07} \qquad 5.5.3a$$

where,

U is the screen approach velocity (ft/sec),

t is the theoretical debris thickness (ft), and

ΔH is the head loss (ft of water).

The same equations can be expressed in S. I. units as:

for mineral wool:

$$\Delta H = 111.2\ U^{1.51}\ t^{1.36} \qquad 5.5.1b$$

for fiberglass:

$$\Delta H = 2738.5\ U^{1.84}\ t^{1.54} \qquad 5.5.2b$$

for NUKON™:

$$\Delta H = 61\ U^{1.79}\ t^{1.07} \qquad 5.5.3b$$

---

[17] Theoretical debris thickness is defined as: Mass of the debris/as fabricated density/area of the strainer.

where,

U is the screen approach velocity (m/sec),

t is the theoretical debris thickness (m), and

ΔH is the head loss (bars).

These equations clearly emphasize the strong dependence of head loss on the material characteristics. NUREG-0897, Rev. 1 (Ref. 5.2) recommended usage of these equations for head loss calculations.

The major drawback of these equations is that they are based on experimental data obtained for non-uniform beds formed by relatively large shreds of insulation. Typical shreds of insulation generated by break jet impingement are much finer, as demonstrated by HDR tests, than the shreds used in the experiments reviewed above. The accumulation of such fine shreds on the strainer and subsequent compression results in formation of beds much denser than the original material, and thus, higher head losses. This behavior was reported by KKL after experimentation with mineral wool aged up to 20 years (Ref. 5.7). In KKL experiments aged mineral wool was stirred in water to simulate the effects of steam jet and subsequent suppression pool turbulence. The fibrous material was then transferred to the screen type strainer, where it formed a uniform layer. The experiment was started at high velocities to allow for bed compaction before head losses were measured. Measured head losses were correlated using the equation:

$$\Delta H = 141\ U^{1.13}\ t^{1.14} \qquad 5.6a$$

where,

U is the screen approach velocity (m/sec),

t is the theoretical insulation debris thickness (m), and

ΔH is the head loss (bar).

This equation can be expressed in U.S. units as:

$$\Delta H = 318.2\ U^{1.13}\ t^{1.14} \qquad 5.6b$$

where,

U is the screen approach velocity (ft/sec),

t is the theoretical insulation debris thickness (ft), and

ΔH is the head loss (ft of water).

It can be easily shown that equation 5.6a/b predicts head losses approximately 2 to 3 times higher than equation 5.5.1a/b, which is for insulation similar to that used to develop equation 5.6a/b.

Similar test data have recently been obtained for NUKON™. Applicable tests were conducted under PCI sponsorship. In these tests, finer debris were generated from aged insulation blanket by jet impingement, using either two-phase jets typical of BWRs or air jets that are scaled down (Ref. 5.5). These finer debris were then collected and deposited on the strainer to form beds of uniform thickness. Head loss measurements for beds formed in this manner are reported, along with recommended correlations for usage. However, these correlations have drawbacks very similar to those discussed above, and therefore could not be used in this study. The following section summarizes the methodology used to derive the required equations for the present study.

5.5.2 NUKON™ Head Loss Model

The head loss model used in this study was specifically derived for NUKON™ insulation used at DAEC-Unit 1. Similar equations are being developed for other materials (mineral wool and high density fiber glass), and they will be made available once they are finalized. The head loss equation presented below was obtained from experimental data made available by PCI. These experimental data included head loss measurements for (a) as-fabricated NUKON™ blankets, (b) medium to small shreds obtained by manually shredding the data, and (c) finer debris generated by air blast destruction of NUKON™ insulation. Figure 5-4 plots selected experimental data for all three cases[18]. All data were obtained at room temperatures where the water temperatures varied between 70-90 °F. As shown in this figure, the experimental data can be correlated using the following equation:

$$(\Delta H/t) = 61\,U + 54\,U^2 \qquad 5.7$$

where,

U is the screen approach velocity (ft/sec),
t is the theoretical debris thickness (ft), and
ΔH is the head loss (ft of water).

As is evident from Figure 5-4, the correlation is within ± 10-20% of the experimental data. It can be clearly seen that at velocities higher than 2 ft/s, the turbulent flow pressure drop dominates. On the other hand, at very low velocities the laminar component dominates the total pressure drop. At the

[18] Experimental measurements for which the debris bed is sufficiently thick to form uniformly distributed debris were retained in this analysis. Other data, mostly for very thin beds, were eliminated because measured pressure drops are much lower.

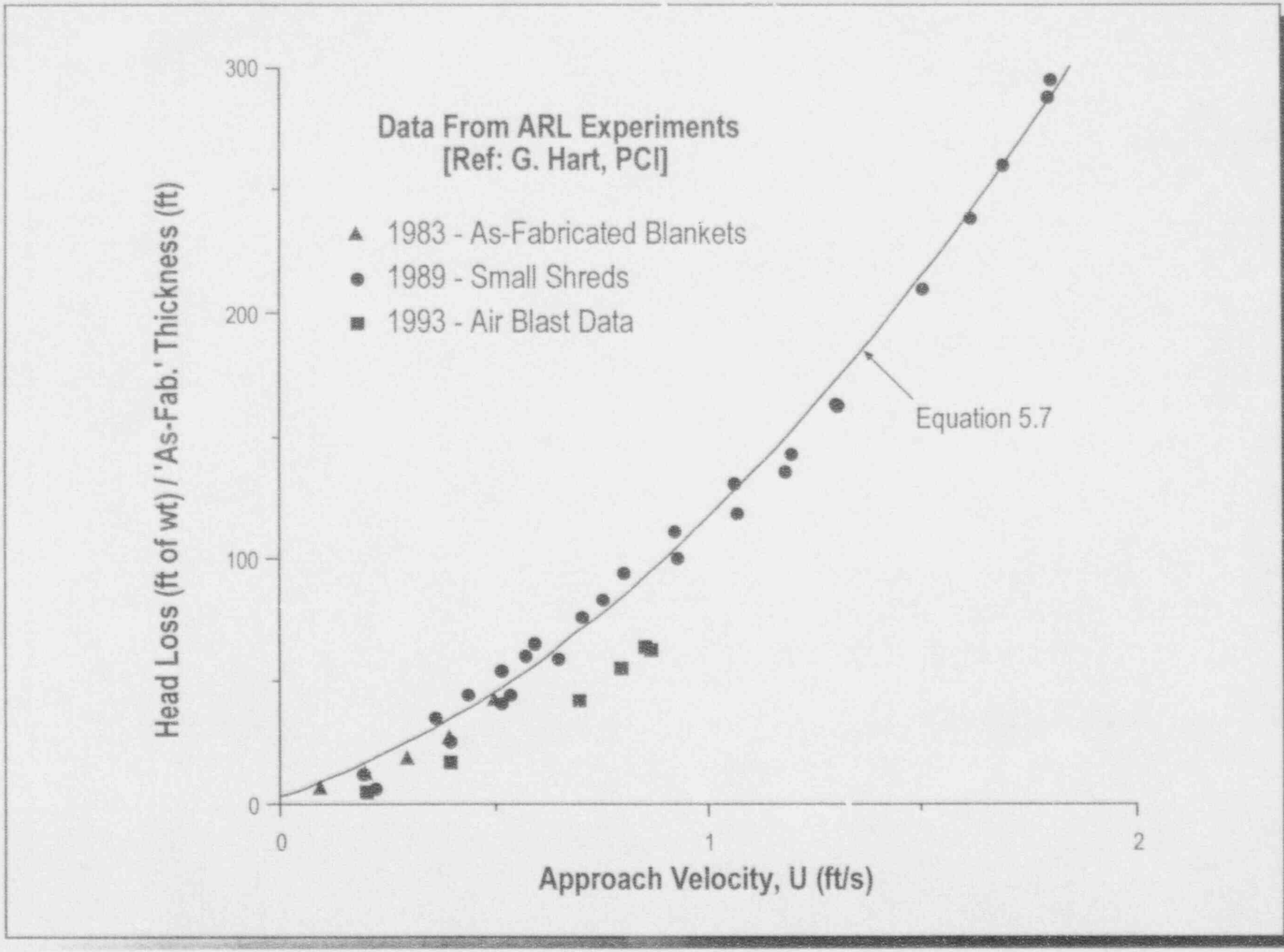

Figure 5-4. Selected Sets of Experimental Data Obtained for NUKON

approach velocity of interest (1.5 ft/s), the head loss is due to a combination of laminar and turbulent flows. This chosen form of the correlation more accurately reflects actual physical processes as compared to the form of equations proposed in NUREG-0897, Rev. 1 (Ref. 5.2). However, for comparison the same data are used to obtain a different correlation in a form consistent with NUREG-0897, Rev.1 (Ref. 5.2), as shown below:

$$\Delta H = 122 \ U^{1.51} \ t. \qquad 5.8a$$

Equation 5.8a gives results essentially equivalent to those of equation 5.7. Because this form more closely matches those used in previous analyses, equation 5.8a is used in the current analysis for the base case evaluations. This equation can be expressed in S.I. units as:

$$\Delta H = 207 \ U^{1.51} \ t. \qquad 5.8b$$

where,

U is the strainer approach velocity (m/sec),
t is the theoretical debris thickness (m), and
ΔH is the head loss (bars).

Equation 5.8a/b lies above equation 5.3.3a/b by up to two times in the velocity range of interest, which is consistent with the trend reported by Sulzer's data for mineral wool (i.e., equation 5.5.1a/b vs 5.6a/b).

For this study, the following conclusions were drawn:

1. Head loss equations presented in NUREG-0897, Rev. 1 (Ref. 5.2), can underpredict pressure drops because (a) relatively larger shreds were used to form the test beds, and (b) some of the test beds were non-uniformly distributed.

2. Beds formed of finer debris and small shreds tend to result in pressure drops as high as 'As-Fabricated' blankets.[19] For such cases, the worst case pressure drop can be predicted using equations 5.7 or 5.8a/b.

---

[19] It is conceivable that compacted beds formed of fines would result in pressure drops even higher than 'As-Fabricated' blankets. However, experimental data on such beds was not available for review and hence was not included in deriving equation 5.7.

3. Equation 5.7 is only applicable to NUKON™ insulation. Similar equations can be made available for other insulations after pertinent data are released from proprietary restrictions.

5.5.3 Appl[illegible]tion to DAEC-Unit 1 Plant

Mo[illegible] than 95% of the fibrous insulation used in DAEC-Unit 1 drywell is NUKON™. As a result equation 5.7 is adequate to estimate pressure drop due to strainer blockage. Required coefficients were input to BLOCKAGE 2.0, which calculates theoretical bed thicknesses using equation 5.4, and strainer approach velocities using the following equation:

$$U = QC/A_s \qquad 5.9$$

where

U is strainer approach velocity (ft/s),

Q is ECCS flow rate (GPM),

C is conversion factor (0.1337/60), and

A_s is the strainer surface area (ft^2).

Sensitivity analyses, documented in Section 10.2.3, calculated pressure drops using equation 5.3.3a/b, 5.7 and by simply multiplying 5.3.3a/b by a factor of 2. These analyses were carried out to examine the effect of the pressure drop equation on the blockage frequency.

5.6 Loss of ECCS NPSH Model

As suggested in NUREG-0897, Rev. 1 (Ref 5.2), loss of ECCS pumps is assumed when the $NPSH_{margin}$ (i.e., $NPSH_{available}$ - $NPSH_{required}$) is less than the predicted head loss due to strainer blockage by insulation debris (i.e., equation 5.7). Available and required NPSH values are plant-specific, and can be estimated for a given plant using the methodology described in Section 3.2.3 of NUREG-0897, Rev. 1 (Ref. 5.2).

For the DAEC-Unit 1 plant, available and required NPSH values for both LPCI and CS pu[illegible] were provided by the utility. NPSH requirements are shown in Figure 3.16 and 3.17 for LPCI and [illegible] pumps, respectively. The available NPSH estimat[illegible]d after assuming atmospheric containment pressure and a 120 °F pool temperature is about 24 and 32 ft of water for LPCI and CS pumps respectively. This provides a $NPSH_{margin}$ of about 14 ft of water for the RHR pump and 17 ft of water for the CS pump. In the present analysis, both the RHR and CSs strainer were combined together to forr[illegible] a single strainer of area equal to the total areas of the individual strainers. The strainer was assumed to be completely blocked when predicted head loss is larger than 14 ft of water, i.e.,

$$\Delta H \geq NPSH_{margin} = 14 \text{ ft. of water.} \qquad 5.10$$

Although the CS pumps can operate beyond this point due to their higher $NPSH_{margin}$ for them, it is not clear if they alone can provide adequate core cooling.

This present analysis assumed that all of the ECCS flow (25,000 GPM) is lost when equation 5.10 is exceeded. Variations to NPSH margin due to either increased containment pressure or increases in suppression pool temperature were not modeled.

References for Section 5

5.1 J. Wysocki and R. Kolbe, "Methodology for Evaluation of Insulation Debris Effects," Burns and Roe, Inc., published as Sandia National Laboratories Report No. SAND82-7067, NUREG/CR-2791, September 1982.

5.2 A. W. Serkiz, "Containment Emergency Sump Performance," US Nuclear Regulatory Commission, NUREG-0897, Rev. 1, October 1985.

5.3 G. G. Weigand et al., "Two-Phase Test Loads," published as Sandia National Laboratories Report SAND82-1935, NUREG/CR-2813.

5.4 D.N. Brocard, "Buoyancy, Transport, and Head Loss of Fibrous Reactor Insulation," Alden Research Laboratory, published as Sandia National Laboratories report No. SAND82-7205, Rev, NUREG/CR-2982, Rev. 1, July 1983.

5.5 T. Kegel, "Air Blast Destructive Testing of NUKON™ Insulation Simulation of a Pipe Break LOCA," Colorado Engineering Experiment Station, Inc., October 1993.

5.6 W. W. Durgin and J. F. Noreika, "The Susceptibility of NUKON™ Insulation Pillows to Debris Formation Under Exposure to Energetic Jet Flows," Alden Research Laboratory, September 1983.

5.7 KKL Specific ECCS Strainer Plugging Analysis According to Regulatory Guide 1.82, Rev. 1, for a Loss-of-Coolant Accident, Technical Report, BET/93/031, KERNKRAFTWERK, LEIBSTADT, AG.

6.0 COMPUTER PROGRAM BLOCKAGE 2.0

6.1 Background

The analysis assisting in the resolution of USI A-43 relied on computer programs PRA and TABLE to probabilistically assess recirculation sump blockage in PWRs due to LOCA induced debris from destroyed insulation. Program PRA calculates ECCS strainer blockage probability as a product of frequency of occurrence of the initiating event and the probability of sump blockage as a result of the initiating event. The program then sorts the overall ECCS strainer blockage frequency into several bins by systems, by pipe diameter, etc. The second program TABLE reads output generated by PRA and restructured the data into table formats that were ultimately used in NUREG-0869, Rev. 1 (Ref. 6.1), and NUREG/CR-3394 (Ref. 6.2). Design features of these programs and various calculations performed by these programs are presented in NUREG/CR-3394. Also, source code listings were enclosed as Appendices B and C of Ref. 6.2.

These programs were developed specifically for PWRs. Based on scoping analyses it was determined that regeneration of PRA and TABLE from the source code listing[20] and, subsequent modifications needed to model BWRs would be a time consuming process. Instead, it was decided to create a new computer program, named BLOCKAGE, that would be versatile enough to perform the above described functions for both BWRs and PWRs. Also, BLOCKAGE added several important features that were missing in PRA. The following sections provide an overview of BLOCKAGE 2.0, including functional description, user interface and input/output description.

6.2 BLOCKAGE Overview

BLOCKAGE was designed to be a PC-based software written in FORTRAN. It was developed in two stages. BLOCKAGE 1.0 was developed first and was validated by reproducing the NUREG/CR-3394 (Ref. 6.2) results for the Salem nuclear plant. Development and validation of BLOCKAGE 1.0 established that results of USI A-43 for PWRs are reproducible and that there is consistency between the past and the present studies. Further descriptions of the development of BLOCKAGE 1.0 and its validation are presented in Appendix B.

BLOCKAGE 2.0 was generated by modifying BLOCKAGE 1.0. It was also designed to be a PC-based software that performs all the functions that were important for resolution of USI A-43, while accommodating input for a representative BWR. A brief description of BLOCKAGE 2.0 is provided below, while details on its validation are presented in Appendix B.

---

[20] Programs PRA and TABLE were developed in FORTRAN-IV, which is obsolete and not supported by FORTRAN compiles presently available.

6.3 Functional Description of BLOCKAGE 2.0

6.3.1 Input Description

Figures 6-1 and 6-2 are the input/output flow chart and functional flow chart, respectively, of BLOCKAGE 2.0. As shown in Figure 6-2 the program reads in and validates user input. WELD.INP and PARAMETR.INP are the specific computer portions of the program that account for general parameter input and specific weld input, respectively. WELD.INP contains a unique identifier, diameter, type, location, and a system for each weld in the primary piping subjected to high pressure during regular operation; number, diameter, and length of each pipe targeted by the jet generated by failure of each weld; and type and thickness of insulation on each target pipe. The input data are plant specific and should be obtained in a manner similar to that described in Sections 3.0 and 5.0. This input file for DAEC-Unit 1 was obtained by combining Tables 5-1 (recirculation lines), 5-2 (feedwater lines) and 5-3 (main steam lines); welds in other lines are screened out as explained in Section 3.0. The contents of the input file PARAMETR.INP are illustrated in Figure 6-1. Base case values for flow rates (PM), screen areas (ft^2) and allowable head loss (ft of water) are plant-specific; however, these values can be varied over a range of interest to the user as part of parametric study. Similarly, insulation destruction fractions (F_I, F_{II} and F_{III} described in Section 5.2) and transport factors (T_H, T_M and T_L described in Section 5.3) can be varied over a range of interest. Two options are provided to input break frequency. In the first method, the one used in the present study, the input for computing break frequencies is a table of weld break frequencies by weld type and diameter class. In the second method, the input for computing break frequencies is a table of plant pipe break frequency by diameter class, together with weighting factors by type of weld. Additional details on the input parameters are discussed in Appendix B. Table 6-1 displays the input file used for base-case runs described in Section 7.0.

6.3.2 Calculational Algorithm

As shown in Figure 6-2, the first step performed by BLOCKAGE 2.0 is to validate user input data, and generate diagnostic files that can be used to correct/modify the input files. Once the validation process is completed, the program proceeds to calculate available fibrous insulation volume in each region (i.e., Regions I, II and III of Figure 5-2) corresponding to each weld using equation 5.1. These calculated values together with some of the user input are output at this stage as TARGET.OUT. The program then sorts the welds by diameter class and weld type, and outputs weld data as WELD.OUT. Using simple table look-up logic the program then assigns a weld break frequency for each weld. The program then follows each weld and determines whether or not it results in ECCS strainer blockage. As shown in Figure 6-1, the calculation proceeds in five steps:

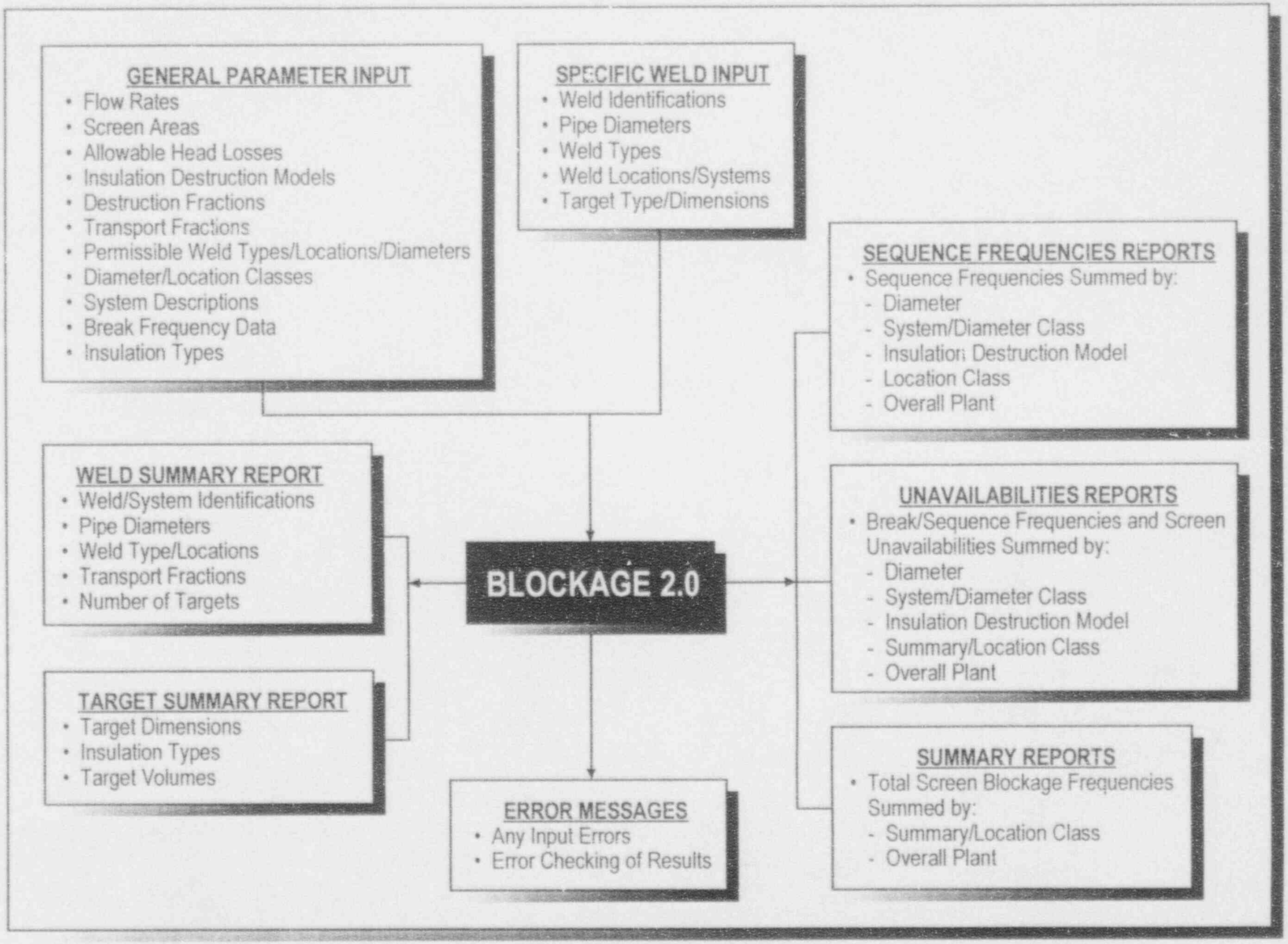

Figure 6-1. BLOCKAGE 2.0 Input/Output Flow Chart

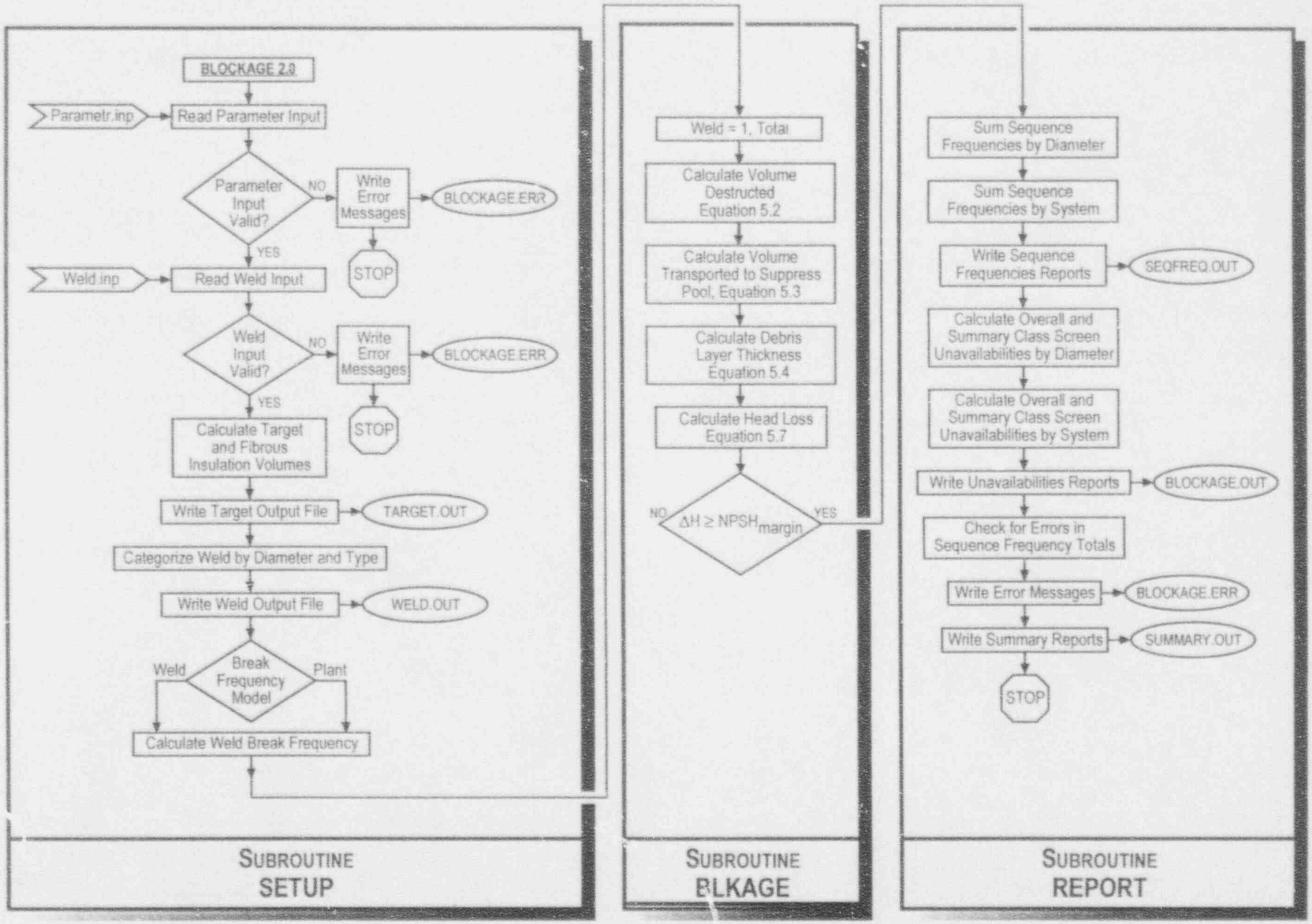

Figure 6-2. BLOCKAGE 2.0 Flow Chart by Function

Table 6-1: Duane Arnold (BWR) Base Case Parameter Input

Input	Description
3. 5. 7.	insulation destruction model L/Ds
.75 .60 .40	destruction fractions
1	number of flow rates
25000.	flow rates (GAM)
1	number of head losses
14.	allowable head losses
1.51 1.00 121.5	head loss parameters A, B, C
1	number of screen areas
37.62	screen areas(sq.ft)
6	number of permissible weld types
S1 S2 S3 C1 C3 C4	permissible weld types
3	number of permissible weld locations
'H' 'M' 'L'	permissible weld locations
0.25 0.5 0.75	transport fractions
3	number of systems
'Recirculation Loop'	1st system descriptor
'Main Steam'	2nd system descriptor
'Feedwater'	3rd system descriptor
9	no. of weld diameters
1.0 1.25 2.0 4.0 6.0	diameters 1 - 5
10.0 16.0 20. 22. /	diameters 6 - 9
W	method for calculating break frequencies
4	no.of pipe diameter classes
0.75 4.0 12.0 18.0	smallest diam.in diameter class
'.75-2' '4-10' '12-16' '18-+'	diameter class label
1.e-6 1.e-6 2.e-6 2.e-7	weld break freq, weld type S1
1.e-6 1.e-6 2.e-6 2.e-7	weld break freq, weld type S2
1.e-6 1.e-6 2.e-6 2.e-7	weld break freq, weld type S3
2.e-7 2.e-7 2.e-7 2.e-7	weld break freq, weld type C1
2.e-7 2.e-7 2.e-7 2.e-7	weld break freq, weld type C3
2.e-7 2.e-7 2. -7 2.e-7	weld break freq, weld type C4
3	no.of location classes
'High '	label
'H ' ' '	selection criteria
'Above 776 ft Grating'	descriptor
'Med. '	label
'M ' ' '	selection criteria
'Between 757/776 Gratings'	descriptor
'Low '	label
'L ' ' '	selection criteria
'Below 757 ft Grating'	descriptor
4	no.of perm. insulation materials
'NK' 'MR' 'CS' 'NN'	insulation type identifiers
'F' 'N' 'N' 'N'	fibrous insulation flags

1. Calculate the actual volume of insulation destructed into transportable form (fines and small shreds) using equation 5.2.

2. Calculate the total volume of this insulation transported to the suppression pool using equation 5.3, which uses transport factors provided by the user.

3. Calculate the thickness of the layer of debris on the strainer using equation 5.4.

4. Calculate the head-loss due to debris accumulation using a head loss equation. Coefficients of this equation are provided by the user as part of PARAMETR.INP.

5. Check to determine if the head-loss calculated in step 4 is larger than the allowable head-loss (or NPSH-margin) provided by the user as an input.

This procedure is repeated for each weld, and a tally of each weld resulting in ECCS strainer blockage is kept. The program then calculates the overall ECCS strainer blockage frequency, which is a sum of break frequencies of the welds resulting in ECCS strainer blockage. In addition the program bins each weld by system, by pipe diameter, by location, etc. The program then calculates ECCS strainer blockage frequency for each bin by summing the frequency of welds resulting in ECCS strainer blockage for each weld that falls in that bin/clan. These calculated values are output as SEQFREQ.OUT and BLOCKAGE.OUT. Finally, the program checks for errors in sequence frequency totals, and outputs summary reports into SUMMARY.OUT.

6.3.3 Output Description

BLOCKAGE 2.0 generates the following output report files:

File Description	File Name
Weld Summary Report	WELD.OUT
Target Summary Report	TARGET.OUT
Sequence Frequency Report	SEQFREQ.OUT
Unavailabilities Report	BLOCKAGE.OUT
Summary Reports	SMMARY.OUT
Error Messages	BLOCKAGE.ERR

6.4 Application to DAEC-Unit 1 Plant

BLOCKAGE 2.0 was used to estimate ECCS strainer blockage frequency for DAEC-Unit 1 plant. The plant-specific weld data used as input are presented in Tables 5-1, 5-2, and 5-3. The input parameters was previously presented in Table 6-1, which includes weld break frequencies. Output tables are enclosed as Appendix B. The analysis results are presented and discussed in the following section.

References for Section 6

6.1 A. W. Serkiz, "USI A-43 Regulatory Analysis," US Nuclear Regulatory Commission, NUREG-0869, Rev. 1, October 1985.

6.2 J. J. Wysocki, "Probabilistic Assessment of Recirculation Sump Blockage Due to Loss of Coolant Accidents, Containment Emergency Sump Performance USI A-43," Vols. 1 and 2, Burns and Roe, Inc., published as Sandia National Laboratories Report No. SAND83-7116, NUREG/CR-3394, July 1983.

7.0 DUANE ARNOLD BLOCKAGE ESTIMATES

This section of the report presents results and findings related to the BLOCKAGE 2.0 analyses. To facilitate the presentation of these results and findings, relevant information is contained within several subsections. Each subsection focuses on a specific aspect of the analysis.

Subsection 7.1 below describes the results of BLOCKAGE 2.0 analyses for a set of base case parameters. Included in this subsection is a presentation and discussion of the overall blockage frequency estimate. Also included in this subsection are the contributions to blockage frequency based on the piping system, pipe size, and pipe location. Subsection 7.2 summarizes the major assumptions and limitations of the analysis effort. Subsection 7.3 presents the results from a limited set of sensitivity analyses that involved the variation of several important parameters. Major conclusions of the study are summarized in subsection 7.4. Finally, subsection 7.5 presents a set of recommendations that could serve to further refine and enhance this analysis.

7.1 Base Case Results

An estimate of the probability of ECCS sump blockage for Duane Arnold Unit 1 was obtained using the base case input to BLOCKAGE 2.0. Tables 5-1, 5-2, and 5-3 summarize the weld input data used in this analysis. As discussed in Section 3.0, only welds in recirculation piping, feedwater piping and main steam lines were included in the input. Table 6-1 presents the parametric input provided to BLOCKAGE 2.0. As shown in this table, the base-case run used destruction factors of 0.75, 0.60 and 0.40 for Regions I, II, and III of Figure 5-2. These destruction factors represent conservative upper bounds for steel jacketed NUKON™ insulation. For other insulation materials and/or other forms of jacketing, these destruction factors would be expected to be different. The base case used a strainer flow rate of 25000 GPM, a strainer surface area of 37.62 ft^2, and a NPSH-margin (or allowable head loss) of 14 ft of water. These values were obtained based on P&IDs for the strainers and on discussions with the plant systems engineers. The base case run used transport factors of 0.25, 0.50 and 0.75 for welds located in High, Medium and Low drywell elevations, respectively. The methodology used to derive weld break frequencies for input for this run was discussed in Section 4.0.

Before presenting the results from this study, it is useful to note that some of the results are presented in the form of a "conditional blockage probability". A conditional blockage probability is derived by dividing the frequency estimate for a specific blockage scenario by the corresponding initiator frequency. This type of mathematical expression provides a measure of the probability or likelihood that blockage will occur given a specific pipe break initiating event.

7.1.1 ECCS Strainer Blockage Frequency Estimates for the Base Case

The point estimate for the overall pipe break frequency (for breaks that could potentially result in ECCS intake screen blockage) at DAEC-Unit 1 was estimated to be 1.5E-04/Rx-yr. The corresponding overall ECCS strainer blockage frequency was estimated to be 4.6E-05/Rx-yr, resulting in a overall conditional blockage probability of 0.31. The estimated ECCS strainer blockage frequency falls in the range of 3E-06 to 5E-05/Rx-yr discussed in NUREG-0869, Rev. 1 (Ref. 7.1), for PWRs and Mark I BWRs.

7.1.2 ECCS Strainer Blockage Frequency Estimates by System

The postulated pipe breaks were subdivided according to the three systems found to pose the greatest threat for causing blockage: recirculation loop, main steam lines, and feedwater loops. The ECCS strainer blockage frequency was sorted by system as shown in Table 7-1. As is evident from this table, the recirculation system made the largest contribution to the total ECCS strainer blockage frequency, simply because the pipe break frequency for this system was much larger than those of the other two systems. On the other hand, a main steam line break was more likely to cause ECCS strainer blockage as demonstrated by the conditional blockage probability of 0.68. This result is a direct reflection of the fact that a main steam line break, would, on average, generates a much larger volume of debris compared to a postulated break in a recirculation loop[21].

Table 7-1: Blockage Estimates by System

System	Weld Break Frequency (1/Rx-yr)	Distribution (%)	Blockage Frequency (1/Rx-yr)	Distribution (%)	Conditional Blockage Probability
Recirculation	1.2E-04	79	3.1E-05	67	0.26
Main Steam	1.8E-05	12	1.3E-05	28	0.68
Feedwater	1.4E-05	9	2.2E-06	5	0.16
Overall Plant	1.5E-04	100	4.6E-05	100.	0.31

7.1.3 ECCS Strainer Blockage Frequency Estimates by Pipe Size

The ECCS strainer blockage frequencies were sorted by size as shown in Table 7-2. As shown in this table, the contribution of breaks postulated in pipes less than 6 inches in diameter is negligible; in fact, none of these breaks, including breaks in the recirculation discharge by-pass lines, resulted in generation

[21] Note that the recirculation loops contain several 1" and 2" instrumentation welds. If one of these small welds were to break, only very small volumes of insulation debris would be released.

of sufficient debris volume to cause blockage. This conclusion is consistent with the USI A-43 finding for PWRs. Note, however, that this conclusion may not be valid if the insulation used is different from steel jacketed NUKON™. For other insulations, such as the non-jacketed mineral wool in Barsebäck, the analysis should be repeated using more appropriate destruction factors. On the other hand, it is evident from Table 7-2 that LOCAs postulated in 20 inch or larger pipes would almost certainly result in ECCS strainer blockage. It is important to recognize that the conditional blockage probability of 0.95 estimated for 22 inch pipes was due to two cap welds in the recirculation manifolds (e.g. weld RMA-J6 in Figure 5-3) that generate small quantities of insulation debris. The conditional blockage probabilities for 10 and 16 inch pipe breaks was estimated to be 0.31 and 0.56, respectively.

Table 7-2: Blockage Estimates by Diameter

Diameter (in)	Weld Break Frequency (1/Rx-yr)	Distribution (%)	Blockage Frequency (1/Rx-yr)	Distribution (%)	Conditional Blockage Probability
1	2.8E-05	19	0	0	0.0
1-1/4	2.0E-06	1	0	0	0.0
2	4.4E-06	3	0	0	0.0
4	2.6E-05	17	0	0	0.0
6	2.0E-07	<1	0	0	0.0
10	5.2E-05	34	1.6E-05	35	0.31
16	1.8E-05	12	1.0E-05	22	0.56
20	1.3E-05	9	1.3E-05	28	1.0
22	7.4E-06	5	7.0E-06	15	0.95
Overall Plant	1.5E-04	100	4.6E-05	100	0.31

7.1.4 ECCS Strainer Blockage Frequency Estimates by Pipe Location

The blockage estimates were correlated by containment location as shown in Table 7-3. The containment was subdivided into three location classes 'H', 'M', and 'L' by the drywell gratings located at the 757 and 776 ft elevations. Although there is an equal likelihood of weld breaks in 'H' and 'M' locations, the majority of the ECCS strainer blockage frequency (70%) was contributed by weld breaks in 'M' location class. It was determined that welds in this location class also have the highest conditional blockage probability. Breaks below the 757 ft. grating have a very low conditional blockage probability

(0.10) primarily because a relatively large number of welds in this location class are instrumentation and drain pipe welds.

Table 7-3: Blockage Estimates by Location

Location Class	Weld Break Frequency (1/Rx-yr)	Distribution (%)	Blockage Frequency (1/Rx-yr)	Distribution (%)	Conditional Probability
H	5.6E-05	37	1.0E-05	22	0.18
M	5.7E-05	38	3.2E-05	70	0.56
L	3.8E-05	25	3.8E-06	8	0.10
Overall Plant	1.5E-04	100	4.6E-05	100	0.31

Figures 7-1 and 7-2 combine the effects of pipe diameter and pipe location, and pipe diameter and system, to facilitate better understanding of their individual effects on the ECCS strainer blockage frequency. These figures together illustrate the data in Tables 7-1 through 7-3.

7.2 Major Analysis Assumptions and Limitations

As was previously discussed, the analysis was based on a number of major assumptions. In addition, there were certain limitations associated with the analysis methods. The purpose of this subsection is to summarize the major assumptions and limitations inherent in this study.

7.2.1 Major Analysis Assumptions

Major assumptions used in the analysis are listed below. For convenience, these assumptions are grouped according to subject.

7.2.1.1 Pipe Break Initiator Assumptions

- The initiator type was assumed to be a DEGB event. Other breaks that represent a less severe form of pipe failure were not considered.

- Recirculation piping whose rupture could cause a LOCA event was assumed to be constructed of a material (304SS) susceptible to IGSCC effects.

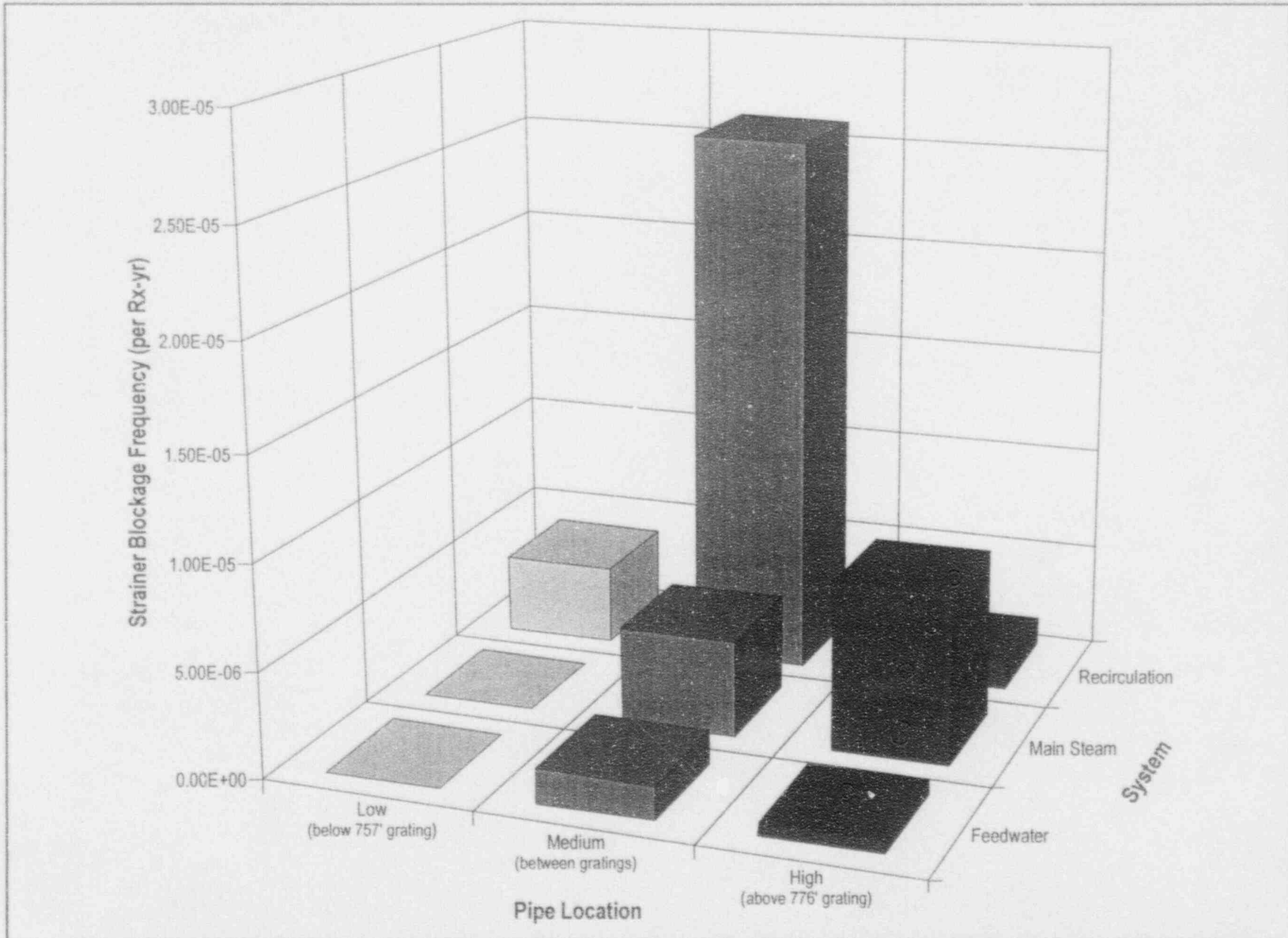

Figure 7-1. Blockage Frequency by System and Location

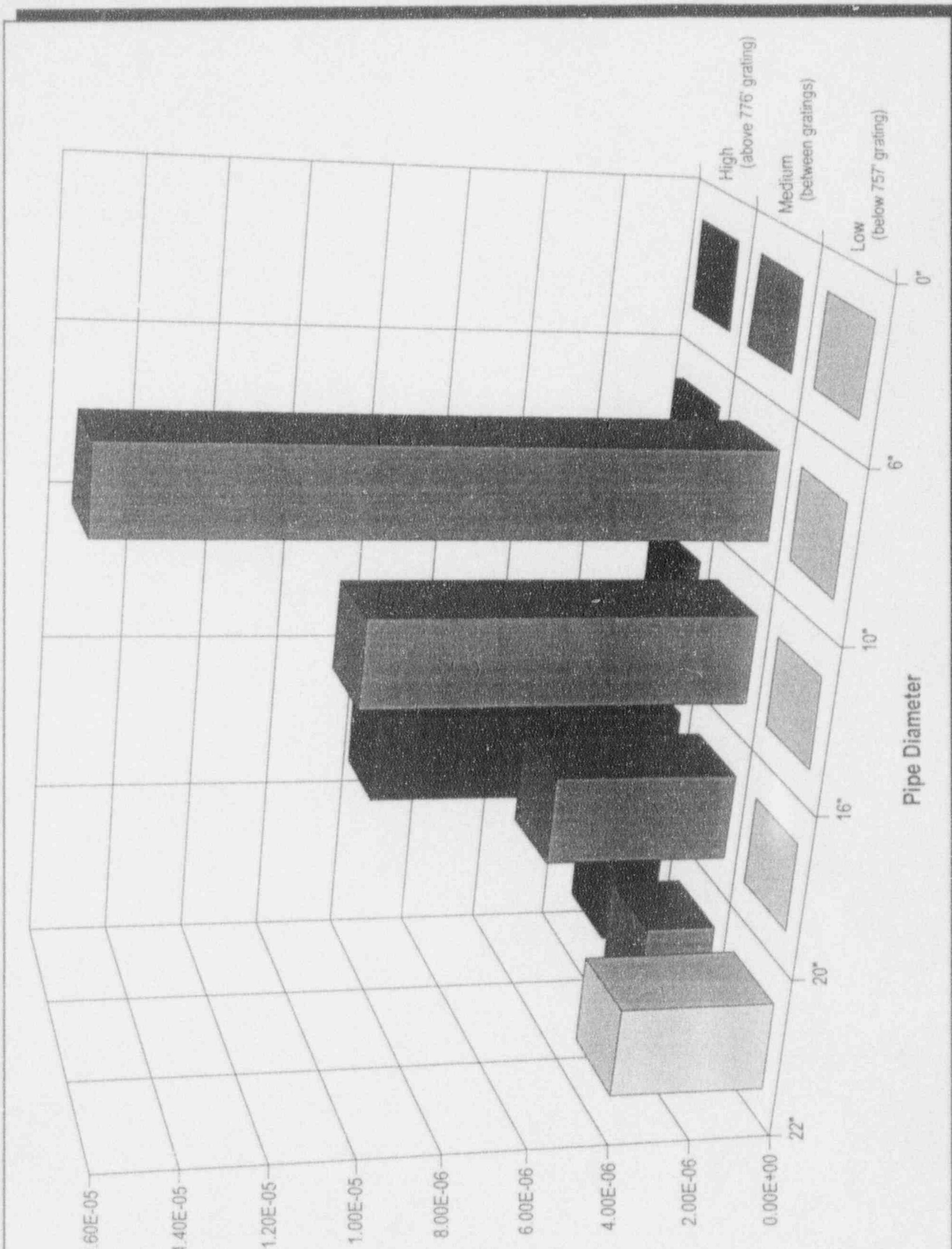

Figure 7-2. Blockage Frequency by Diameter and Location

- Welds associated with main steam and feedwater piping were assumed to have the same break frequencies as 22"-28" recirculation system welds.

- It was assumed that only one IGSCC mitigating action would be in place, namely an in-service inspection program. Appropriate credit for in-service inspection was given as described more fully in Appendix A.

7.2.1.2 Debris Generation Assumptions

- The three region zone of influence model, similar to that suggested in NUREG-0897, Rev. 1 (Ref 7.2), was assumed for BWRs.
- Only insulation on the pipe with the break was assumed to be dislodged. Insulation on the surrounding pipes, but within the zone influence, was not included in this analysis.
- Destruction factors of 0.75, 0.6, and 0.4 were assumed for Regions I, II and III, respectively.

7.2.1.3 Debris Transport Assumptions

- No distinction was made between short-term (blowdown phase) and long-term (recirculation phase) transport of debris to the suppression pool.
- Only a fraction of the debris (0.75-0.25) generated in the drywell was assumed to reach the suppression pool.
- It was assumed that all fines (fiber-size debris and shreds) would remain suspended in the suppression pool for long periods of time and would be deposited on the strainer as a function of the concentration in the flow. It was further assumed that the remaining large pieces would undergo further shredding and ultimately reach the strainer in a condition similar to the fines. This approach was expected to provide a conservative prediction for debris cake thickness.
- The time dependance of debris accumulation on the strainer was not considered.

7.2.2 Major Analysis Limitations

Major limitations associated with the analysis are listed below. Note, however, that some of the limitations discussed below will be addressed by on-going efforts involving hydraulics modeling and value impact analyses.

7.2.2.1 General Limitations

- The analysis was based on a BWR 4/Mark I plant, specifically the DAEC-Unit 1 plant. The analysis results and conclusions may be significantly different for other BWR designs. For example, there are significant plant-to-plant variations in the types of insulation that was used. Also note that plant-specific layout features can significantly affect the migration of debris.

- The results contained in this report were expressed solely in terms of point estimates. There was no work done to generate pertinent statistical information, for example means, medians, and other uncertainty distribution parameters.

7.2.2.2 Pipe Break Initiator Limitations

As previously described in Section 4.0, pipe weld break analyses contained in a LLNL study [NUREG/CR-4792 (Ref 7.3)] was used as the basis of the pipe break frequency estimates used herein. Consequently, some of the LLNL study limitations had direct impact on the blockage analysis. Those LLNL limitations that were judged to have the greatest impact on the blockage analysis are listed below.

- Certain local phenomena were not considered in the LLNL analysis, for example the effect of coolant flow velocity on possible flushing of impurities that otherwise could aggravate the susceptibility to IGSCC.

- The LLNL model used "harsh" laboratory conditions to predict growth rates and times-to-initiation. It is conservative to extrapolate the "harsh" laboratory data to the relatively benign conditions that exist in reactor facilities.

- Pipe weld failure probabilities are very sensitive to the type of residual stress assumed in the LLNL analysis. Consequently, plant-to-plant experiences could significantly vary depending on residual stresses that remain following pipe assembly welding and "fit up". Worst case stress assumptions were used in the analysis.

- The main objective of the LLNL analysis was to compare the behavior of different types of materials to IGSCC. This emphasis may have introduced additional uncertainties in the absolute value of the break frequencies.

- There were discrepancies between the LLNL predictions and field tests done at a BWR site. These discrepancies most likely were the result of field variations in various pertinent phenomena and in analytical assumptions needed to model these phenomena. However, it is important to note that both the LLNL analysis and field results gave highest priority to riser and bypass welds.

- Pipe breaks caused by water hammer or a projectile from pump failures were not considered.

- The LLNL analysis did not consider scenarios that involved IGSCC-weakened piping coupled with other pipe challenges, for example water hammer or seismic events.

7.2.2.3 Debris Generation Limitations

The debris generation model used in this study is similar to the three-region model described in NUREG-0897 (Ref. 7.2). Those limitations that were judged to have largest impact on the overall analysis outcome are listed below.

- This study focused on the expected behavior of metallic-jacketed NUKON material, because this insulation material is used in the reference plant (DAEC-Unit 1). The applicability of the results of this analysis to plants with other types of insulation, especially unjacketed insulation, therefore, is limited.

- This study did not include pipes, tanks, or other insulated components in the surrounding areas to calculate total debris generated by a break. This may limit the applicability of the results of this analysis to small diameter breaks, particularly 4" DEGBs in recirculation discharge bypass lines.

7.2.2.4 Debris Transport Limitations

Major limitations of the study related to debris transport are listed below.

- The analysis used transport factors to calculate the volume of debris transported from the various drywell elevations - where the breaks occur. However, there are no experimental data that can be used to verify the adequacy or realism of these transport factors for various containment types.

- Transport time dependencies were not considered in this study. This was a limitation because, in reality, the time at which blockage occurs strongly influences accident outcome.

Future analyses, planned as part of the on-going hydraulics modeling, will address these issues. However, note that the lack of experimental data may limit the extent to which these issues will be resolved.

7.2.2.5 Head Loss Limitations

This study used an experimental correlation, similar in form to that proposed in NUREG-0897, Rev. 1 (Ref. 7.2). This correlation predicts head loss as a function of approach velocity and debris bed thickness. Major limitations associated with the usage of this correlations are listed below.

- The head loss equation used in this study was developed using experimental data obtained for NUKON™ shreds generated by manual means or from small scale air blast experiments. Its applicability to debris generated by energetic two-phase jets during a blowdown phase is not clear. The debris fibers may undergo further destruction during transport to the sump by the impact of the blowdown flow recirculation within the drywell. This situation could cause formation of a much denser debris-bed on the strainer than was modeled herein, resulting in a higher head loss than predicted by the head loss equation used in this study.

- The head loss equations for materials other than NUKON have not been finalized because the necessary data has not been made available until recently.

- The impact of paint, rust, and particulate debris from some types of insulation were not included in this analysis. Their impact on the analysis results may be substantial.

Hydraulics modeling currently in progress will address these issues. Note that related experimental data has recently been made available and it is the intent of future analyses to make use of all available data to derive a head-loss model.

7.2.2.6 Pump Performance Limitations

- The analysis did not account for pressurization of the suppression pool during the blowdown phase or reduction in available NPSH due to an increase of pool water temperature.

Efforts are underway to obtain containment and suppression pool pressures following a large break LOCA as a function of time. Other concerns to be addressed include structural integrity of the strainer when subjected to large pressure drops due to debris accumulation.

7.3 Sensitivity Analyses

As noted in section 5.0, several important parameters used in the debris generation transport models were based on engineering judgement supported by very limited experimental data. To quantify the influence of these parameters on the overall ECCS strainer blockage frequency estimates, a series of BLOCKAGE 2.0 runs were made in which these parameters were varied over a preselected range. Results of this sensitivity analysis are documented below. It should be noted that the sensitivity analyses presented here were very limited in scope and did not address a variety of issues including: insulation type, differences in Mark I, II and III containments, the effect of recirculation loop replacements, or larger strainer surface areas. Results of such analyses will be documented as they become available.

7.3.1 Variation of Head-Loss Correlation Coefficients

The base case estimated head-loss due to debris accumulation on the screen using equation 5.8, which was developed based on selected sets of head loss data for NUKON™ insulation. This equation is reproduced here for convenience:

$$\Delta H = 122\ U^{1.51}\ t^{1.0}. \qquad 5.8$$

Case 1 of the sensitivity analysis examined the effect of using the head-loss equation suggested in NUREG-0897, Rev. 1 (Ref. 7.2), for NUKON™ given by

$$\Delta H = 68.3\ U^{1.79}\ t^{1.07}. \qquad 5.6.3$$

Also, another analysis was run (Case 2) where the head loss was assumed to be simply twice that predicted by equation 5.6.3[22]. Table 7-4 presents the effect of head loss equation on the ECCS blockage frequency. As is evident from this table, the ECCS strainer blockage frequency increases by a factor of 1.6 if the new head-loss equation (base case) is used instead of that suggested in NUREG-0897, Rev. 1 (Ref. 7.2). On the other hand, there is little difference between calculations using the head loss predicted in equation 5.8 or the head loss assumed to be twice that of equation 5.6.3 (Case 2). These results are not surprising considering that the new correlation (equation. 5.8) was based on sets of data carefully selected to reflect the worst case scenario.

It should be noted that additional experimental results, presently unavailable, may reveal that the actual head-loss is even larger than predicted by equation 5.8. In that case, the ECCS strainer blockage estimates should be reevaluated.

Table 7-4: Blockage Correlation Sensitivity Results

Case	Break Frequency (1/Rx-yr)	Blockage Frequency (1/Rx-yr)	Conditional Probability
Base	1.5E-04	4.6E-05	0.31
Case 1	1.5E-04	2.8E-05	0.19
Case 2	1.5E-04	4.6E-05	0.31

7.3.2 Variation of NPSH Margin

The sensitivity of the screen blockage to the allowable head loss was investigated by varying the minimum required input head from zero to 20 ft. This sensitivity is shown as the percentage of plant overall blockage as a function of allowable head in Figure 7-3. These results illustrate that the blockage is relatively insensitive to the allowable head around the base case head of 14 ft. However, the blockage would decrease from 31 to 25% if the head were increased from 14 to 15 ft. Upon decreasing the allowable head loss from the base case, the blockage did not increase from the 31% value until the head loss decreased to 7 ft.

---

[22] This head loss value was selected for the following reason: Following the Barsebäck event, Sulzer reported that the measured head loss for fine debris generated by jet impingement on aged mineral wool blankets is about two- to three-times that predicted by equation 5.6.1 developed using experimental data for small shreds. Using the same argument, this study assumed that actual head-loss for NUKON™ fines is twice as large as that predicted by equation 5.6.3, also obtained for small shreds.

For accident conditions where the suppression pool heats due to insufficient cooling, the allowable head loss may decrease due to the heating. Figure 7-3 helps visualize how an inlet screen might not be effectively blocked initially but could become blocked later as a result of suppression pool heating. This effect could be countereacted to some extent by containment pressurization.

7.3.3 Variations of Debris Generation Insulation Destruction Fractions

The sensitivity of the screen blockage to the insulation destruction fractions was investigated by varying the input destruction fractions from the base case fractions. This sensitivity is shown in Figure 7-4 as the percentage of plant overall blockage as a function of percentage change from the base case fractions. The base case fractions were 0.75, 0.60, and 0.40, i.e., 75% of the insulation in Region I ($L/D \leq 3$), followed by 60% in Region II ($3 \leq L/D \leq 5$), and 40% in Region III ($5 \leq L/D \leq 7$). The destruction fractions for the 5% increase calculation, for example, were 0.80, 0.65, and 0.45.

Increasing the destruction fractions from the base case did not increase the blockage percentage for significantly for the range of increases tested. However, reducing the destruction fractions did reduce the blockage as shown.

7.3.4 Variations of Debris Transport Fractions

The sensitivity of the screen blockage to the debris transport fractions was investigated by varying the input transport fractions from the base case fractions. This sensitivity is shown in Figure 7-5 as the percentage of plant overall blockage as a function of percentage change from the base case fractions. The base case fractions were 0.25, 0.50, 0.75 for the high, medium, and low location classes, i.e., 25% of the debris formed above the 776 ft grating was transported to the suppression pool, followed by 50% of the debris formed between the 757 and 776 ft gratings, and by 75% of the debris formed below the 757 ft grating. The transport fractions for the 5% increase calculation, for example, were 0.30, 0.55, and 0.80.

Increasing the transport fractions from those of the base case did not increase blockage until the fractions were increased to 25% above the base case, then the blockage was 52%. A worst case calculation run with both destruction and transport fractions all set to 1.0 resulted in a blockage percentage of 54%. Decreasing the transport fractions resulted in a blockage decrease for the -5% calculation but then remained nearly constant down to the -25% case.

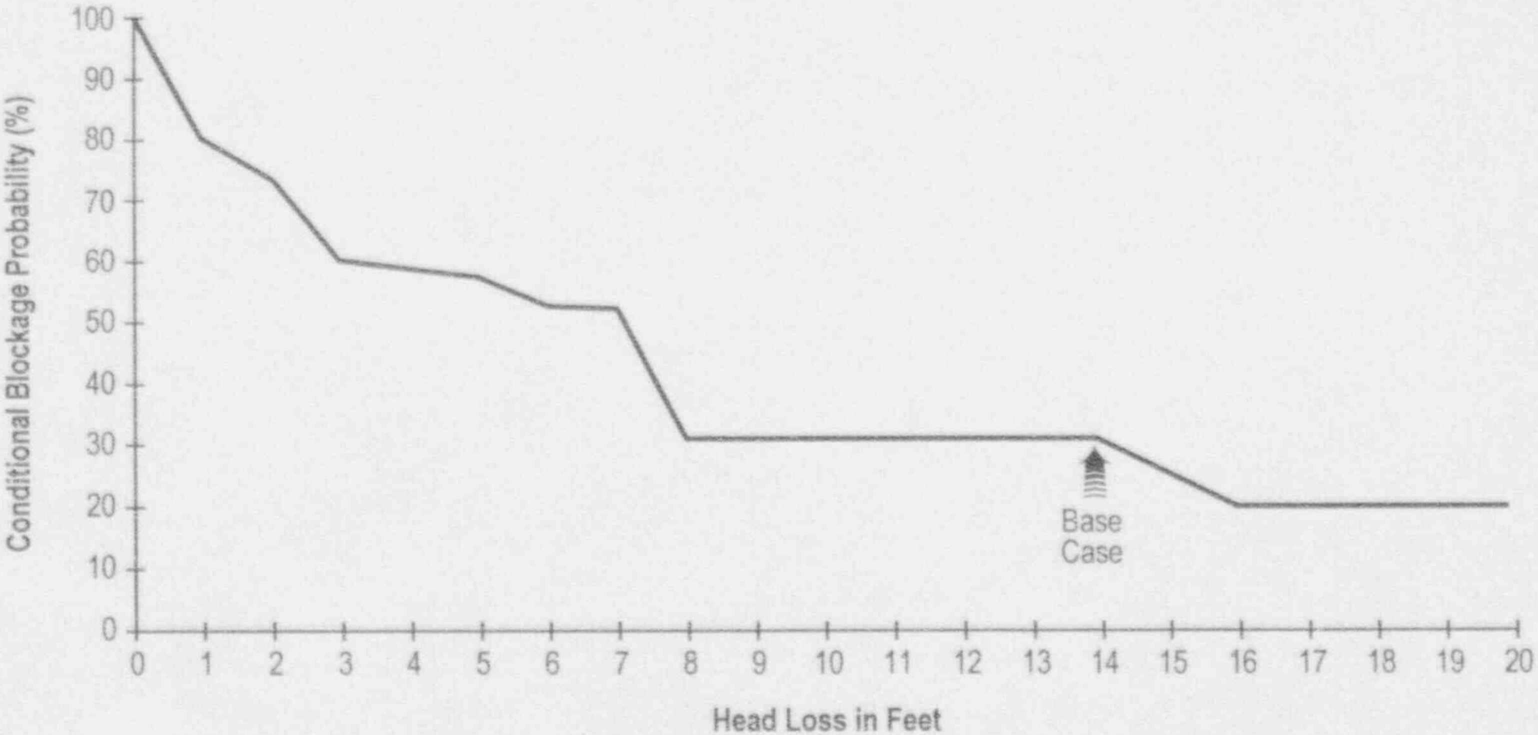

Figure 7-3. Blockage Sensitivity to Allowable Head Loss

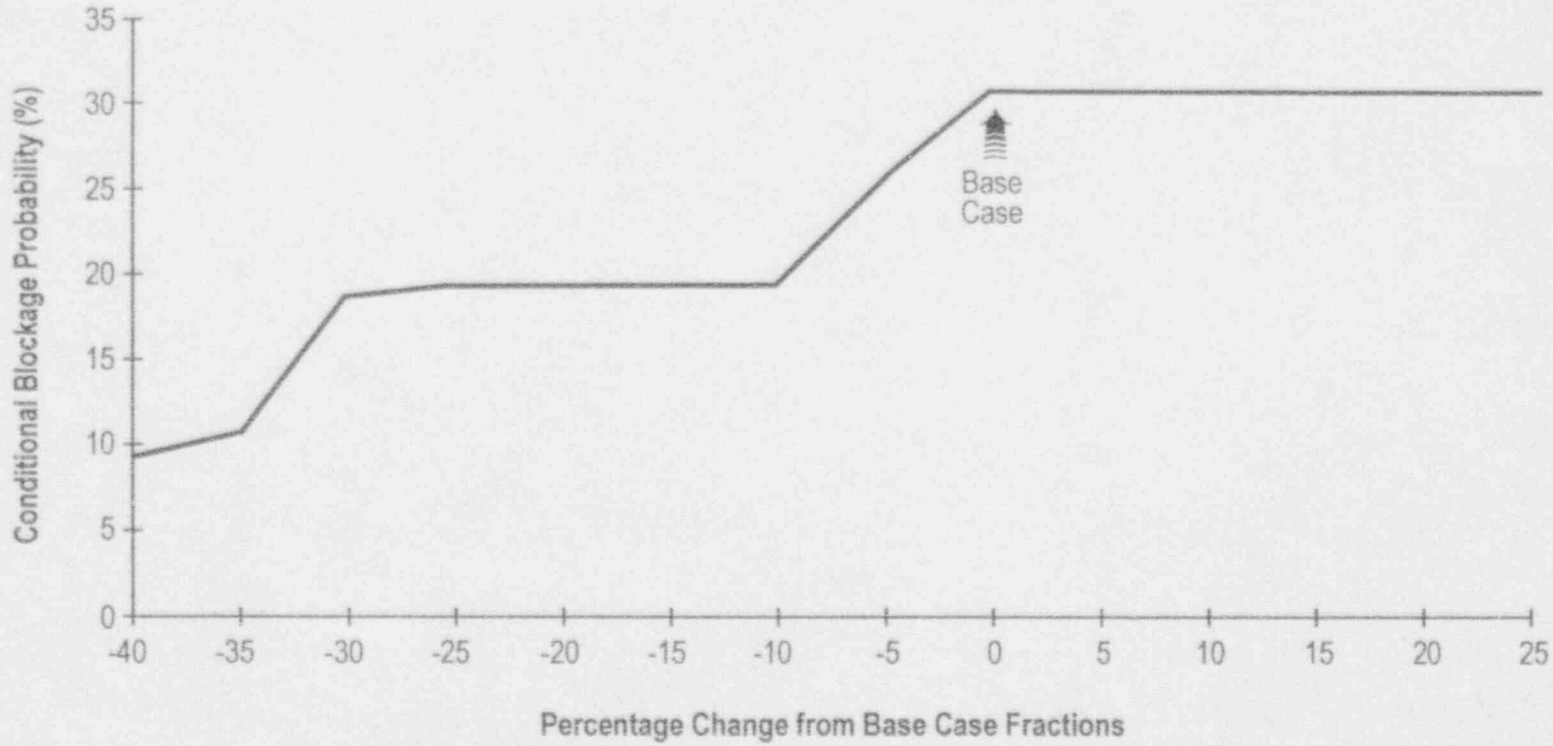

Figure 7-4. Blockage Sensitivity to Destruction Fractions

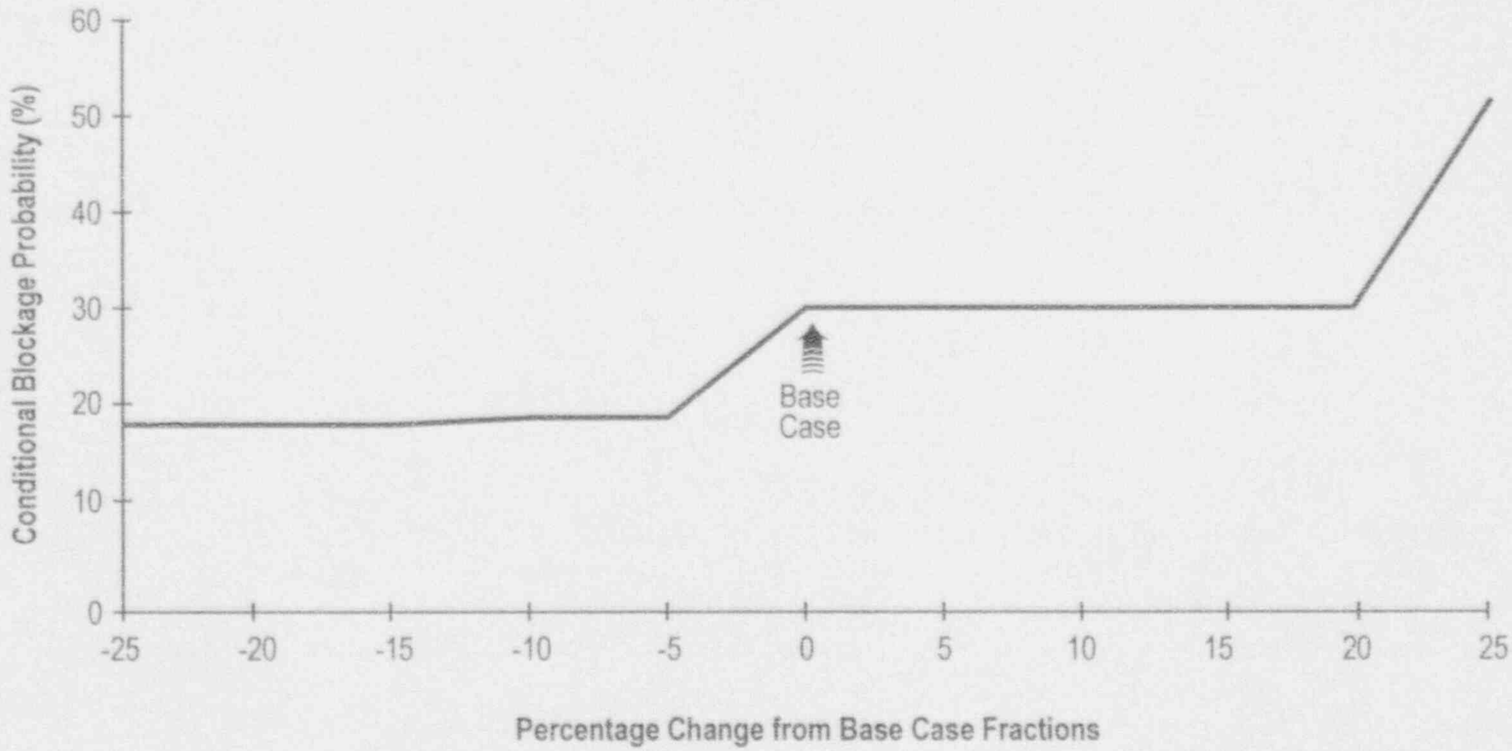

Figure 7-5. Blockage Sensitivity to Transport Fractions

7.4 Summary and Conclusions

The major findings of the blockage analysis can be summarized as follows:

- The results predicted an overall point-value blockage frequency of 4.6E-05/Rx-yr, which is in the upper portion of the frequency range discussed in NUREG-0869, Rev. 1 (Ref. 7.1) for PWRs and Mark 1 BWRs.

- On an overall basis, the conditional probability of blockage given a LOCA initiator was 0.31. In other words, given a LOCA and the assumptions used, there is a 31% probability that it would lead to a ECCS strainer blockage scenario.

- The recirculation system contributed the largest fraction to the blockage frequency. This result is due to the fact that most of the pipe break initiator frequency is contributed by recirculation system welds.

- Main steam line breaks had the highest conditional blockage probability (0.68) of the three piping systems considered in this analysis. This high conditional blockage probability is due to the relatively high volume of debris generated, on average, by a steam line break as compared to recirculation or feed water breaks. The only breaks in main steam lines that do not result in blockage are the 1-2" instrumentation welds.

- The majority of the contribution to blockage frequency is due to breaks in the mid-location class. This result is primarily due to the larger volumes of debris generated by LOCAs in this region as compared to LOCAs in other regions.

- The contribution of breaks less than 6 inches in diameter to blockage frequency was negligible due to the small volume of debris generated. This result can be attributed to the fact that the amount of debris generation is a direct function of the break diameter. However, this conclusion may not hold true if all the surrounding pipes are included as the targets.

- Parametric studies confirmed that the results can change, in some instances significantly, with variations in NPSH margin, debris destruction fractions, and debris transport fractions.

References for Section 7

7.1 A. W. Serkiz, "USI A-43 Regulatory Analysis," US Nuclear Regulatory Commission, NUREG-0869, Rev. 1, October 1985.

7.2 A. W. Serkiz, "Containment Emergency Sump Performance," US Nuclear Regulatory Commission, NUREG-0897, Rev. 1, October 1985.

Appendix A

BWR Coolant Pipe Weld Break Frequencies for Estimating The Potential for LOCA-Generated ECCS Strainer Blockage (Revision 3)

Table of Contents

Section		Page
1.0	Introduction	1
	1.1 Background	1
	1.2 Objective of Study	2
2.0	Review of General Approaches to Quantification of Pipe/Weld Breaks	3
	2.1 Operational Data	3
	2.2 Analytical Methods	3
	2.3 Expert Judgment	4
	2.4 Combined Approach	4
3.0	BWR Weld Break Frequency Estimates	5
	3.1 Approach Used to Estimate Weld Break Frequencies	5
	3.2 Limitations of the LLNL Analysis	14
	3.3 Recommended Weld Break Frequency Data	15
	3.4 Comparisons of Recommended Data With Other Data Sources	17
4.0	Summary and Recommendations	19
REFERENCES		20

List of Figures

3-1	Weld Locations in a Recirculation Loop	7
3-2	Weld Locations in Feedwater Paths	8
3-3	Weld Locations in a Main Steam Path	9
3-4	Cummulative System Probabililties of DEGB in One Recirculation Loop	10
3-5	Relative Contribution of Various Welds to DEGB in Recirculation Loop	13

List of Tables

3-1	Frequencies for Directly-Caused DEGBs, Exclusive of IGSCC Effects	11
3-2	Frequencies for IGSCC-Caused DEGBs to Recirculation Piping	11
3-3	Frequencies for Indirectly-Caused DEGBs to Reactor Coolant Piping	12
3-4	Frequencies for IGSCC-Caused DEGBs to Recirculation Welds in Susceptible Material (304SS)	14
3-5	Recommended DEGB Frequency Estimates	17
3-6	Comparison of Recommended Mark 1 Large LOCA Data with Industry Risk Assessment Data	18

1.0 Introduction

This report provides break frequency estimates of pipe welds in the reactor coolant piping of a representative BWR 4/Mark I plant. The break frequencies were generated for the purpose of estimating Emergency Core Cooling System (ECCS) unavailability caused by blockage of BWR suppression pool suction strainers following a Loss of Coolant Accident (LOCA).

1.1 Background

The following subsections briefly discuss background information pertinent to this study. Subsection 1.1.1 provides an overview of the debris blockage issue, while subsection 1.1.2 discusses the issue of intergranular stress corrosion cracking (IGSCC) as it relates to susceptible piping at older BWR plants.

1.1.1 Overview of Debris Blockage Issue

As described in NUREG-0869, Rev. 1 (Ref. 1), USI A-43 has addressed concerns about the availability of adequate recirculation cooling water in a PWR following a LOCA. One concern was the effects of LOCA-generated insulation debris that is transported to the sump debris screen and blocks the screen, reducing net positive suction head (NPSH) margin below that required for the Emergency Core Cooling System (ECCS) pumps to maintain long-term recirculation cooling.

For the resolution of USI A-43, the NRC Staff evaluated the loss of recirculation capability due to debris generation, focusing primarily on PWRs. The blockage probabilities for PWRs were calculated on the basis of a detailed analysis in NUREG/CR-3394 (Ref. 2). The methodology described in NUREG/CR-3394 (Ref. 2) is also generally applicable to BWRs. The recent Barseback and Perry Nuclear Plant debris blockage of ECCS intake strainers extended the concern about debris blockage to BWRs as well. The BWR Residual Heat Removal (RHR) system provides the Low Pressure Coolant Injection (LPCI) function of the ECCS. The suction strainers in the suppression pool of a BWR RHR system are analogous to the PWR sump debris screen, and both BWRs and PWRs must have adequate recirculation cooling capacity to prevent core damage.

1.1.2 Intergranular Stress Corrosion Cracking Concerns at BWR Plants

As noted in NUREG/CR-4792 (Ref. 3), older BWR plants, particularly those with a Mark I containment design, have recirculation piping that has been found to be susceptible to intergranular stress corrosion cracking (IGSCC). The susceptible (sensitized) Type 304 stainless steel piping used in Mark 1 BWRs can experience IGSCC as the result of significant tensile stress caused by the normal welding practice and a corrosive environment. If susceptible piping has not been replaced with resistant materials, Stress Improvement (SI) can be accomplished on weldments already installed by the Induction Heating

Stress Improvement process, or by the Mechanical Stress Improvement Process (MSIP). For piping with more than 2 years of operation, SI is considered to be less effective, because cracking may already be present. If the oxygen levels in the primary coolant are reduced by implementing Hydrogen Water Chemistry (HWC), stress corrosion cracking of even sensitized material will be reduced. Another potential mitigation is an augmented inspection schedule.

NUREG-0313, Rev. 2 (Ref. 4) lists the following austenitic materials considered to be adequately resistant to sensitization by welding:

1. Low carbon wrought austenitic steel. These include 304L, 304NG, 16L, 316NG, 347NG, and similar types.
2. Low carbon weld metal of type 308L and similar grades with a minimum of 7.5% ferrite as deposited. This may also be used as a cladding on the inside of the pipe.
3. Cast austenitic stainless steel with less than 0.035% carbon and a minimum of 7.5% ferrite.
4. Inconel 82 nickel base weld metal.

1.2 Objectives of Study

The objective of the work described in this paper is to estimate the frequency of BWR pipe weld breaks that have the potential to lead to strainer blockage accident scenarios. The work was limited to the consideration of piping features in a reference BWR 4/Mark I plant. It was assumed that this reference plant would contain susceptible type 304 stainless steel piping.

2.0 Review of General Approaches to Quantification of Weld Breaks

A number of various types of reactor equipment items are normally considered in a reactor probabilistic safety assessment, for example pumps, valves, motors, diesels, switchgear, instrumentation, and piping. Of the reactor equipment items considered in these types of analyses, piping and associated welds are generally among the most difficult to treat in regard to failure quantification. This situation exists because of the scarcity of incidents involving actual pipe failures and the difficulties associated with developing detailed analytical predictive models. The following subsections briefly discuss general methods that could be used to address pipe/weld break frequencies, and their respective advantages and disadvantages.

2.1 Operational Data

As was noted above, there is a scarcity of actual pipe failure events that can be applied to the quantification of reactor pipe breaks. For example, there have been no BWR recirculation system pipe breaks that have occurred to date. Actual pipe breaks of significant size have been limited to non-LOCA sensitive systems.

It is important to recognize that the limited available data are not sufficiently detailed to provide insight into specific expected break locations and time-dependent variability in equipment failure frequency. On the other hand, limited data can in some cases be used as general benchmarks of "reasonableness".

Bayesian statistical techniques, such as those discussed in NUREG/CR-4407 (Ref. 5), have been used to address the issue of very limited operational experience. For a situation involving no failures, these techniques can be used estimate a failure rate by dividing an assigned numerator ("assumed number of failures") by the population in which no breaks have actually occurred. This numerator is typically in the range of approximately 0.2 to 1. These techniques are not ideal, in that they may not be able to adequately account for phenomena that are strongly dependent on aging (such as corrosion effects).

2.2 Analytical Methods

Probabilistic structural methods can be used to estimate pipe break frequencies. These types of analytical methods can address possible material flaws, material properties, and loadings. An example of this type of analysis is the Lawrence Livermore National Laboratory (LLNL) analysis presented in NUREG/CR-4792 (Ref. 3).

In using an analytical approach, it is imperative that the dominant failure causes are adequately addressed. Because of the complexities and assumptions used in the required models, the analytical approach can be expected to have rather large uncertainties. On the other hand, insights obtained from these calculations can be used to predict specific phenomena of interest, for example pipe locations having the highest probability of break and the progression of aging-related phenomena. In addition, analytical methods can be effective in evaluating the relative behavior of different types of materials.

2.3 Expert Judgment

Systematic procedures have been developed as described in NUREG-1150, Vol. 1 (Ref. 6) and NUREG/CR-4550, Vol. 2 (Ref. 7) to conduct expert elicitations that can be used to predict equipment failure rates. In general, the use of expert judgment is recommended only in situations where a) an issue has a significant impact on risk and/or uncertainty, and b) other sources or means of generating data are not available.

2.4 Combined Approach

Under some circumstances, it may to useful to combine operational and analytically-derived data to estimate pipe failure rates. In a combined approach, it may be possible to account for detailed phenomena in a deterministic model, while at the same time using operational data to judge the reasonableness of the predicted failure rates.

3.0 BWR Weld Break Frequency Estimates

In making a decision on an approach to quantify BWR weld break frequencies for later use in estimating ECCS unavailability due to debris blockage, particular attention was given to recently published cautionary information in CRTD-Vol. 20-2 (Ref. 8) that contains ASME-sponsored work related to risk-based inspection guidelines for light water reactor components. In particular, p. 15 of Ref. 8 notes that conservative design practices have made it very unlikely that pipe failures would occur for a number of anticipated modes of failure, including excessive elastic or plastic deformation, brittle fracture, stress rupture/creep deformation (inelastic), and plastic instability. This document goes on to state that "it is generally believed within the nuclear industry that other causes not addressed in design, by ASME BPVC[1] calculations or otherwise, are most likely to cause structural failures. Two common examples are intergranular stress corrosion cracking (IGSCC) of stainless steel piping and erosion-corrosion wall thinning of carbon steel piping."

3.1 Approach Used to Estimate Weld Break Frequencies

Given the ASME cautionary note above about potential IGSCC degradation and the relative lack of suitable historical data for pipe failures, an analytical approach was selected as the foundation for generating pipe weld break frequency estimates. The analytical model chosen for this study was developed by the Lawrence Livermore National Laboratory (LLNL) and is described in detail in NUREG/CR-4792 (Ref. 3). The LLNL model was chosen because it is comprehensive in nature. As will be discussed in more detail below, the LLNL model addressed both indirect and direct causes of weld breaks, including IGSCC. While the LLNL analysis was generally conservative, areas of conservatism were identified so that future refinements to the break frequency data can be made.

3.1.1 Brief Description of LLNL Analysis Method

The LLNL analysis combined probabilistic and deterministic techniques to estimate the chances that weld breaks will occur in reactor coolant piping at a BWR 4/Mark I plant. The following categories of weld breaks were considered by LLNL:

a) Breaks due to direct causes, specifically:
   i) Crack growth at welded joints related to the combined effects of thermal, pressure, seismic, and other loads, and
   ii) Crack growth at welded joints related to IGSCC.

---

[1] Boiler and Pressure Vessel Code

b) Breaks due to indirect causes, specifically the seismically-induced failure of equipment, including piping and component supports, that could lead to the break of a reactor coolant pipe.

The LLNL analysis considered three major piping systems: the recirculation, main steam and feedwater systems. However, the evaluation of IGSCC effects was limited to the recirculation system. Also, note that the main objective of the IGSCC analysis was to compare relative behavior of different types of recirculation piping materials. Typical layouts of a BWR 4/Mark 1 plant recirculation, main steam, and feedwater systems are shown in Figures 3-1, 3-2, and 3-3.

The LLNL analysis provides results both in terms of "leaks" and Double Ended Guillotine Breaks (DEGBs). As will be explained later in Section 3.2, it was assumed that of these two break categories, only the DEGBs would be of concern for later use in the debris blockage analysis. Table 3-1 summarizes probability data extracted from Tables 3.2 and 3.6 in the LLNL analysis for DEGBs related to direct causes, exclusive of IGSCC effects. Note that the LLNL results have been converted to frequencies, assuming a 40 yr plant lifetime.

To address potential IGSCC effects, it is useful to consider the data contained in Figure 3-4. This figure presents the cumulative system probability that a BWR 4/Mark 1 recirculation loop made from 304SS and a (fictitious) 316NG replacement loop with the same configuration will experience a DEGB given IGSCC effects. This figure is reproduced from Figure 4.9(a) in the LLNL analysis. Note that LLNL has not provided a corresponding uncertainty analysis for these results. Over a 40 year plant lifetime, these probability data predict that a recirculation loop made from 304SS will experience a DEGB event with a frequency of approximately 5E-04/Rx-yr. In contrast, the fictitious 316NG replacement loop was predicted to fail with a frequency of approximately 4E-05/Rx-yr. These data indicate that the susceptible (304SS) material is over 10 times more likely to experience a DEGB over a 40 yr plant life than the resistant (316NG) material. Table 3-2 expresses the data in terms of total DEGB frequency of the recirculation system based on a total of two recirculation loops.

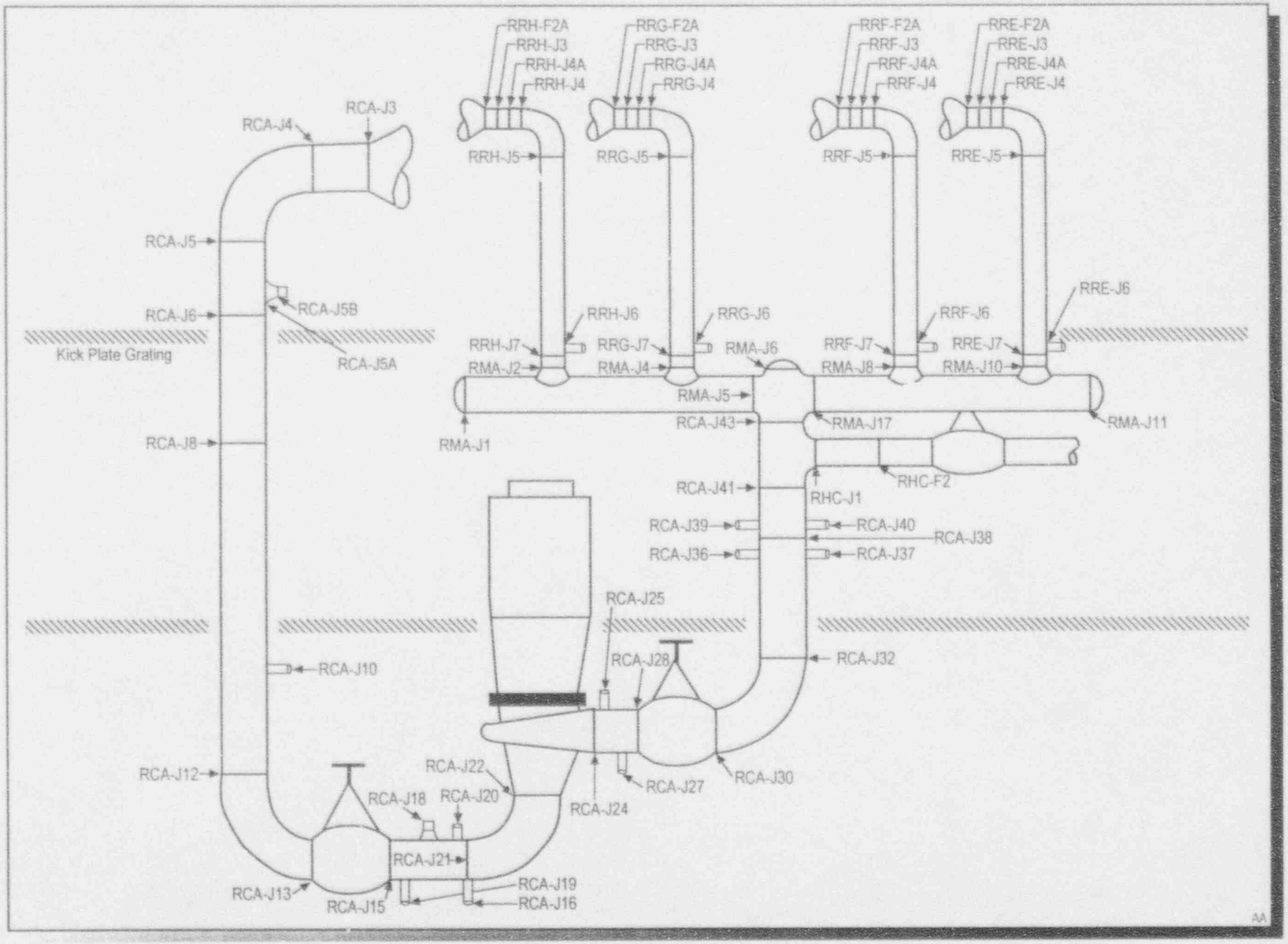

Figure 3-1. Weld Locations in a Recirculation Loop

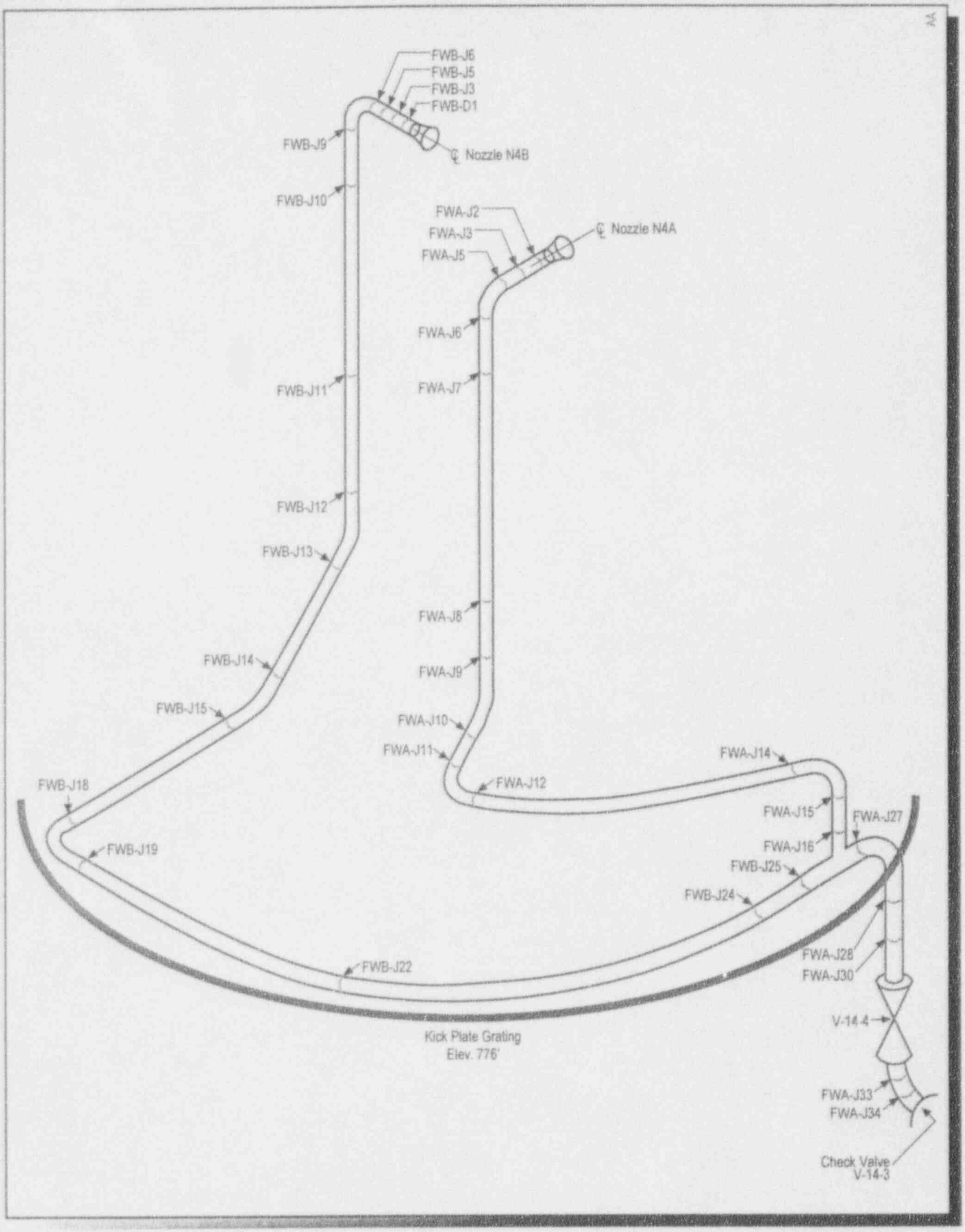

Figure 3-2. Weld Locations in Feedwater Paths

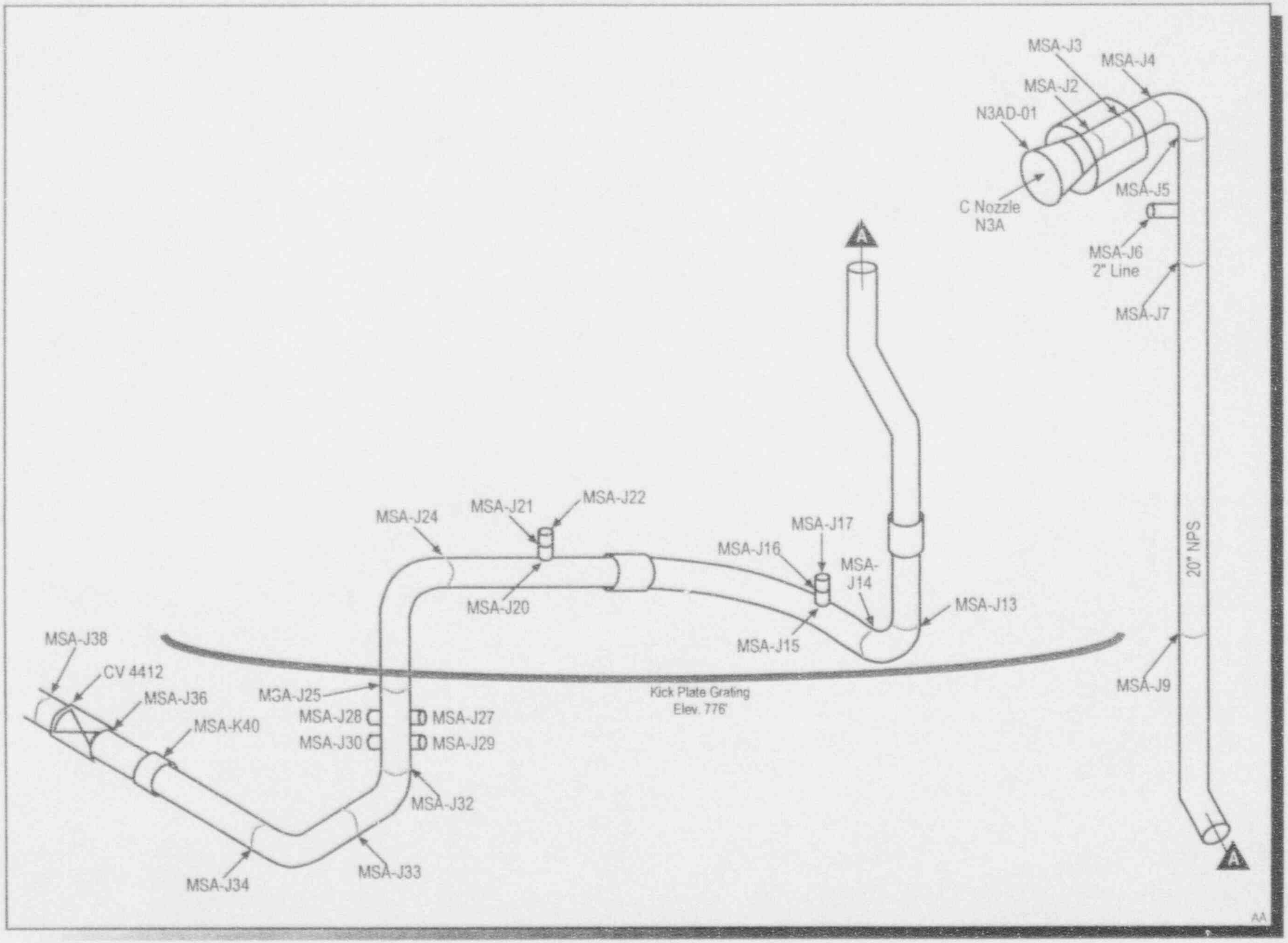

Figure 3-3. Weld Locations in Main a Steam Path

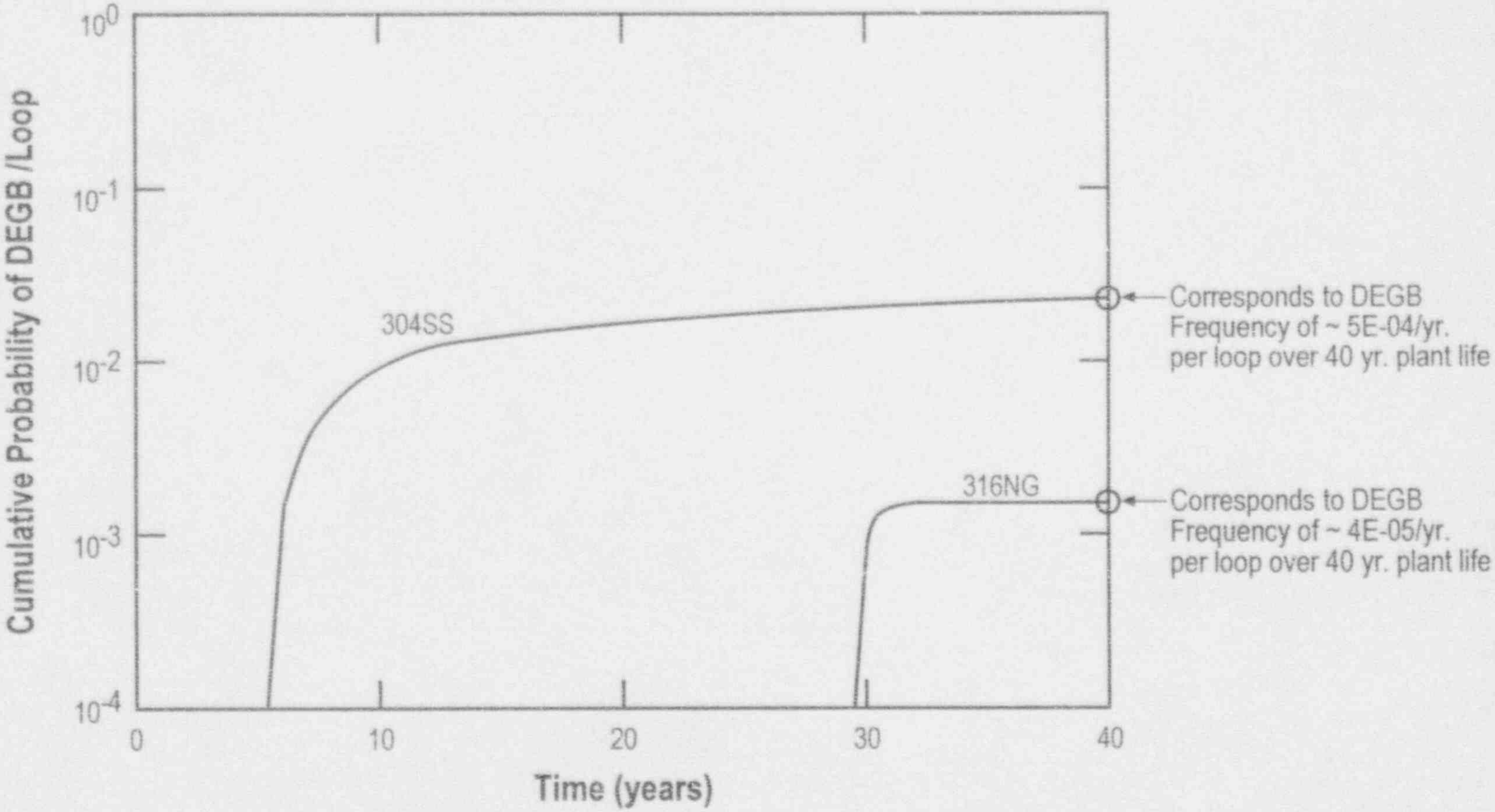

Reproduced from Fig. 4.9(a), Vol. 1 of NUREG/CR-4792

Figure 3-4. Cumulative System Probabilities of DEGB in One Recirculation Loop

Table 3-1
Frequencies for Directly-Caused DEGBs, Exclusive of IGSCC Effects[1]

	DEGB Frequency (1/Rx-yr.) Uncertainty Distribution Percentiles			
	10%	50%	90%	LLNL Best Estimate
Recirculation Loop[2]	-	-	-	3.8E-11
Main Steam Line[3]	5E-15	3E-13	1.4E-10	2.5E-13
Feedwater Line[3]	1.1E-14	1.5E-12	1.2E-09	1E-12

Notes:
1. Data extracted from Tables 3.2 and 3.6 of NUREG/CR-4792, Vol. 1 (Ref. 3).
2 Uncertainty distribution data not given for existing recirculation piping.
3. IGSCC routinely disregarded in evaluation of main steam and feedwater piping.

Table 3-2
Frequencies for IGSCC-Caused DEGBs to Recirculation Piping[1]

Material	DEGB Frequency (1/Rx-yr.) Point Estimate
Susceptible (304SS)	~1E-03[2]
Resistant (316NG)	~8E-05[3]

Notes:

1. Data extracted from Figure 3-4 of this report which has been reproduced from Fig. 4.9(a), Vol. 1 of NUREG/CR-4792 (Ref. 3).
2. DEGB frequency = ~5E-04/Rx-yr. per loop over 40-year plant life. Given a total of 2 loops, net DEGB frequency = ~1E-03/Rx-yr.
3. DEGB frequency = ~ 4E-05/Rx-yr. per loop over 40-year plant life. Given a total of 2 loops, net DEGB frequency = ~8E-05/Rx-yr.

Data pertaining to breaks caused by indirect means are summarized in Table 3-3. Again, these data were extracted from the LLNL analysis.

Table 3-3
Frequencies for Indirectly-Caused DEGBs to Reactor Coolant Piping[1]

Cause	DEGB Frequency (1/Rx-yr.) Uncertainty Distribution Percentiles 10%	50%	90%
Major Containment or Reactor Pressure Vessel Support Fails	5.1E-10	1.9E-07	2.8E-06
Failure of "Intermediate" Pipe Supports[2]	-	-	5.0E-06

Notes:
1. Data extracted from NUREG/CR-4792 (Ref. 5), p. 5-14 of Vol. 1 and p. 5-6 of Vol. 4.
2. Conservatively includes snubber relief valve failures and seismic hazard curve truncation level of 5 times Safe Shutdown Earthquake (SSE).

Based on a review of the information presented in Tables 3-1, 3-2, and 3-3, it was noted that the overwhelming contribution to the overall frequency of DEGB LOCA events at the reference BWR4/Mark I plant is predicted to be due to IGSCC effects on recirculation piping. Even in the case of resistant material (316NG), the IGSCC-induced DEGB frequencies are approximately an order of magnitude higher than the next most significant category, namely breaks caused by indirect means.

The LLNL study also presented the IGSCC DEGB frequency data in terms of specific weld categories. As is shown in Figure 3-5, about 80% of the postulated 304SS recirculation piping DEGBs were associated with 12" riser welds, while about 20% of the 304SS DEGBs were associated with 4" bypass line welds. The header (22"), discharge (28"), and suction (28") welds were each judged to contribute less than 10% to the recirculation loop DEGB frequency, based on the statistical accuracy of the LLNL calculations. Failure data for a proposed 316NG replacement recirculation loop having no bypass piping are also displayed in Figure 3-5.

Failure data extracted from Table 3-2 and Figure 3-5 were used to generate IGSCC DEGB frequencies on a per-weld basis for the categories of susceptible (304SS) recirculation loop material. As shown in Table 3-4, these calculations were made by multiplying the overall recirculation DEGB frequency estimate from Table 3-2 by the fractional contributions given in Figure 3-5, and subsequently dividing by the number of welds in a given category. The number of welds in a given category were obtained from the LLNL report.

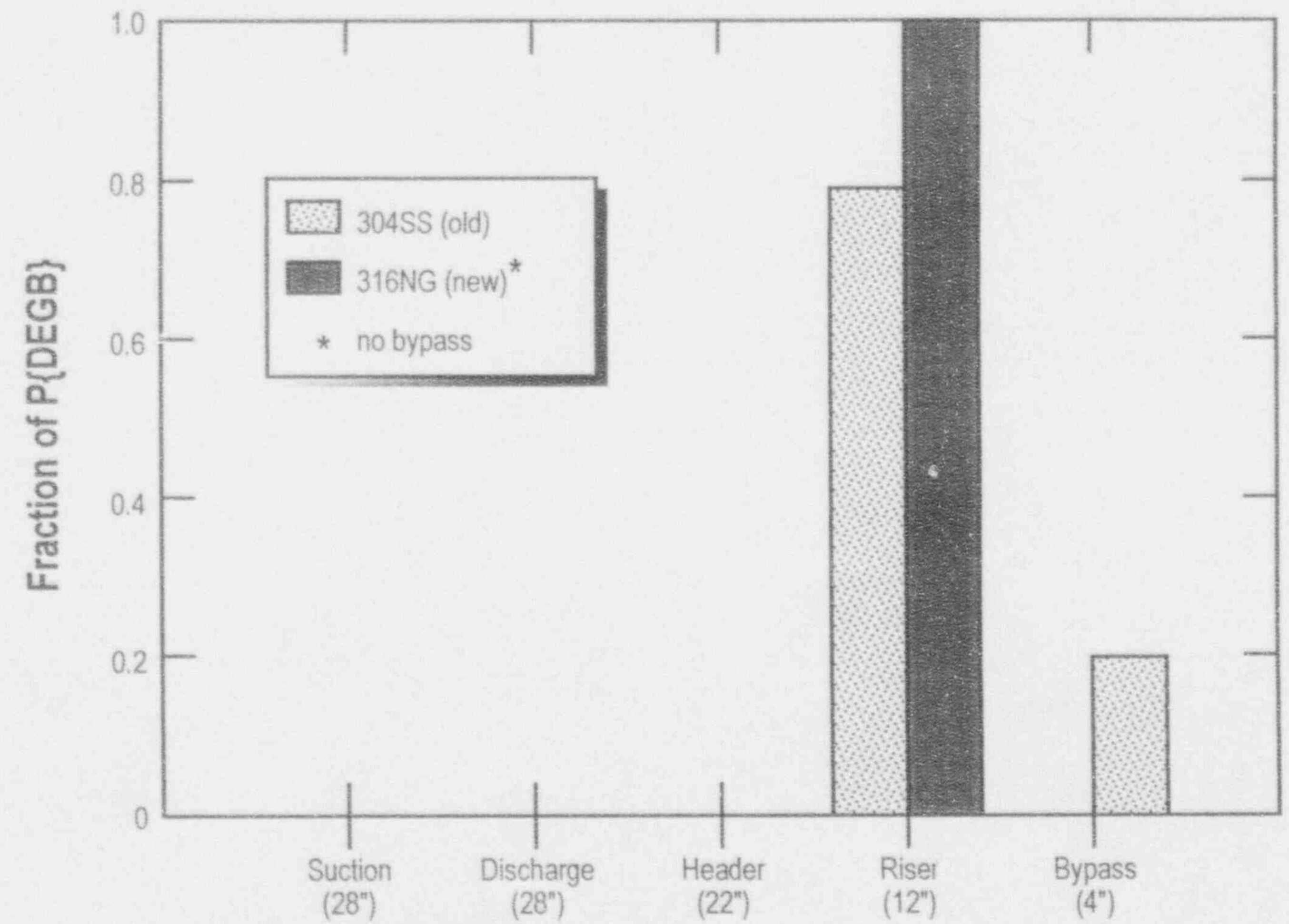

Reproduced from Fig. 4.11(b), Vol. 1 of NUREG/CR-4792

Figure 3-5. Relative Contribution of Various Welds to DEGB in Recirculation Loop

Table 3-4
Frequencies for IGSCC-Caused DEGBs to Recirculation Welds in Susceptible Material (304SS)

Weld Category	Total Welds in Category[1]	Fractional Contribution to Overall DEGB[2]	Weld DEGB Frequency Point Estimate[3]
4" Bypass	20	0.2	(0.2) x (1E-03/Rx-yr)/20=1E-05/Rx-yr
12" Riser	40	0.8	(0.8) x (1E-03/Rx-yr)/40=2E-05/Rx-yr
22"-28" (header discharge, suction)	42	<0.10	<(0.10) x (1E-03/Rx-yr)/42, ~2.E-06/Rx-yr

Notes:
1. Total welds in both recirculation loops
2. Data extracted from Figure 3-2 of this report which has been reproduced from Figure 4.11(b), Vol 1 of NUREG/CR-4792 (Ref. 3)
3. (1E-03/Rx-yr) frequency used in calculations was extracted from Figure 3-1 of this report which has been reproduced from Figure 4.11(a), Vol. 1 of NUREG/CR-4792 (Ref. 3)

3.2 Limitations of the LLNL Analysis

There were a number of limitations associated with the LLNL analysis. Because of the overwhelming contribution of IGSCC to the predicted weld break frequencies, efforts were focused on identifying the most significant limitations associated with the IGSCC portion of the analysis. Some of the limitations of the LLNL IGSCC analysis that were identified in this study include:

1) Certain local phenomena were not considered in the LLNL analysis, for example the effect of coolant flow velocity on possible flushing of impurities that otherwise could aggravate the susceptibility to IGSCC.

2) The model used "harsh" laboratory conditions to predict growth rates and times-to-initiation. It is conservative to extrapolate the "harsh" laboratory data to the relatively benign conditions that exist in reactor facilities.

3) The failure probability is very sensitive to the type of residual stress assumed in the analysis. Consequently, plant-to-plant experiences could vary significantly depending on residual stresses that remain following pipe assembly welding and "fit up". Worst case stress assumptions were used in the analysis.

4) The analysis did not give credit for actions to mitigate the effects of IGSCC, specifically in-service inspections, weld overlay, or inductive heating stress improvement (IHSI). In addition, the analysis did not address the mitigating effects of corrosion control programs.

5) The main objective of the analysis was to compare the behavior of different types of materials to IGSCC. This emphasis may introduce additional uncertainties in the absolute value of the break frequencies.

6) There were discrepancies between the LLNL predictions and a field test done at a BWR site. As noted in NUREG/CR-5486 (Ref. 9), these discrepancies most likely are the result of field variations in various pertinent phenomena and analytical assumptions needed to model these phenomena. However, it is important to note that both the LLNL analysis and field results give highest priority to riser and bypass welds.

7) The LLNL analysis assumed that IGSCC effects could be ignored regarding pipe breaks of the main steam and feedwater piping.

8) Pipe breaks caused by water hammer or a projectile from pump failures were not considered.

9) The analysis did not consider scenarios that involved IGSCC-weakened piping coupled with other pipe challenges (i.e., water hammer, seismic events).

3.3 Recommended Weld Break Frequency Data

The IGSCC-induced DEGB data were used as a starting point in deriving estimates of weld break frequencies for use in the debris blockage analysis. In using the LLNL predictions of IGSCC-induced DEGB frequency for this analysis, adjustments were made to give credit for in-service inspection activities. Subsection 3.3.1 discusses the assumptions made in the use and refinement of the LLNL IGSCC data. Subsection 3.3.2 presents point estimates of the weld frequencies.

3.3.1 Assumptions Made in the Use and Refinement of LLNL IGSCC Data

In applying the LLNL data to this study, the following assumptions were made:

1) Of the two categories of breaks evaluated in the LLNL analysis (leaks and DEGBs), only breaks in the DEGB category were considered. It was assumed that the predicted breaks in the "leak" category would either represent mathematically-predicted flaws that do not actually

pass coolant, or would only allow the passage of coolant at a rate less than needed for ECCS actuation. If either of these two conditions were to exist, sump blockage would not be of concern.

2) Susceptible material (304SS) was assumed to be the material of interest.

3) Welds associated with main steam and feedwater piping would have the same break frequencies as the 22"-28" recirculation welds.

4) Only one IGSCC mitigating action would be in place, namely an in-service inspection program. In adjusting the data for an in-service inspection program, use was made of a discussion of risk-based inspection activities contained in CRTD-Vol. 20-2 (Ref. 8). In particular, it was noted on p. 81 of CRTD-Vol. 20-2 (Ref. 8) that "a high level of inspection can significantly reduce the failure probabilities of BWR piping systems (by a factor of 10 or more)." Supporting data and analyses are contained in Table 2-12 of this reference. For the purpose of this analysis, it was decided that the LLNL frequency estimates would be reduced by a factor of 10 to account for in-service inspection. The effect on this in-service inspection adjustment is to lower the 304SS DEGB frequency to a value slightly above that predicted for the non-susceptible material (316NG). This situation is illustrated in Figure 3-4.

3.3.2 Recommended Frequency Estimates for Weld Breaks

By using the LLNL IGSCC data for the DEGB category and the assumptions discussed above in Subsection 3.3.1, estimates for weld break frequencies were generated. The recommended frequency estimates are given in Table 3-5. The data in Table 3-5 were generated by applying the in-service inspection reduction factor of 10 discussed above to the LLNL IGSCC DEGB data presented earlier in Table 3-4. As noted in Table 3-5, the welds associated with main steam and feedwater piping were assumed to have the same break frequencies as the 22"-28" recirculation welds.

It is important to recognize that there are large uncertainties associated with the recommended point-value frequency estimates. Because an uncertainty analysis has not been performed, it is not possible to further interpret the statistical significance of the point-value estimates given in Table 3-5.

Table 3-5
Recommended DEGB Frequency Estimates

Pipe Category	DEGB Frequency (1/Rx-yr) - Point Estimate
a) Per Weld	
4" Recirculation (304SS)	1E-06[1]
12" Recirculation (304SS)	2E-06[1]
22 - 28" Recirculation (304SS)	2E-07[1]
Main Steam[2]	2E-07
Feedwater[2]	2E-07
b) All Welds	
All Recirculation (102 weld total)	1E-04[3]
Main Steam (64 welds total): 64 x 2E-07/Rx-yr = ~1E-05/Rx-yr.	1E-05
Feedwater (58 welds total): 58 x 2E-07/Rx-yr = ~1E-05/Rx-yr.	1E-05
Total	~1E-04[4]

Notes:
1. Derived by reducing Table 3-4 data by a failure of 10 to account for in-service inspection.
2. Main steam and feedwater welds assumed to have same failure frequency as 22-28" recirculation system welds.
3. Overall recirculation DEGB frequency estimate given earlier in Table 3-2 and reduced by a factor of 10 to account for in-service inspection
4. Total estimated DEGB frequency for all pipe categories for LLNL reference BWR..

3.4 Comparisons of Recommended Data With Other Data Sources

A comparison of the recommended frequency data was made with large LOCA data given in several BWR 4/Mark I risk assessment studies, specifically: the Duane Arnold IPE (Ref. 10), the Cooper Level 1 PRA (Ref. 11), the FitzPatrick IPE (Ref. 12), the Browns Ferry Unit 2 IPE (Ref. 13), and a Peach Bottom PRA described in NUREG/CR-4550 (Ref. 14). This comparison is displayed in Table 3-6. The point-estimate value for the DEGB frequency, 1E-04/Rx-yr, was extracted from Table 3-5, and represents a summation of our DEGB frequency estimates over all welds for the LLNL reference plant. The total number of welds in each category is based on data provided in the LLNL analysis.

Table 3-6
Comparison of Recommended Large LOCA Data with Other BWR 4/Mark I Risk Assessment Data

Data Source	LOCA Type	Estimated Frequency (1/Rx-yr)	Statistical Category	Notes
1. Recommended Data (LLNL Reference BWR)	DEGB (≥ 4")	1E-04	Point Estimate	Based on LLNL study
2. Duane Arnold IPE	Large LOCA	3E-04	?	Based on Brunswick study
3. Peach Bottom PRA (NUREG -1150)	Large LOCA	1E-04	Mean	Based on WASH-1400
4. Cooper IPE	Large LOCA	1F-04	Mean	Based on WASH-1400
5. J. A. FitzPatrick IPE	Large LOCA	1E-04	Mean	Based on WASH-1400
6. Browns Ferry Unit 2 IPE	Large LOCA:			Based on PLG Proprietary Data Base
	a. Recirc. suction line	9.2E-05	Mean	
	b. Recirc. disch. line	3.1E-04	Mean	
	c. Core spray line	8.3E-05	Mean	
	d. Other	1.1E-04	Mean	

It can be seen from the data in Table 3-6 that the recommended DEGB point estimate is in agreement with large LOCA frequency estimates used in other BWR studies. It can also be seen that several plants have chosen to base their frequency estimates on data from WASH-1400 (Ref. 15). The Browns Ferry IPE data were primarily based on generic data that have been derived from cumulative experience at a large number of plants, with adjustments for Browns Ferry plant-specific features. The data used to support the Browns Ferry IPE were given in PLG-0500 (Ref. 16), a proprietary data base.

It is recognized that IPE results have generally concluded that LOCA initiated-accidents are small contributors to core damage. Consequently, there has not been a strong motivation for licensees to expend large efforts to refine LOCA initiating event frequencies.

4.0 Summary and Recommendations

This study has used results from an analytical approach to estimate the failure frequency of DEGB weld breaks at BWR 4/Mark I plants. The analysis focused on effects related to IGSCC, as this phenomena appeared to be the dominant mechanism involved in weld breaks for the susceptible material of interest (304SS). An adjustment was made to the data to account for in-service inspection activities. Consideration of other mitigating mechanisms, for example aggr[illegible] corrosion control, was not evaluated. It is important to recognize that an uncertainty analysis [illegible]t been performed. Consequently, it is not possible to interpret the statistical significance of the point-value estimates. It is also important to note that future studies may identify important weld break phenomena that have not been included in this analysis.

It is recommended that additional study be done to refine the proposed weld break data. For example, it is recommended that additional sensitivity studies be [illegible] address IGSCC mitigating mechanisms so that areas of conservatism can be better understoo[illegible] [illegible]s also recommended that an analysis be done to address the expected distribution of leak rates that are associated with predicted "leak events" (as opposed to DEGB events). Sor[illegible] fraction of the "leak" category events may pass coolant with rates large enough to be considered initiators for the debris blockage analysis. In addition, it is recommended that a comprehensive uncertainty analysis be done to establish statistical parameters of interest (i.e., mean values). Finally, note that work to address sor[illegible] the above recommendations will most likely involve additional computer analyses using the LLNL [illegible]odology.

REFERENCES

[1] A. W. Serkiz, "USI A-43 Regulatory Analysis," US Nuclear Regulatory Commission, NUREG-0869, Rev. 1, October 1985.

[2] J. J. Wysocki, "Probabilistic Assessment of Recirculation Sump Blockage Due to Loss Of Coolant Accidents, Containment Emergency Sump Performance USI A-43," Vols. 1 and 2, Burns & Roe, Inc., published as Sandia National Laboratories Report No. SAND83-7116, NUREG/CR-3394, July 1983.

[3] G. S. Holman and C. K. Chou, "Probability of Failure in BWR Reactor Coolant Piping," published as Lawrence Livermore National Laboratory report UCID-20914, NUREG/CR-4792, March 1989.

[4] W.S. Hazelton and W. H. Koo, "Technical Report on Material Selection and Processing Guidelines for BWR Coolant Pressure Boundary Piping," U. S. Nuclear Regulatory Commission, NUREG-0313, Rev. 2, January 1988.

[5] R. E. Wright et. al, "Pipe Break Frequency Estimation for Nuclear Power Plants," EG&G Idaho, Inc, EGG-2421, NUREG/CR-4407, May 1987.

[6] U. S. Nuclear Regulatory Commission, "Severe Accident Risks: An Assessment for Five U. S. Nuclear Power Plants," NUREG-1150, Vol. 1, December 1990.

[7] T. A. Wheeler, et. al, "Analysis of Core Damage Frequency from Internal Events: Expert Judgment Elicitation," published as Sandia National Laboratories report, SAND86-2084, NUREG/CR-4550, Vol. 2, April 1989.

[8] "Risk-Based Inspection -- Development of Guidelines, Volume 2, Part 1, Light Water Reactor (LWR) Nuclear Power Plant Components," The American Society of Mechanical Engineers, CRTD-Vol. 20-2, 1992.

[9] G.S. Holman, "Application of Reliability Techniques to Prioritize BWR Recirculation Loop Welds for In-Service Inspection," published as Lawrence Livermore National Laboratory report UCID-21838, NUREG/CR-5486, December 1989.

[10] Iowa Electric Light & Power Co., "Duane Arnold Energy Center Individual Plant Examination (IPE)," November 1992.

[11] Nebraska Public Power District, "Cooper Nuclear Station Probabilistic Risk Assessment Level 1," March 1993.

[12] New York Power Authority, "James A. FitzPatrick Nuclear Power Plant Individual Plant Examination," August 1991.

[13] Tennessee Valley Authority, "Browns Ferry Nuclear Plant Unit 2 Probabilistic Risk Assessment Individual Plant Examination," September, 1992.

[14] A. M. Kolaczkowski, et. al., "Analysis of Core Damage Frequency: Peach Bottom, Unit 2 Internal Events," published as Sandia National Laboratories report SAND86-2084, NUREG/CR-4550, Vol. 4, Rev. 1, Part 1, August 1989.

[15] U.S. Nuclear Regulatory Commission, "Reactor Safety Study - An Assessment of Accident Risks in U.S. commercial Nuclear Power Plants," WASH-1400 (NUREG 75/014), October 1975.

[16] Pickard, Lowe and Garrick, Inc., "Database for Probabilistic Risk Assessment of Light Water Nuclear Power Plants," Vol. 7, BWR Initiators, PLG-0500, May 1992.

APPENDIX B

Overview of BLOCKAGE 2.0

Table of Contents

Section — Page

B.1 Background B-1

B.2 Functional Requirements B-1

B.3 Description B-2
- B.3.1 BLOCKAGE 2.0 General Features B-2
- B.3.2 BLOCKAGE 2.0 Program Structure B-5

B.4 Verification and Validation B-8
- B.4.1 BLOCKAGE 1.0 Testing B-9
- B.4.2 BLOCKAGE 1.0 Qualification Test B-9
- B.4.3 BLOCKAGE 2.0 Testing B-9
- B.4.4 BLOCKAGE 2.0 Validation Testing B-10
- B.5.2 Output Description B-11

References B-18

List of Figures

B.3-1 BLOCKAGE 2.0 Input/Output Flow Chart B-4
B.3-2 BLOCKAGE 2.0 Flow Chart by Function B-6
B.3-3 BLOCKAGE 2.0 Flow Chart by Subroutine B-7

List of Tables

B.4-1 BLOCKAGE 1.0 and 2.0 Quality Assurance B-8
B.5-1 BLOCKAGE 2.0 File Structure B-10
B.5-2 Parameter Input File B-12
B.5-3 Weld Input File B-13
B.5-4 Sample Parameter Input File B-14
B.5-5 Sample Weld Input File B-16

APPENDIX B:
Overview of BLOCKAGE 2.0

B.1 Background

This appendix provides additional details of the PC-based BLOCKAGE 2.0 computer code that was used to generate the strainer blockage analysis results. As was previously noted in the main body of the report, the BLOCKAGE 2.0 code was developed in two stages. In the first stage, BLOCKAGE 1.0 was developed to reproduce the NUREG/CR-3394 (Ref. 1) results for the Salem PWR plant. Subsequently, BLOCKAGE 2.0 was generated by modifying BLOCKAGE 1.0 to accommodate BWRs.

Section B.2 below provides a discussion of the BLOCKAGE 2.0 functional requirements. A description of the code is given in Section B.3, including general features and the program structure. Section B.4 describes pertinent verification and validation activities, specifically the testing of BLOCKAGE 1.0 and 2.0. Finally, the user interface is described in Section B.5, including descriptions of the code input and output.

B.2 Functional Requirements

As noted above, the BLOCKAGE 2.0 code was developed in two stages. The BLOCKAGE 1.0 code was developed first and validated by reproducing the previous results. The BLOCKAGE 1.0 code was subsequently modified to accommodate BWRs.

The functional requirements for the BLOCKAGE 1.0 code are that it:

1. Is a Level 1 technical application PC-based software,

2. Reproduces the functions of the calculational program documented in NUREG/CR-3394, Vol. 2 (Ref. 1) important to the resolution of USI A-43,

3. Meets quality assurance in accordance with the "Software Quality Assurance Program and Guidelines", NUREG/BR-0167 (Ref. 2), as applicable, and that as a minimum, its development includes verification and validation, configuration management, and documentation control,

4. Is developed for intended use by those under the supervision of engineers who are experienced with the phenomena, are knowledgeable of the methodology, and who will perform critical reviews of the calculations,

5. Has software documentation which includes a software requirements document, a software design document, and a qualification test report, placed under configuration control, and

6. Has initial break probabilities developed by weld type weighting method.

Since no qualification tests were readily available to validate BLOCKAGE 2.0, it had to be subjected to more stringent verification procedures such as line-by-line internal peer inspection and simple tests compared with hand calculations. The verification and validation of the BLOCKAGE 2.0 code is described more thoroughly in Section B.4.

B.3 Description

BLOCKAGE 2.0 is PC-based software that reproduces the functions of PRA and TABLE that were important to the resolution of USI A-43, while accomodating input for a representative BWR. The code calculates the frequency, per Rx-yr, of a sequence involving a LOCA followed by inadequate NPSH in the recirculation cooling system due to insulation debris generated by the LOCA.

B.3.1 BLOCKAGE 2.0 General Features

The user provides a list of welds whose failure can initiate a LOCA. BLOCKAGE 2.0 uses one of two methods to determine a break frequency for each weld. If the user chooses the first method, the input for computing break frequencies is a table of weld break frequencies by weld type and diameter class.

In the second method, the input for computing break frequencies is a table of plant pipe break frequency by diameter class, together with weighting factors by type of weld. If this method is chosen by the user, the list of welds must include all piping included in the plant break frequencies, including secondary systems. The software allocates the plant frequencies among the individual welds such that the plant pipe break frequency is the sum of the weld break frequencies. If the plant has appropriate symmetry, the list of welds need include only the welds in one loop; each weld will represent all of the corresponding welds in other loops.

Using the general parameter input and specific weld input data supplied by the user, BLOCKAGE 2.0 generates six output report files:

- Weld summary report
- Target summary report
- Sequence frequencies reports

- Unavailabilities reports
- Summary reports
- Error messages.

A flow chart for the BLOCKAGE 2.0 input/output is shown in Figure B.3-1. The specific formats, parameters, and data are described in Section B.5.

BLOCKAGE 2.0 contains a number of features not contained in the PRA and TABLE software. For example, BLOCKAGE 2.0 provides for input of a destruction fraction for each value of L/D. This factor is applied to the fibrous insulation generated between that value of L/D and the next lower value (or zero), and represents the fraction of fibrous insulation that is pulverized into individual fibers or small bundles. The software also provides for input of a transport fraction for each permissible weld location. For fibrous debris generated at that location, the transport represents the fraction that reaches the suppression pool. Finally, the parameters for the head loss formula are now variables determined by user input.

Different terminology is used in the BLOCKAGE 2.0 reports than in the USI A-43 analysis software. In the BLOCKAGE 2.0 specification, frequencies have units of inverse time, and probabilities are dimensionless, consistent with current nomenclature conventions. This is the opposite of the nomenclature used in NUREG/CR-3394 (Ref. 1).

Many of the reports generated by the USI A-43 analysis software were not used in the regulatory analysis. Although the unused reports presumably were not important to the resolution of USI A-43, their content has been reviewed to verify that they would not be relevant to the study of BWR strainer clogging. In particular, BLOCKAGE 2.0 is not required to create Tables A.2-1 through A.2-6 of NUREG/CR-3394 (Ref. 1), "Event Probabilities by Pipe Diameter" and "Event Probabilities by Pipe System," which were not used in the regulatory analysis. This capability was unnecessary because the break frequencies are reported by diameter class and by system in the Probability Reports.

Similarly, BLOCKAGE 2.0 was not required to create Tables B.5-4 through B.5-45 of NUREG/CR-3394 (Ref. 1), "Debris Summary for Maximized Fibrous Debris" and "Debris Summary for Maximized Total Debris" which were not used in the regulatory analysis. The only output of debris volume required was included in the table of targets. This volume does not include destruction fractions, but assumed 100% destruction.

Another omitted capability was the capability to perform calculations based on allocation of LOCA frequency assuming longitudinal pipe breaks; that is, in proportion to the length of the pipe segment. The earlier programs, PRA and TABLE, produce reports for both weld-basis and length-basis using the same

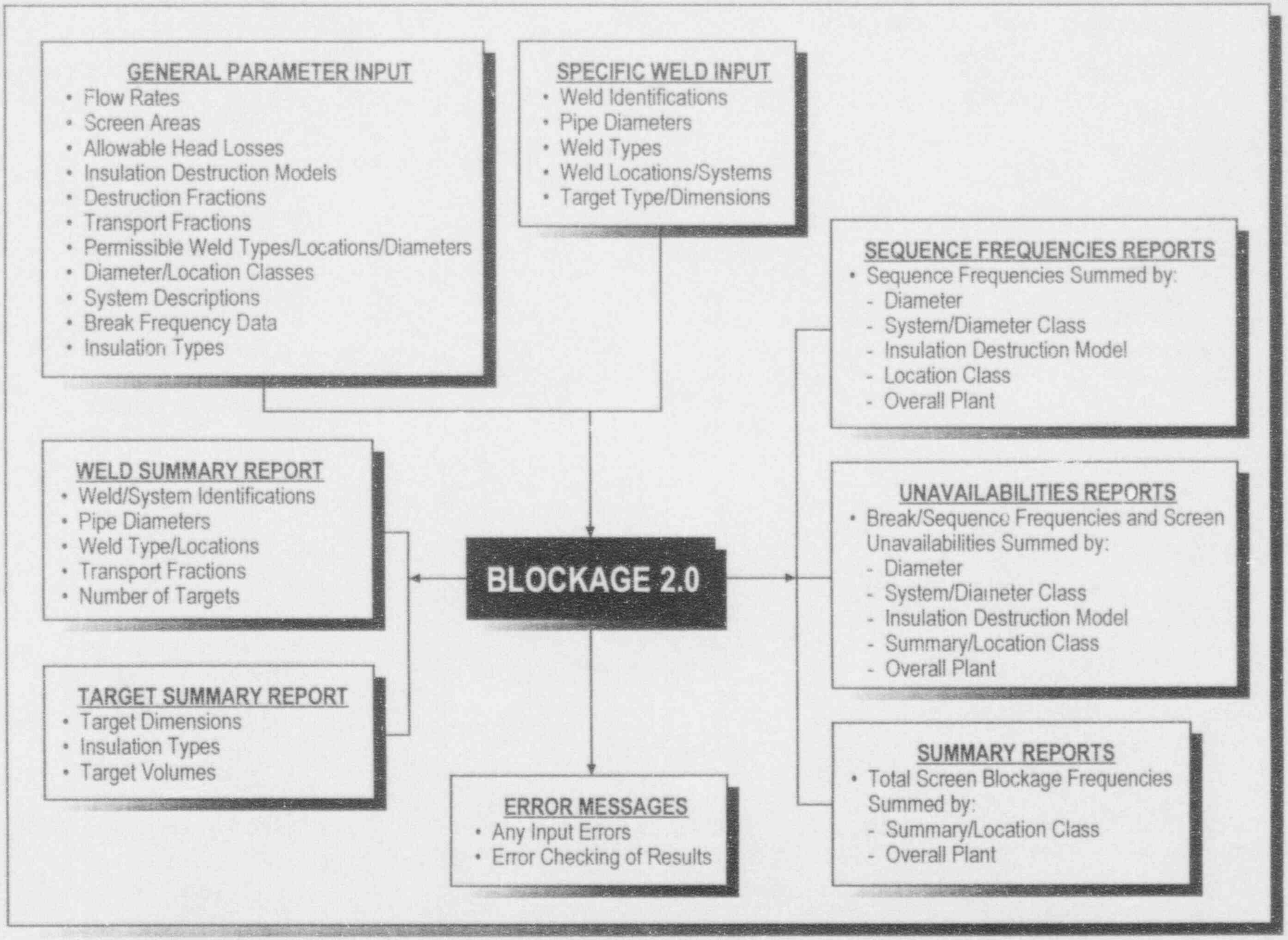

Figure B.3-1. BLOCKAGE 2.0 Input/Output Flow Chart

target data. However, the length-basis results were not used in the subsequent regulatory analysis because the weld-basis frequencies were considered to be more realistic. Furthermore, the length-basis calculations should have used target data derived for longitudinal breaks rather than circumferential breaks.

Finally, BLOCKAGE 2.0 does not provide for blockage summaries that contain counts of potential break locations. Such tables appear in appendix B of NUREG/CR-3394 (Ref. 1), with the counts weighted either by weld factor or by segment length. There is no accompanying text to explain these tables, and they were not used in the regulatory analysis.

B.3.2 BLOCKAGE 2.0 Program Structure

The BLOCKAGE 2.0 software development and quality assurance followed the general guidelines in NUREG/BR-0167 (Ref. 2) and ANSI/IEEE Std. 830-1984 (Ref. 3). A functional flow chart for BLOCKAGE 2.0 is shown in Figure B.3-2. The three major functions required are performed within three major subroutines: SETUP, BLKAGE, and REPORT. Within SETUP, the parameter and weld input files are read and validated. Any error messages are written to BLOCKAGE.ERR. The program then calculates the target and fibrous insulation volumes and writes the target summary report, TARGET.OUT. The welds are characterized by diameter and type for output to the weld summary report, WELD.OUT. Finally, the subroutine calculates weld break frequencies based on the break frequency model. Subroutine BLKAGE calculates head losses and tests for blockage. The remaining reports are generated in REPORT, resulting in output files SEQFREQ.OUT, BLOCKAGE.OUT, and SUMMARY.OUT. In addition, any error messages are written to BLOCKAGE.ERR.

The subroutine flow chart in Figure B.3-3 illustrates the relationship of the functional subroutines within the threee main subroutines. The specific equations used in each calculation were previously given in Section 5 of of this report.

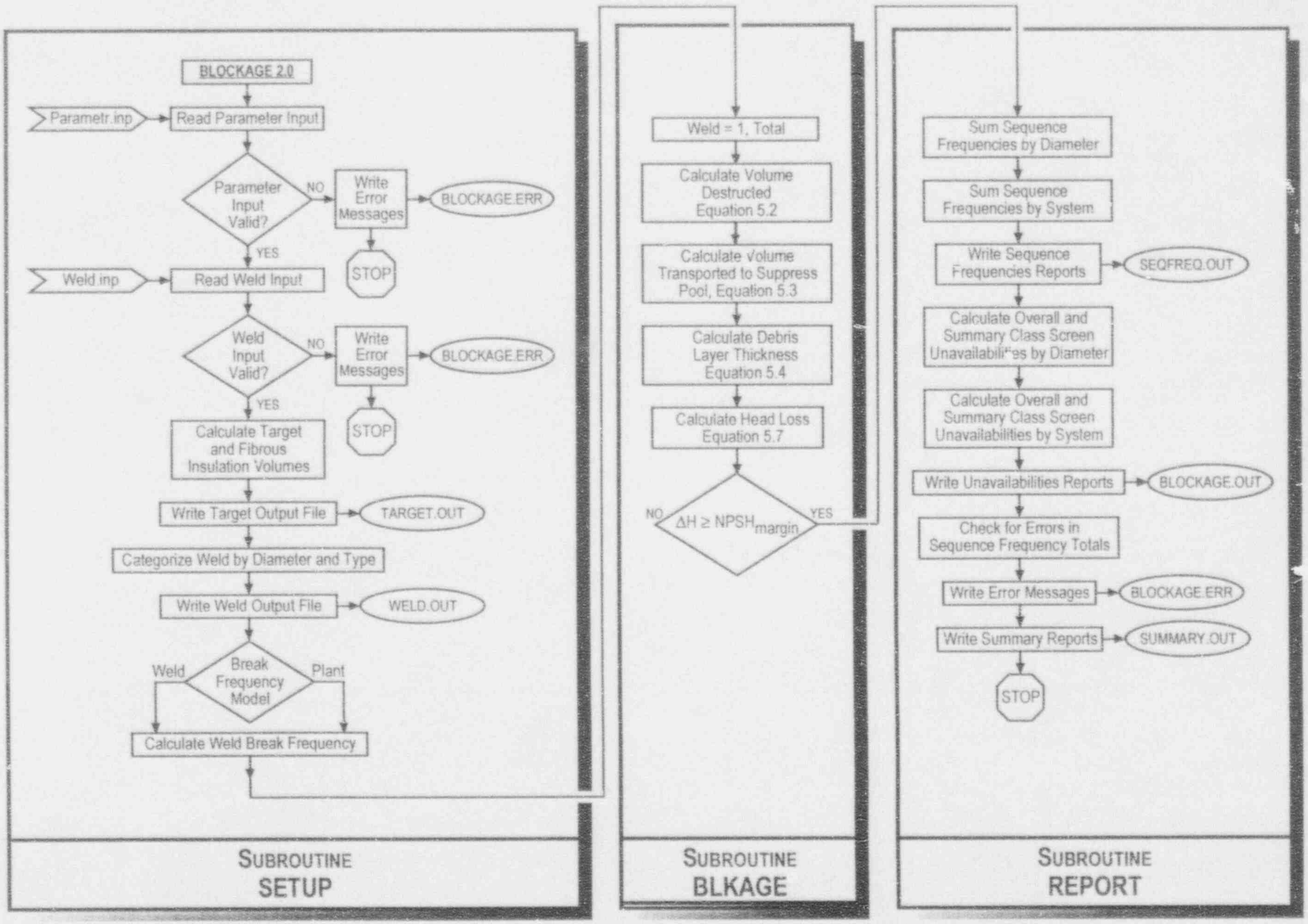

Figure B.3-2. BLOCKAGE 2.0 Flow Chart by Function

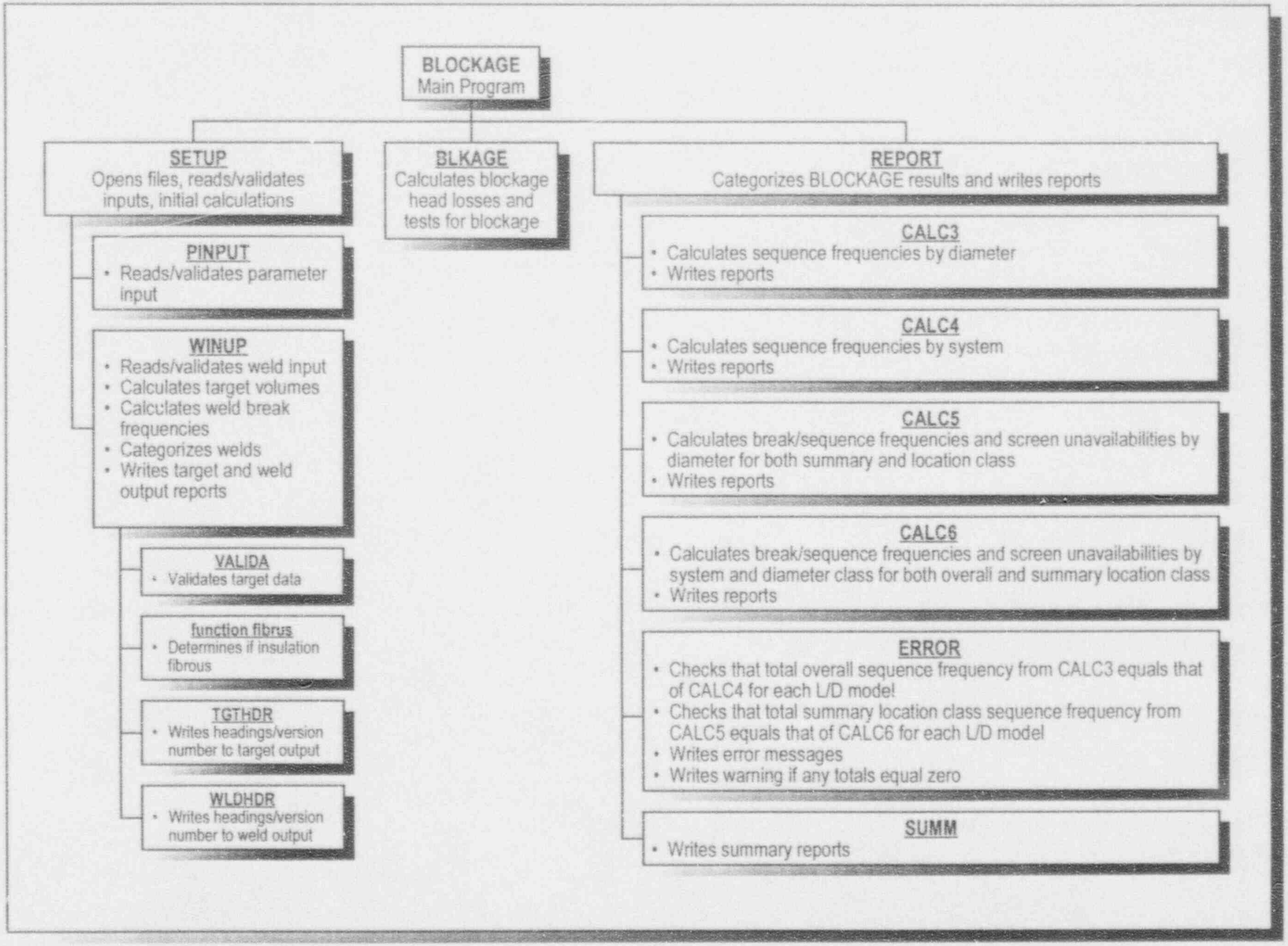

Figure B.3-3. BLOCKAGE 2.0 Flow Chart by Subroutine

B.4 Verification and Validation

The BLOCKAGE 2.0 code was verified and validated by coding review, by test calculations and by comparing its results to those of a previous calculation documented in NUREG/CR-3394 (Ref. 1). The code was developed in two separate steps to facilitate the code verification. The first development step resulted in BLOCKAGE 1.0 which was coded to reproduce the results of NUREG/CR-3394 (Ref. 1) and the direct comparison of these two results produced by different codes represented a qualification test of the coding of BLOCKAGE 1.0. The second developmental step was to add models to BLOCKAGE 1.0 allowing the user to specify break frequencies per weld type and diameter class, to specify an insulation destruction fraction for each insulation destruction model, to specify a transport fraction for each permissible weld location, and to specify the constant parameters in head loss formula. The code with these modifications then became BLOCKAGE 2.0.

The verification of the BLOCKAGE code was mainly accomplished through a number of software quality assurance activities based on guidance in NUREG/BR-0167 (Ref. 2) and ANSI/IEEE Std. 830-1984 (Ref. 3), and outlined in Table B.4-1.

Table B.4-1
BLOCKAGE 1.0 and BLOCKAGE 2.0 Quality Assurance

Date	QA Activity
19 October 1993	BLOCKAGE 1.0 Software Requirements Review
2 November 1993	Inspection of Draft BLOCKAGE 1.0 Software Design Document
15 November 1993	Inspection of Draft BLOCKAGE 1.0 Software Design Document
17 November 1993	BLOCKAGE 1.0 Design Review
17 November 1993	BLOCKAGE 2.0 Software Requirements Review
27 November 1993	Inspection of BLOCKAGE 1.0 code
27 November 1993	Inspection of BLOCKAGE 2.0 Software Design
27 November 1993	BLOCKAGE 1.0 Test Readiness Review
29 November 1993	BLOCKAGE 1.0 Qualification Test
10 December 1993	BLOCKAGE 2.0 Validation Test

B.4.1 BLOCKAGE 1.0 Testing

The BLOCKAGE 1.0 code was tested with a test calculation small enough that the results could be calculated by hand but large enough to sufficiently exercise the code models and logic. The calculation consisted of 12 welds selected to exercise the majority of the code logic. The code calculated weld break frequencies and the blockage array were printed out for verification. Hand calculated results were compared with the corresponding code results for the weld and target classifications (i.e., weld diameter, weld type, and insulation type), the target volume calculations, the blockage calculation, weld break frequencies, sequence frequencies, and unavailabilities. Totals were also compared. No differences were found between the hand and code generated results other than those resulting from numerical roundoff.

B.4.2 BLOCKAGE 1.0 Qualification Test

The qualification test for BLOCKAGE 1.0 involved executing the BLOCKAGE 1.0 code using the weld input data from NUREG/CR-3394 (Ref. 1). The values reported in NUREG-0869, Rev. 1 (Ref. 4) were compared to the corresponding output from BLOCKAGE 1.0. In addition, 31 representative output tables were chosen for comparison from NUREG/CR-3394 (Ref. 1). The values from BLOCKAGE 1.0 agreed within one in the second significant decimal digit with the referenced values. The only major difference involved a mismatch of the location categories in the system-basis sequence frequency tables. The qualification test team determined that the PRA code had printed the values corresponding to "PI-Inside Crane Wall" under the heading "PO-Outside Crane Wall" and vice-versa. In summary, the required reference data compared favorably with the output of BLOCKAGE 1.0, and all discrepancies were resolved.

B.4.3 BLOCKAGE 2.0 Testing

The BLOCKAGE 2.0 code was tested with the 12 weld BLOCKAGE 1.0 test calculation modified to include the insulation destruction and destruction fractions. This test calculation was sufficiently diverse to exercise the logic of the code modifications and to verify that the remaining BLOCKAGE 1.0 logic was still valid. The calculation of the volumes of destroyed target material transported to the screen was verified. The volume calculation was tested and verified using non-equal destruction and transport fractions and was also tested using the bounding fractions of zero and one. The weld break frequency calculation was tested and verified for both types of input (i.e., by plant or by weld). The screen blockage calculation was tested and verified. The weld and target classifications (i.e., by diameter, system and types), the summations of break and sequence frequencies, the computation of screen unavailabilities, and totals were all tested and verified. No differences were found between the hand and code generated results other than those resulting from numerical roundoff.

B.4.4 BLOCKAGE 2.0 Validation Testing

BLOCKAGE 2.0 validation testing also used the weld input data from the BLOCKAGE 1.0 qualification test. The program was first executed using parameter and weld input files to test the plant mode for specifying break frequencies. The first and last pages of all output files were compared to the BLOCKAGE 1.0 qualification test output. All values were the same. Next, the program was executed again using parameter and weld input files corresponding to the weld method for specifying break frequencies. Again, the first and last pages of each output file was compared to the BLOCKAGE 1.0 qualification test output. The values were again the same.

B.5 User Interface

The BLOCKAGE 2.0 source Fortran source code is located in six separate files. Compilation is accomplished by compiling BLOCKAGE.FOR. The other Fortran files are included into BLOCKAGE by INCLUDE statements. The code was compiled with Lahey Computer Systems, Inc. Fortran 77 Version 5.01 (Ref. 5). The execution of the code requires two input files and results in six output files. These files are described in Table B.5-1.

Table B.5-1: BLOCKAGE 2.0 File Structure

File Name	File Description
PARAMETR.INP	Parameter Input
WELD.INP	Weld and Target Input
WELD.OUT	Weld Summary Output
TARGET.OUT	Target Summary Output
SEQFREQ.OUT	Sequence Frequencies Reports
BLOCKAGE.OUT	Unavailabilities Reports
SUMMARY.OUT	Summary Reports
BLOCKAGE.ERR	Error Messages

B.5.1 Input Description

User input is arranged in a free-format and read into the code using list-directed READ statements. Data are entered starting in column 1 and where multiple parameters are entered on a line, they must be separated by either commas or spaces and entered in the following prescribed order. Character data input should be enclosed in single quotes. Comments may follow the data on each line. No line should be left blank.

The BLOCKAGE 2.0 code required two separate input files. These files are a parameter input file named PARAMETR.INP and a weld and target input file named WELD.INP. The input specifications are listed in Tables B.5-2 and B.5-3 for the parameter and weld, respectively. Sample input files are provided for further guidance in Table B.5-4 and B.5-5, for parameter and weld input, respectively.

B.5.2 Output Description

The BLOCKAGE 2.0 code produces six types of reports. Two reports located in output files, WELD.OUT and TARGET.OUT, echo the weld and target input, respectively, for inspection and for inclusion in reports. The calculational results are written in sequence frequencies and probabilities reports located in output files, SEQFREQ.OUT and BLOCKAGE.OUT, respectively. Summary information is written to the output file, SUMMARY.OUT. Any errors encountered in reading the input or during the calculations are written to the output file BLOCKAGE.ERR. The information reported is now described further by output file.

<u>WELD.OUT</u> The data for each weld input into the calculation is printed separate from its associated target data. The information listed for each weld includes: 1) a sequence number, 2) the weld identification, 3) the system identification, 4) the pipe diameter in inches, 5) the type of weld, 6) the location class, 7) the transport fraction for this location class, and 8) the number of targets for this weld.

<u>TARGET.OUT</u> The calculated total volume of each target and the data input for each target is printed. The information listed for each target includes: 1) the identification of its associated weld, 2) the number of the target associated with the weld, 3) the inner diameter of this target in inches, 4) the insulation type identifier, 5) the thickness of the insulation in inches, 6) the reference information, and 7) the target length and volume for each insulation destruction model. The incremental destruction fractions associated with each insulation destruction model is printed at the top of the table.

Table B.5-2: Parameter Input File

Line	Variable	Description	Limits and Conditions
1	ld(i)	Insulation Destruction Model L/D Ratios	i=1,3
2	dfract(i)	Target Insulation Destruction Fractions	i=1,3
3	nfr	Number of Flow Rates	1 to 3
4	pfrs(i)	Flow Rates (gpm)	i=1,nfr; >0., <100000.
5	nhl	Number of Allowable Head Losses	1 to 3
6	ahls(i)	Allowable Head Losses (feet of water)	i=1,nhl; >0., < 20.
7	a, b, c	Coefficients in Head Loss Correlation	
8	nsa	Number of Screen Areas	1 to 4
9	psas(i)	Screen Areas	i=1,nsa; >0., <1000.
10	npwt	Number of Permissible Weld Types	1 to 10
11	pwts(i)	Permissible Weld Types	i=1,npwt; characters*2
12	npwl	Number of Permissible Weld Locations	1 to 20
13	pwls	Permissible Weld Locations	i=1,npwl; character*2
14	tfract(i)	Debris Transport Fractions	i=1,npwl
15	nsys	Number of Systems	1 to 10
16i[a]	systbl(i)	System Descriptions	i=1,nsys; character*26
17	npwd	Number of Permissible Weld Diameters	1 to 30
18j[b]	pwds(i)	Permissible Weld Diameters (in)	i=1,npwd; j=1,npwd/5
19	break	Method of Calculating Break Frequencies	character*1[c]
20	ndc	Number of Pipe Diameter Classes	1 to 4
21	wdctbl(i)	Smallest Diameter in Diameter Class (in)	i=1,ndc; >0., <99.99
22[d]	wdcffr(i)	Weld Failure Frequencies (Rx-yr)	i=1,ndc; >0., <1.
23	wdclbl(i)	Diameter Class Labels	i=1,ndc; character*5
24j	wwffwf(i,j)	Weld Weighting Factors for Plant Method or Weld Failure Frequencies for W Method	i=1,ndc; j=1,npwt
25	nlc	Number of Location Classes	1 to 5
26a[f]	lclabl(i)	Location Class Label[e]	i=1,nlc; character*5
26b	lcsel1(i),lcsel2(i)	Location Class Selection Criteria	i=1,nlc; character*2
26c	lcdesc(i)	Location Class Description	i=1,nlc; character*50
27	npim	Number of Permissible Insulation Materials	1 to 10
28	pims(i)	Insulation Type Identifiers	i=1,npim; character*2
29	fibflg(i)	Fibrous Insulation Flags[g]	i=1,npim; character*1

a - One Line for Each system
b - 5 Diameters per Line of Input Until npwd Diameters are Entered, end last line with /
c - Enter Either a P for Plant Method or a W for Weld Method
d - Enter only if Plant Method was Selected
e - The First Location Class is the Summary Location Class
f - Each location class requires 3 lines of input in series (i.e., a, b, c, then a, b, c, etc.) for a total of 3 x nlc lines
g - Either an F for Fibrous or an N for Non-Fibrous

Table B.5-3: Weld Input File

Line	Variable	Description	Limits and Conditions
1	probid	Problem Identification and Description	character*40
2i[a]	weldid(i)	Weld Identification	character*9
	sysid(i)	System Identification	integer 1 to 10
	wdiam(i)	Weld Diameter (in)	agree with pwds[b]
	wtype(i)	Weld Type	character*2
	wloc(i)	Weld Location	character*2[c]
	ntgts(i)	Number of Targets for this Weld	1 to 40
	tgtno(1)	First Target Number for Weld i	Must be 1
	tgtdia(1)	Target Diameter (in)	> 0., <1000.
	tgtsys(1)	Reference Information	character*4[d]
	tgttyp(1)	Insulation Type	character*2[e]
	tgtthk(1)	Insulation Thickness (in)	>0., <100.
	tgtlen(1,k)	Target Length for each L/D Model (ft)	k=1,3
3ij[f]	tgtno(j)	Sequential Target Number for Weld i	2 to ntgts
	tgtdia(j)	Target Diameter (in)	>0., <1000.
	tgtsys(j)	Reference Information	character*4[d]
	tgttyp(j)	Insulation Type	character*2[e]
	tgtthk(j)	Insulation Thickness	>0., <100.
	tgtlen(j,k)	Target length for each L/D Model (ft)	k=1,3

a - Index of Each Weld (i.e., 1 to Number of Weld)

b - Weld Diameters Must Equal One of the Permissible Weld Diameters

c - Weld Location Must Match One of the Permissible Weld Locations

d - Reprinted in TARGET.OUT but Not Used

e - Insulation Type Must Match One of the Insulation Type Identifiers

f - The Order of Line Input is 2_1, $3_{1,2}$, $3_{1,3}$, ..., $3_{1,ntgts(1)}$, 2_2, $3_{2,2}$, $3_{2,3}$, ..., $3_{2,ntgts(2)}$, ..., etc.

Table B.5-4: Sample Parameter Input File

Input	Comments
3. 5. 7.	insulation destruction model L/Ds
1. 1. 1.	destruction fractions
3	number of flow rates, 1-3
6000. 8000. 10000.	flow rates (gpm), >0.0, <100000.0
3	number of head losses, 1-3
1. 2. 5.	allowable head losses, >0.0, <20.0
1.84 1.54 1653.	headloss parameters A, B, C
4	number of screen areas, 1-4
50. 75. 100. 200.	screen areas(sq.ft) >0.0, <1000.0
3	number of permissible weld types, 1-10
'N' 'A' 'E'	permissible weld types, any 2 characters
4	number of permissible weld locations, 1-20
'IP' 'IS' 'OP' 'OS'	permissible weld locations, any 2 chars.
1. 1. 1. 1.	transport fractions
9	number of systems, 1-10
'Hot Leg'	1st system descriptor, up to 26 char.
'Cold Leg'	2nd system descriptor, up to 26 char.
'Crossover'	3rd system descriptor, up to 26 char.
'Safety Inj. (cold leg)'	4th system descriptor
'Safety Inj. (hot leg)'	5th system descriptor, up to 26 char.
'Chem./Vol. Control System'	6th system descriptor
'Feedwater'	7th system descriptor, up to 26 char.
'Main Steam'	8th system descriptor, up to 26 char.
'Pressurizer'	9th system descriptor, up to 26 char.
13	no. of weld diameters
2.0 3.0 4.0 6.0 8.0	diameters 1 - 5
10.0 14.0 16.0 30.0 32.0	diameters 6 - 10
32.3 34.0 36.3 /	diameters 11-15, end with /
P	method for calculating break frequencies
4	no.of pipe diameter classes, 1-4; for each:
2.0 8.0 12.0 18.0	smallest diam.in class(0.00-99.99 in.)
3.E-4 4.E-5 3.E-5 3.E-6	failure frequency/Rx-yr, 0.-1.
'2-6' '8-10' '12-16' '18-+'	diameter class label
0.7 0.5 0.5 0.5	weld wgtg factors, weld type N
0.15 0.3 0.3 0.3	weld wgtg factors, weld type A
0.15 0.2 0.2 0.2	weld wgtg factors, weld type E
5	no.of location classes, 1-5, and:
'IP'	summary location class label,
'IP' ' '	its 1st & 2nd sel. criteria(weld type)
'Primary systems in crane wall'	its loc.class descriptor;
'Out'	2nd loc.class label,
'OP' 'OS'	1st & 2nd selection criteria(weld type),
'Outside crane wall'	50-char.summary loc.class descriptor;
'In'	3rd location class label,
'IP' IS'	its 1st & 2nd sel. criteria(weld type),
'Inside crane wall'	its 50-char.loc.class descriptor;
'Prim'	4th location class label,
'IP' 'OP'	its 1st & 2nd sel. criteria(weld type)

Table B.5-4: Sample Parameter Input File
(Continued)

'Primary systems'	its 50-char.loc.class descriptor;
'Sec'	5th location class label,
'IS' 'OS'	its 1st & 2nd sel. criteria(weld type),
'Secondary systems'	its 50-char.loc.class descriptor;
4	no.of perm. insulation materials, 1-10
'RM' 'FE' 'SE' 'AS'	insul. type identifiers, any 2 chars.
'N' 'F' 'F' 'N'	fibrous insulation flags, F or N

Table B.5-5: Sample Weld Input File

Qual. Test for BLOCKAGE 2.0/Plant

'1A'	1	34.0	N	IP	3	1	34.00	'28'	RM	3.50	4.17	4.17	4.16
						2	34.00	'28'	RM	3.50	2.17	2.17	2.10
						3	32.26	'28'	RM	3.50	2.25	2.25	2.25
'1B'	1	34.0	N	IP	3	1	34.00	'28'	RM	3.50	2.00	2.00	2.00
						2	34.00	'28'	RM	3.50	5.17	5.17	5.16
						3	32.26	'28'	RM	3.50	5.50	5.50	5.50
'2A'	1	34.0	E	IP	2	1	34.00	'28'	RM	3.50	2.83	2.83	2.83
						2	32.26	'28'	RM	3.50	0.75	0.75	0.75
'2B'	1	34.0	E	IP	3	1	34.00	'28'	RM	3.50	3.00	3.00	3.00
						2	34.00	'28'	RM	3.50	6.00	6.00	6.00
						3	32.26	'28'	RM	3.50	6.17	6.17	6.16
'3A'	1	34.0	E	IP	24	1	34.00	'28'	RM	3.50	6.00	6.00	6.00
						2	138.0	'28'	RM	3.50	6.00	6.00	6.00
						3	138.0	'28'	SE	3.50	2.33	8.00	13.67
						4	32.26	'28'	RM	3.50	0	1.83	5.25
						5	36.32	'28'	RM	3.50	0	3.33	29.50
						6	81.00	'28'	RM	3.00	0	0	26.00
						7	138.0	'28'	RM	3.50	0	0	6.00
						8	138.0	'28'	SE	3.50	0	0	13.67
						9	2.00	'4'	SE	1.50	15.7	15.8	15.83
						10	1.00	'4'	SE	1.50	3.42	10.5	10.50
						11	3.00	'4'	SE	1.50	0	6.25	13.00
						12	2.00	'26'	FE	1.50	2.75	10.8	13.50
						13	3.00	'26'	FE	1.50	5.25	11.5	14.25
						14	0.75	'26'	FE	2.00	0	1.50	1.50
						15	0.75	'26'	FE	2.00	0	1.50	1.50
						16	2.00	'26'	FE	1.50	0	2.00	2.00
						17	2.00	'16'	AS	1.00	0	0	7.00
						18	1.00	'32'	SE	1.00	0	0	9.08
						19	0.75	'32'	SE	1.00	0	0	1.40
						20	2.00	'33'	SE	1.00	0	0	5.00
						21	10.00	'25'	RM	3.00	0	0	20.58
						22	10.00	'25'	FE	1.50	0	0	11.25
						23	10.00	'37'	FE	1.50	0	0	11.66
						24	6.00	'37'	FE	1.50	0	0	4.75

SEQFREQ.OUT The sequence frequencies were correlated by both diameter and system. A pair of reports is therefore printed for each combination of screen area, flow rate, allowable head loss, and insulation destruction model. The header information in all of these reports includes the code version identification , the problem identification, the screen area, the flow rate, the allowable head loss, and the length to diameter ratio of the insulation destruction model. The sequence frequencies are compiled for each of location classes as well as for the overall plant. The sequence frequencies are totaled for the overall plant and for each location class. In the diameter report, the sequence frequencies are correlated by permissible weld diameters. In the system report, the sequence frequencies are correlated by both system and by diameter class. The descriptions of the location classes are printed at the bottom of each diameter report and the system descriptions are printed at the bottom of each system reports. If the maximum number of screen areas, flow rates, and allowable head losses are input, the code will produce a total of 216 sequence frequencies reports.

BLOCKAGE.OUT Probabilities of screen unavailability are correlated both by system and diameter class and by permissible weld diameter for the overall plant and the summary location class (first location specified in the input). The break and sequence frequencies associated with the unavailabilities are also correlated in these reports. Each report includes results for the three insulation destruction models. A set of four reports is printed for each combination of screen area, flow rate, and allowable head loss. The break frequencies do not depend upon the selection of the insulation destruction model since they are not a function of screen blockage. The frequencies are totaled for each category. The header information in all of these reports includes the code version, the problem identification, the screen area, the flow rate, the allowable head loss, and the insulation destruction model. The description of the summary location class is printed at bottom of each report. If the maximum number of screen areas, flow rates, and allowable head losses are input, the code will produce a total of 144 reports.

SUMMARY.OUT The total sequence frequencies are saved in this file for each combination of screen area, flow rate, allowable head loss, and insulation destruction model. There is a summary report for the overall plant sequence frequencies and a report for the summary location class sequence frequencies.

BLOCKAGE.ERR If any errors are encountered in reading or validating the input or during the calculations, an error message is written to this file. An error message identifies the portion of the code originating the message and indicates the error. The following message, for example, identifies an error encountered in validating a weld diameter in the subroutine WINPUT.

```
WINPUT: Error in WDIAM =     19.0000     I=          9
WINPUT: Not a permissible weld diameter
```

The ninth weld in the weld input file has a diameter of 19 inches which does not correspond to any of the permissible weld diameters provided in the parameter input.

References

[1] J.J. Wysocki, "Probabilistic Assessment of Recirculation Sump Blockage Due to Loss of Coolant Accidents, Containment Emergency Sump Performance USI A-43," Vols. 1 and 2, Burns & Roe, Inc., published as Sandia National Laboratories Report No. SAND83-7116, NUREG/CR-3394, July 1983.

[2] US Nuclear Regulatory Commission, "Software Quality Assurance Program and Guidelines," NUREG/BR-0167, February 1993.

[3] The Institute of Electrical and Electronics Engineers, Inc., "IEEE Guide to Software Requirements Specifications, Software Engineering Standards," ANSI/IEEE Std 830-1984, October 1987.

[4] A.W. Serkiz, "USI A-43 Regulatory Analysis," US Nuclear Regulatory Commission, NUREG-0869, Rev. 1, October 1985.

[5] Lahey Computer Systems, Inc., Fortran 77 Version 5.01, 1993.